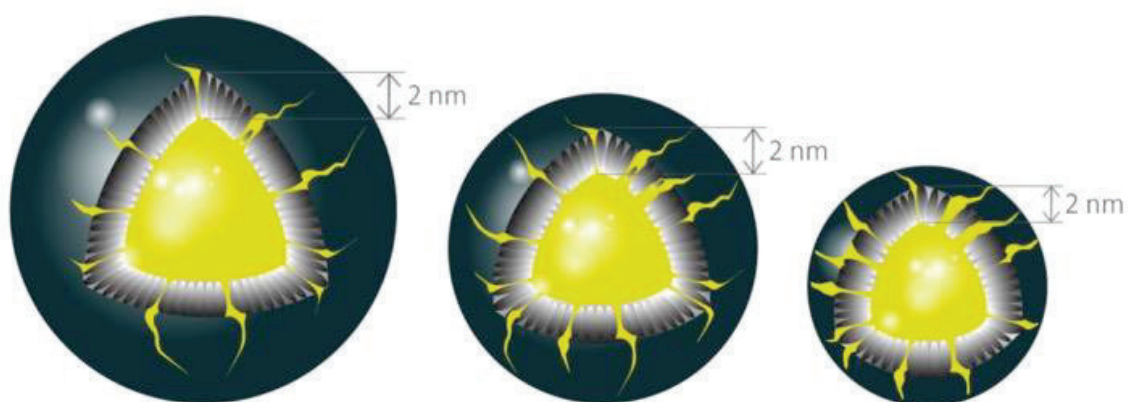


LIPOPROTEIN ANALYSIS BY 2D DIFFUSION-ORDERED  
 $^1\text{H}$ -NMR SPECTROSCOPY

NÚRIA AMIGÓ GRAU



DOCTORAL THESIS

2017



UNIVERSITAT  
ROVIRA i VIRGILI

Núria Amigó Grau

**LIPOPROTEIN ANALYSIS BY 2D DIFFUSION-ORDERED  $^1\text{H}$ -NMR  
SPECTROSCOPY**

DOCTORAL THESIS

Supervised by Prof. Xavier Correig Blanchar

Department of Electronic, Electric and Automatic Engineering



UNIVERSITAT ROVIRA I VIRGILI

Reus

2017





Escola Tècnica Superior d'Enginyeria

Departament d'Enginyeria Electrònica, Elèctrica i Automàtica

Av. Paisos Catalans 26

Campus Sescelades

43007 Tarragona

I STATE that the present study, entitled: "**LIPOPROTEIN ANALYSIS BY 2D DIFFUSION-ORDERED <sup>1</sup>H-NMR SPECTROSCOPY**", presented by **Núria Amigó Grau** for the award of the degree of Doctor, has been carried out under my supervision at the Department of Electronic, Electric and Automatic Engineering (DEEEA) of this university and meets the requirements to qualify for International Mention.

Tarragona, August 2017

Xavier Correig Blanchar



“Science is not only a disciple of reason but, also, one of romance and passion”

**Stephen Hawking**





L'elaboració d'aquesta tesi ha estat un procés llarg, agradable, difícil, intens, canviant, fascinant... Un viatge a través de la ciència i de l'aprenentatge, de la mà de molts companys que han guiat i fet possible que es realitzés i que, finalment, es tanqués aquesta etapa.

Agraeixo profundament al Dr. Xavier Correig l'haver-me donat aquesta oportunitat. Agraeixo la seva manera d'escoltar-nos i respectar-nos; i la seva capacitat per saber veure en cada un de nosaltres allò en el que podem créixer i gaudir. És difícil trobar algú excepcional, i més difícil encara, excepcional tant en l'àmbit professional com en el personal.

A la Universitat Rovira i Virgili i a l'Institut d'Investigació Sanitària Pere i Virgili el seu suport i facilitats, permetent la realització d'aquesta tesi; així com al personal del departament d'Enginyeria Electrònica, Elèctrica i Automàtica, la seva ajuda constant.

Agraeixo afectuosament haver pogut coincidir amb cada un dels companys de viatge, que al llarg d'aquesta etapa han esdevingut amics. Moltes gràcies Mariona, Sara, Míriam, Ruben, Óscar i Miguel, per ser-hi, per la vostra ajuda, per tan bons moments compartits, reflexions i aprenentatges. Gràcies Serena, Josep, Lorena, Sílvia, Jordi, Mabel, Salva, Pol, Rita, Irene, Xavi, Noelia, Dídac i Pere per les bones experiències; així com als professors Nicolau Canyelles i Jesús Brezmes. Gràcies amics de Biosfer, Miguel, Miriam, Rocío i Dani, és un plaer treballar amb vosaltres, sou un equip increïble.

Agraeixo també a tots els companys de la URLA, unitat amb la que he tingut la sort de poder treballar sovint i que m'ha permès tenir contacte amb un entorn científic diferent, més pròxim a la realitat clínica. Gràcies Dr. Lluís Masana per la seva calidesa, així com a tot el grup que m'ha fet sentir part de la unitat: Daiana, Josefa, Núria, Josep, Montse, Joan Carles, Cèlia, Alba, Paula, Iris, Sandra i Marina; i especialment a la Merche, a qui he tingut la sort de trobar al llarg d'aquesta etapa, i amb qui sé que puc comptar sempre.

A la Dra. Samia Mora agraeixo l'experiència al Brigham and Women's Hospital, una oportunitat molt valuosa a nivell professional i personal, que m'ha donat un enfocament complementari de la recerca, menys creatiu potser, però eficient i molt ben estructurat.

Agraeixo de tot cor a tota la meva família el seu suport incondicional, paciència i ànims constants.

Finalment, vull agrair especialment al Dr. Roger Mallo l'aprenentatge, la seva visió, la seva perseverança i passió; aquesta tesi és fruit de molt treball en comú, de moltes discussions i moltes reflexions mantingudes al llarg d'aquests anys.

## TABLE OF CONTENTS

LIST OF PUBLICATIONS

LIST OF CONGRESSES

LIST OF PATENTS

INDUSTRIAL R+D COMPETITIVE PROJECTS

Chapter 1. Introduction, 1

- 1.1 Background, 3
- 1.2 Motivation, 13
- 1.3 Hypothesis and objectives, 19
- 1.4 Organization of the document, 23
- 1.5 References, 27

Chapter 2. State of the art. Lipoprotein analysis by  $^1\text{H-NMR}$  and its clinical relevance, 35

- 2.1 Lipoproteins, metabolism and standard quantification methods, 37
- 2.2 Serum/Plasma lipoprotein analysis by  $^1\text{H-NMR}$  spectroscopy, 47
  - 2.2.1 Sample Handling procedures, 51
  - 2.2.2 Serum/plasma lipoprotein analysis by 1D  $^1\text{H-NMR}$  spectroscopy, 53
  - 2.2.3 Serum/plasma lipoprotein analysis by 2D  $^1\text{H-NMR}$  spectroscopy, 59
- 2.3 The Liposcale Test, 65
  - 2.3.1 The technology, 69
  - 2.3.2 Industrial Development, 106
  - 2.3.3 Clinical applications developed by Biosfer Teslab, 112
- 2.4 References, 115

Chapter 3. Study of the HDL fraction of diabetic patients by diffusion edited  $^1\text{H-NMR}$  spectroscopy, 125

- 3.1 Introduction, 127
- 3.2 Lipoprotein hydrophobic core lipids are partially extruded to surface in smaller HDL: "Herniated" HDL, a common feature in diabetes, 131
  - 3.2.1 Abstract, 133
  - 3.2.2 Introduction, 133
  - 3.2.3 Results, 136
  - 3.2.4 Discussion, 148
  - 3.2.5 Methods, 151
  - 3.2.6 References, 157
  - 3.2.7 Supporting information, 162

- 3.3 Remarkable quantitative and qualitative differences in HDL after niacin or fenofibrate therapy in type 2 diabetic patients, 169
  - 3.3.1 Abstract, 171
  - 3.3.2 Introduction, 172
  - 3.3.3 Patients and methods, 174
  - 3.3.4 Results, 179
  - 3.3.5 Discussion, 186
  - 3.3.6 References, 189

#### Chapter 4. Lipoprotein analysis for diet and nutritional interventions assessment, 193

- 4.1 Introduction, 195
- 4.2 Fish consumption, omega-3 fatty acids and NMR lipoprotein subfractions in 26,034 apparently healthy women, 199
  - 4.2.1 Abstract, 201
  - 4.2.2 Introduction, 202
  - 4.2.3 Methods, 203
  - 4.2.4 Results, 210
  - 4.2.5 Discussion, 224
  - 4.2.6 References, 231
- 4.3 Improvement of the omega 3 index of healthy subjects does not alter the effects of dietary saturated fats or n-6PUFA on LDL profiles, 237
  - 4.3.1 Abstract, 239
  - 4.3.2 Introduction, 240
  - 4.3.3 Material and Methods, 241
  - 4.3.4 Results, 247
  - 4.3.5 Discussion, 251
  - 4.3.6 References, 255
- 4.4 Effect of diets rich in either saturated fat or n-6 polyunsaturated fatty acids and supplemented with long-chain n-3 polyunsaturated fatty acids on plasma lipoprotein profiles, 259
  - 4.4.1 Abstract, 261
  - 4.4.2 Introduction, 262
  - 4.4.3 Material, Subjects and Methods, 263
  - 4.4.4 Results, 266
  - 4.4.5 Discussion, 272
  - 4.4.6 References, 277

#### Chapter 5. Discussion and conclusions, 283

## **LIST OF PUBLICATIONS**



J. Girona, C. Rodríguez-Borjabad, D. Ibarretxe, M. Heras, **N. Amigó**, A. Feliu, L. Masana and N. Plana (2017). Plasma IDOL, soluble LDLR and PCSK9 Levels as Potential Biomarkers of Familial Hypercholesterolemia in Children. *J. Clin. Lipidol.* (In press, accepted).  
doi:10.1016/J.JACL.2017.10.003

R. Barrilero, N. Ramírez, JC. Vallvé, D. Taverner, R. Fuertes, **N. Amigó** and X. Correig (2017). Unravelling and quantifying the “NMR-invisible” metabolites interacting with human serum albumin by binding competition and T2 relaxation-based decomposition analysis *J Proteome Res.* 2017;16(5).  
doi:10.1021/acs.jproteome.6b00814.

AJ. Amor, M. Pinyol, E. Solà, M. Catalan, M. Cofán, Z. Herreras, **N. Amigó**, ... and E. Ortega (2017). Relationship between noninvasive scores of nonalcoholic fatty liver disease and nuclear magnetic resonance lipoprotein abnormalities: A focus on atherogenic dyslipidemia. *J Clin Lipidol.* 2017;11(2).  
doi:10.1016/j.jacl.2017.02.001.

C. B. Dias, **N. Amigó**, L.G. Wood, X. Correig and ML. Garg (2017). Effect of diets rich in either saturated fat or n-6 polyunsaturated fatty acids and supplemented with long-chain n-3 polyunsaturated fatty acids on plasma lipoprotein profiles. *Eur J Clin Nutr.* May 2017.  
doi:10.1038/ejcn.2017.56.

C. B. Dias, **N. Amigó**, L.G. Wood, R. Mallol, X. Correig and ML. Garg (2016). Improvement of the omega 3 index of healthy subjects does not alter the effects of dietary saturated fats or n-6PUFA on LDL profiles. *Metabolism.* 2017;68.  
doi:10.1016/j.metabol.2016.11.014.

J. Girona, D. Ibarretxe, N. Plana, S. Guaita-Esteruelas, **N. Amigó**, M. Heras and L. Masana (2016). Circulating PCSK9 levels and CETP plasma activity are independently associated in patients with metabolic diseases *Cardiovasc Diabetol.* 2016;15(1).  
doi:10.1186/s12933-016-0428-z.

**N. Amigó**, R. Mallol, M. Heras, S. Martínez-Hervás, F. Blanco-Vaca, J. C. Escolà-Gil, N. Plana, Ó. Yanes, L. Masana and X. Correig. (2016) Lipoprotein hydrophobic core lipids are partially extruded to surface in smaller HDL: "Herniated" HDL, a common feature in diabetes. *Sci Rep.* 2016;6:19249.  
doi:10.1038/srep19249.

D. Ibarretxe, J. Girona, N. Plana, A. Cabré, R. Ferré, **N. Amigó**, S. Guaita, R. Mallol, M. Heras and L. Masana. (2015) Circulating PCSK9 in patients with type 2 diabetes and related metabolic disorders. *Clin Investig Arterioscler.*  
doi:10.1016/j.arteri.2015.11.001.

D. Ibarretxe, J. Girona, **N. Amigó**, N. Plana, R. Ferré, S. Guaita, R. Mallol, M. Heras and L. Masana. (2015) Impact of epidermal fatty acid binding protein on 2D-NMR-Assessed atherogenic dyslipidemia and related disorders *J Clin Lipidol.* 2016;10(2):330-338.e2.  
doi:10.1016/j.jacl.2015.12.012.

R. Mallol, **N. Amigó**, M. A. Rodríguez, M. Heras, M. Vinaixa, N. Plana, E. Rock, J. Ribalta, O. Yanes, L. Masana and X. Correig. (2015). Liposcale: a novel advanced lipoprotein test based on 2D diffusion-ordered <sup>1</sup>H-NMR spectroscopy. *J Lipid Res.* 2015;56(3):737-746.  
doi:10.1194/jlr.D050120.

L. Masana, A. Cabré, M. Heras, **N. Amigó**, X. Correig, S. Martínez-Hervás, ... and F. Blanco-Vaca. (2015). Remarkable quantitative and qualitative differences in HDL after niacin or fenofibrate therapy in type 2 diabetic patients. *Atherosclerosis.* 2015;238(2):213-219.  
doi:10.1016/j.atherosclerosis.2014.12.006.

**N. Amigó**, A.O. Akinkuolie, S.E. Chiuve, X. Correig, N. Cook and S. Mora. Fish consumption, omega-3 fatty acids (n-3), and NMR lipoprotein subfractions in 26034 apparently healthy women (Preparing manuscript for submission, *Circulation*).

G. Pichler, **N. Amigó**, M Tellez-Plaza, MA. Pardo, A. Dominguez-Lucas, JC. Martin-Escudero, JF Ascaso, FJ. Chaves, R. Carmena and J. Redon. LDL-particles composition and incident cardiovascular disease in a south-



European population: The Hortege-LIPOSCALE Study (Submitted, European Heart journal).



## **LIST OF CONGRESSES**



## Talks

-**N. Amigó.** *“Nueva era en el diagnóstico y valoración del riesgo cardiovascular: Análisis de lipoproteínas mediante RMN”*. 9<sup>th</sup> SEMERGEN National Cardiovascular Meetings, Girona 2017.

-**N. Amigó.** *“La evaluación de patrones de lipoproteínas y su impacto en el manejo de las dislipemias”*. 30<sup>th</sup> Congress of the Spanish Arteriosclerosis Society, Cádiz 2017.

-**N. Amigó.** *“Importancia del tamaño de las lipoproteínas en el cribado del riesgo cardiovascular: LIPOSCALE”*. 8<sup>th</sup> SEMERGEN National Cardiovascular Meetings, Santander 2016.

- **N. Amigó.** *“Importancia del tamaño de las lipoproteínas en el cribado cardiovascular: de la teoría a la práctica clínica”*. 29<sup>th</sup> Congress of the Spanish Arteriosclerosis Society, Granada 2016.

-**N. Amigó** *“La Metabolómica por RMN en el Entorno Clínico. Aplicaciones en la Investigación Biomédica y el Diagnóstico Clínico”*, Valencia 2016.

## Contributions

R. Yahyaoui, E. Rodríguez, M. Gil, MC. García-Jiménez, ML. González-Diéguez, P. Del Valle Loarte, MA Barba-Romero, J. Quintero, D. Gil-Ortega, J. De Las Heras, L. Aldámiz, R. Bernal, E. García, **N. Amigó.** Characterization of plasma lipoprotein particles in Spanish patients with lysosomal acid lipase deficiency (LAL-D). AECOM, Las Palmas, 2017, oral presentation; ICIEM, Rio de Janeiro, 2018, poster presentation.

M. Gil-Serret, D. Ibarretxe, D. Rodriguez, N. Plana, L. Masana, **N. Amigó.** Análisis avanzado de lipoproteínas por RMN en la práctica clínica. Del manejo de la dislipemia al de patrones lipoproteicos. 30<sup>th</sup> Congress of the Spanish Arteriosclerosis Society. Cádiz, 2017. Oral presentation.

M. Gil-Serret, D. Ibarretxe, N. Plana, L. Masana, X. Correig, **N. Amigó**. Normal lipoprotein particle number and size in Spanish population according to sex and age, assessed by Nuclear Magnetic Resonance. 85<sup>th</sup> Congress of the European Atherosclerosis Society. Prague, 2017. Science at a Glance presentation.

R. Fuertes, **N. Amigó**, JC. Vallvé, S. Paredes, D. Taverner, L. Masana, X. Correig. Caracterización del perfil inflamatorio en pacientes con artritis reumatoide frente a población sana mediante <sup>1</sup>H-Resonancia Magnética nuclear (<sup>1</sup>H-NMR). 30<sup>th</sup> Congress of the Spanish Arteriosclerosis Society. Cádiz, 2017. Oral Presentation.

R. Fuertes, **N. Amigó**, JC. Vallvé, S. Paredes, D. Taverner, L. Masana, X. Correig. Characterization of glycoprotein and lipoprotein profile of Rheumatoid arthritis patients by <sup>1</sup>H-Nuclear Magnetic Resonance Spectroscopy (<sup>1</sup>H-NMR). 84<sup>th</sup> European Atherosclerosis Society (EAS) Congress. Prague, 2017. Poster Presentation.

C. Rodríguez-Borjabad, D. Ibarretxe, J. Girona, A. Feliu, **N. Amigó**, L. Masana, N. Plana. Perfil lipoproteico evaluado por RMN 2D-<sup>1</sup>H en niños con hipercolesterolemia familiar y no familiar. 30<sup>th</sup> Congress of the Spanish Arteriosclerosis Society. Cádiz, 2017. Oral presentation.

J. Miranda, RV. Simoes, C. Paules, **N. Amigó**, M. Pardo, ML. García-Martín, F. Figueras, E. Eixarch, F. Crispi, E. Gratacós. Targeted Lipidomics of Maternal and Cord Blood in Term Gestations with Suboptimal Fetal Growth. 9<sup>th</sup> International Symposium on Diabetes, Hypertension, Metabolic Syndrome, and Pregnancy. Barcelona, 2017. Poster presentation -**awarded as best abstract award**.

**N. Amigó**, R. Fuertes, C. Cabré, M. Vinaixa, M. Romeu, M. Muñoz, M. Giralt, J. Soler, J. Aguilera, MT. Compte, X. Correig, A. Martínez-Vea. Pro atherogenic lipoprotein profile associated with white matter lesions in chronic kidney disease patients: A <sup>1</sup>H-NMR metabolomic approach. 84<sup>th</sup> Congress of the European Atherosclerosis Society. Innsbruck, 2016. Science at a Glance presentation -**awarded as best poster award**.

J. Girona, D. Ibarretxe, N. Plana, S. Guaita-Esteruelas, **N. Amigo**, M. Heras, L. Masana. PCSK9 Circulating levels and CETP Plasma activity are

associated independently of lipid lowering therapies. 84<sup>th</sup> Congress of the European Atherosclerosis Society. Innsbruck, 2016. Science at a Glance presentation -**awarded as best poster award**.

**N. Amigó**, R. Fuertes, C. Cabré, M. Vinaixa, M. Romeu, M. Muñoz, M. Giralt, J. Soler, J. Aguilera, MT. Compte, X. Correig, A. Martínez-Vea. Metabolomic approach to white matter lesions in chronic haemodialysis patients identifies a novel metabolic profile associated with these lesions. ERA-EDTA. Viena, 2016. Poster presentation.

**N. Amigó**, R. Fuertes, C. Cabré, M. Vinaixa, M. Romeu, M. Muñoz, M. Giralt, J. Soler, J. Aguilera, MT. Compte, X. Correig, A. Martínez-Vea. Aproximación metabolómica con <sup>1</sup>H-RMN para la caracterización de pacientes con enfermedad renal crónica en hemodiálisis que presentan lesiones en la sustancia blanca cerebral. Spanish Society of Nephrology (SEN). Oviedo, 2016. Poster presentation.

R. Fuertes, **N. Amigó**, JC. Vallvé, S. Paredes, D. Taverner, L. Masana, X. Correig. Caracterización metabolómica de pacientes con artritis reumatoide a través de <sup>1</sup>H-Resonancia Magnética nuclear (<sup>1</sup>H-NMR). 29<sup>th</sup> Congress of the Spanish Arteriosclerosis Society. Granada, 2016. Oral presentation.

**N. Amigó**, R. Mallol, M. Heras, A. Cabré, N. Plana, L. Masana, X. Correig. Smaller and “herniated” high density lipoproteins incremented in type 2 diabetes mellitus patients. Spanish Society of Diabetes. Valencia, 2015. Oral Presentation.

**N. Amigó**, A. O. Akinkuoli, S. E. Chiuve, N. R. Cook, S. Mora. Fish Consumption, Omega-3 fatty acids (N-3) and NMR Lipoprotein Subfractions in 26034 apparently healthy women. Nordic Lipid Forum, Reykjavik 2015, Oral Presentation; International Society of Atherosclerosis, Amsterdam 2015, Oral Presentation; Spanish Atherosclerosis Society, Logroño 2015, Oral Presentation –**awarded as original research**.

S. Parra, N. Canela, M. Heras, **N. Amigó**, P. Sahun, X. Correig, A. Castro. Proteome analyses of HDL particles allows to identify biomarkers of

disease activity in SLE patients: Gelsolin, Indian Hedgehog protein and S100A8. EULAR. Rome, 2015. Poster Presentation.

R. Yahyaoui, E. Rodríguez-García, M. Heras, MC García-Jiménez, ML González-Diéguez, R. Mallol, **N. Amigó**. Characterization of plasma lipoprotein particles in Spanish patients with lysosomal acid lipase deficiency. SSIEM. Lyon, 2015. Poster Presentation.

R. Mallol, **N. Amigó**, M. A. Rodríguez, M. Heras, M. Vinaixa, N. Plana, E. Rock, J. Ribalta, O. Yanes, L. Masana, X. Correig. Discordance analysis between LDL particle concentrations and LDL-C and ApoB values in type 2 diabetic subjects with atherogenic dyslipidemia. International Society of Atherosclerosis. Amsterdam, 2015. Oral Presentation.

MC. García-Jiménez, P. Roncalés, L. Monge, I. Ros, J. Cebolla, E Rodríguez-García, **N. Amigó**, M. Heras, R. Yahyaoui. Deficiencia de lipasa ácida lisosomal: una causa poco reconocida de dislipemia y disfunción hepática. ECM. Pamplona, 2015. Poster Presentation.

CB. Dias, **N. Amigó**, LG. Wood, ML. Garg. Saturated fats and vegetable oil modulate lipoprotein profile similarly when co-administered with omega-3 polyunsaturated fatty acids. FSDH. Wellington, 2015. Oral Presentation.

R. Mallol, A Cabré, **N. Amigó**, M. Heras, L. Masana, X. Correig. Characterization of Atherogenic Dyslipidaemia using a novel NMR-based advanced lipoprotein test in type 2 diabetic subjects. 27<sup>th</sup> Congress of the Spanish Arteriosclerosis Society. Barcelona, 2014. Poster presentation -**3rd award for the best communication award**.

**N. Amigó**, R. Mallol, M. Heras, A Cabré, N. Plana, L. Masana, X. Correig. Smaller and "Herniated" HDL in patients with type 2 diabetes mellitus. 27<sup>th</sup> Congress of the Spanish Arteriosclerosis Society. Barcelona, 2014. Poster presentation.

R. Mallol, A Cabré, M. Rodríguez, **N. Amigó**, M. Vinaixa, N. Plana, M. Heras, L. Masana, X. Correig. Characterisation of Atherogenic Dyslipidemia using a novel NMR-based advanced lipoprotein test in type



2 diabetic subjects. 81<sup>st</sup> European Atherosclerosis Society Congress. Lyon, 2013. Poster presentation

R. Mallol, **N. Amigó**, M. Rodríguez, M. Heras, N. Plana, L. Masana, X. Correig. Advanced Lipoprotein Testing Using Diffusion-edited <sup>1</sup>H-NMR Spectroscopy. 25<sup>th</sup> Congress of the Spanish Arteriosclerosis Society. Reus, 2012. Poster presentation.



## **LIST OF PATENTS**



METHOD FOR THE CHARACTERIZATION OF LIPOPROTEINS, Inventors: Mallol Parera, Roger; Amigo Grau, Núria; Correig Blanchar, Xavier; Masana Marín, Lluís; Rodríguez Martínez, Miguel Ángel; Heras Ibáñez, Mercedes; Plana Gil, Núria; Ribalta Vives, Josep, EP13382478.9, 27 November 2013

METHODS FOR DETERMINING THE LIPID DISTRIBUTION BETWEEN THE CORE AND THE SHELL OF A LIPOPROTEIN PARTICLE, Inventors: Mallol Parera, Roger; Amigo Grau, Núria; Correig Blanchar, Xavier; Masana Marín, Lluís; Rodríguez Martínez, Miguel Ángel; Heras Ibáñez, Mercedes; Plana Gil, Núria, EP13382477.1, 27 November 2013



**INDUSTRIAL**

**R+D COMPETITIVE PROJECTS**





Project: *Development of new in vitro diagnostic tests based on NMR for early diagnosis of cardiometabolic and cardiovascular disease (SNEO-20161091)*

Organism: CDTI, Spanish Government

Initiation date: 01/01/2017

Finalization date: 31/12/2018

Company: Biosfer Teslab

Responsible: Núria Amigó Grau

Project: *Development and validation of advanced diagnostic tests.*

Organism: Acció, Catalan Government

Initiation date: 29/07/2015

Finalization date: 29/07/2017

Company: Biosfer Teslab

Responsible: Núria Amigó Grau



## **Chapter 1. Introduction**



## **1.1 Background**



The prevalence of cardiometabolic diseases, which include chronic cardiovascular disease and diabetes, increases worldwide each year due largely to today's living habits, sedentary lifestyle, stress and consumption of high-calorie, high-fat foods with an elevated content of sugar and salt and poor concentration in micronutrients. The occurrence of this cardiometabolic disorders has dramatically increased the number of cardiovascular accidents, placing cardiovascular disease (CVD) as the leading cause of death worldwide<sup>1</sup>.

Traditionally, these diseases have been diagnosed by analysing the risk factors presented by patients, such as smoking, high cholesterol and high blood pressure, as well as obesity, sedentary lifestyle or type 2 diabetes. However, current medicine has been demonstrated to be incapable of accurately diagnosing individuals at risk of cardiovascular accidents or complications, since today there is still a high incidence of unexpected ischemic events, both in patients with known arteriosclerosis and in subjects classified as healthy.

Cardiovascular (CV) risk functions, such as REGICOR and Framingham Coronary Heart Disease Risk Score, are the usual methods for assessing CV risk in asymptomatic patients. They are multifactorial functions that give a score according to classic CV risk factors which include, among others, a basic lipid profile. A high concentration of cholesterol transported by LDL, a low concentration of cholesterol transported by HDL and/or a high concentration of triglycerides are associated with an increased risk of suffering a CV accident<sup>2,3</sup>. However, most early CV events occur in people not included in high-risk categories. This reflects the poor discriminatory capacity of classical CV risk factors.

## Chapter 1

In recent years, one of the factors considered to be predictive of CV events in asymptomatic populations is the presence of subclinical atherosclerosis (atherosclerotic plaque)<sup>4,5</sup>. In relation to classic CV risk factors, it is known that patients who meet the therapeutic objectives of LDL cholesterol, blood pressure and blood glucose have CV events. According to a recent study<sup>6</sup>, up to the 50% of CV accidents occur in individuals with normal levels of LDL-c. The CV risk of these subjects is known as residual risk. Possible causes of residual risk contributing to a subjacent atherosclerotic disease include lipid fractions other than LDL-c, such as HDL-c and non-HDL cholesterol<sup>7</sup>.

The latter includes all atherogenic particles in addition to LDL-c, and several prospective studies show that it is a better predictor of CVD than LDL concentrations especially in populations with cardiometabolic disorders, which are more vulnerable to suffering CV accidents. In these individuals, LDL-c concentrations are usually normal or slightly elevated, while the amount of LDL particles is clearly increased due to the presence of smaller type of particles, lower in cholesterol and more atherogenic<sup>7,8</sup>.

The presence of this small LDL particles dramatically increases the risk of CVD and goes unnoticed by the traditional scales of risk estimation<sup>9,10</sup>. That is why there are already clinical guidelines that recommend the determination of the size and number of LDL lipoprotein particles, beyond their lipid load, to evaluate a patient's CV risk<sup>11</sup>.

The European ESC/EAS 2016 guidelines<sup>12</sup> for the management of dyslipidaemia in section 3.3.8 recognize the role of the size of the LDL-p



particles in the correct evaluation of cardiovascular risk, although the recommendation on its use cannot be generalized yet for lack of standardization and universal access to the technique. The European ESC 2016 Guidelines on cardiovascular prevention in clinical practice<sup>13</sup>, in their point 3a.7.5, associate a specific pattern of small LDL-p lipoprotein particles with patients with type 2 diabetes mellitus (DM2) along with moderately elevated triglycerides, reduced HDL-c fractions, obesity, and insulin resistance.

Regarding high-density lipoprotein (HDL), HDL particle (HDL-p) concentration or number has shown to perform better than their respective major lipid components, i.e. HDL-c, for assessing CVD risk<sup>14,15</sup>. These clinical studies suggest that HDL-p concentration can provide information on the CV status of an individual that is independent of HDL-c. In the MESA study, taking into account 5,598 men and women, HDL-c was not associated with two measures of cardiovascular disease status after adjusting for LDL-c and the concentration of LDL-p<sup>16</sup>. In contrast, HDL-p remained strongly and independently associated with cardiovascular disease status. In addition, in the JUPITER study, Mora et al. reported that the concentration of HDL-p under pharmacological treatment is a better marker of residual cardiovascular risk than HDL-c or apolipoprotein A1 (ApoA1) concentrations<sup>17</sup>.

#### **Diabetes mellitus and atherosclerosis**

DM is considered an independent risk factor for CVD<sup>18</sup>. People with type 2 DM (DM2) have a 2-fold greater risk of death from myocardial infarction or ictus than people without DM<sup>18</sup>. In patients with type 1 DM (DM1), there is also an increase in CV mortality between 2 and 4 times

## Chapter 1

higher, especially in women and patients with poor glycemic control<sup>19</sup>. In addition, patients with DM present a worse evolutionary course after the acute CV event than those without DM<sup>20</sup>. Despite the different etiology, DM1 and DM2 are associated with an accelerated development of atherosclerotic lesions. In DM patients, atherosclerosis is a complex multifactorial disease characterized by being more extensive (more plaques and territories affected) and progressing more rapidly than atheromatous disease without DM<sup>21</sup>. In addition, none of the CV risk functions (Framingham, SCORE and DECODE) accurately estimates the CV risk for these patients<sup>22</sup>. The mechanisms of high atherogenicity of DM are incompletely understood. Although diabetic arteriosclerosis has a common base with non-DM, undoubtedly hyperglycemia is a determining factor in the acceleration and severity of the atherogenic process<sup>18</sup>.

Differences in the size of different lipoprotein subfractions have been demonstrated in patients with DM1, especially in women, although these have not been correlated with parameters of subclinical atherosclerosis<sup>23</sup>. Regarding the predictive capacity of CVD of different lipoproteins in DM1, the number of VLDL and large and medium HDL particles independently predict the risk of future CV events<sup>24</sup>. On the other hand, a typical feature of DM2 – as well as obesity, insulin resistance and the metabolic syndrome – is atherogenic dyslipidemia (AD), which has emerged as an important risk factor for CVD<sup>25,26</sup>. AD consists of a triad of increased blood concentrations of small and cholesterol-depleted LDL particles, decreased HDL-c levels and increased total triglycerides. In these patients, with DM2 and AD,

advanced lipoprotein analysis can definitely contribute to identify the patients with an increased risk attributable to the presence of lipoprotein abnormalities, such as a shift between large and small LDL and HDL lipoprotein subclasses: DM2 patients with AD have a lower number of medium and large LDL and HDL particles than patients without AD. Patients with DM2 and AD also have a higher total number of LDL-p and, particularly, the small LDL subclass<sup>27</sup>.

Despite the advances, there are still important gaps in the knowledge of diabetic atherosclerosis. The specific contribution of hyperglycemia per se to lipid metabolism disorders potentially implicated in atherogenesis is only partially known, and new markers of atherosclerosis are needed to improve the risk stratification, the patients treatment and the prevention strategies.

#### **Modifiable Factors**

Reduction in LDL-c levels has been shown to reduce the risk of coronary artery disease (CAD) and death. Currently, statins are the agents primarily used to lower LDL-c. Statin efficacy has been proven both in patients with cardiovascular (CV) and cerebrovascular disease in secondary prevention, and in high CV risk patients in primary prevention<sup>28,29</sup>. In the presence of additional CV risk factors, achieving low density lipoprotein (LDL) concentration below 70 mg/dl is recommended<sup>30</sup>. Despite the widespread use of statin therapy, alone or in combination with other agents, many individuals do not achieve LDL-c goals and the rates of CV events and mortality remain high<sup>31</sup>. Therefore, a number of new therapies have been developed which rely on novel mechanisms to further lower LDL-c in patients with high risk for CAD,

## Chapter 1

including mipomersen, inhibitors of PCSK9, inhibitors of cholesteryl ester transfer protein (CETP) and lomitapide<sup>32</sup>. Additional therapies, such as nicotinic acid, fenofibrate and ezetimibe, which also lower LDL-c, often serve as adjunctive therapies. The role of nicotinic acid and fenofibrates for the primary and secondary prevention of CVD is limited although these agents can improve a patient's lipid profile, their effects on clinical outcomes are often neutral or restricted to subgroups of subjects<sup>33,34</sup>.

However, even if the LDL-c target is achieved, an important residual risk remains. A portion of this residual risk has been attributed to lipid and lipoprotein profile alterations. Evidence suggests that coronary heart disease risk is increased by larger very-low-density lipoprotein (VLDL) particle sizes, smaller HDL and LDL particle sizes, and increased concentration of small LDL and large VLDL particles; although the ideal lipoprotein profiles for the prevention of coronary heart disease may vary according to age, gender and health status<sup>10,35</sup>.

A variety of non-pharmacological factors can also modulate the lipoprotein profile, including dietary habits<sup>36,37</sup> and physical exercise<sup>38</sup>. A diet rich in fatty acids such as palmitic acid is associated, in comparison with a diet rich in oleic acid, to a higher concentration in blood and muscle of ceramides (metabolites of sphingomyelin), lipid species related to insulin resistance<sup>39</sup>. In addition, a complex carbohydrate-rich intake supplemented with long-chain polyunsaturated fatty acids is associated with a decrease in triglycerides and free fatty acids in blood; in the same way, several experimental studies have found omega 3 fatty acids to act as a pleiotropic agent which beneficially influences a

number of cardiometabolic risk factors including anti-arrhythmic effects<sup>40</sup>, blood pressure<sup>41</sup>, thrombosis, inflammation<sup>42</sup>, vascular reactivity and lipids<sup>43,44</sup>, although their contribution on the CV risk reduction remains unclear.

The proper evaluation of the cardiometabolic status of the patients, as well as the evaluation of pharmacological and nutritional interventions, could guide clinicians to design and achieve better preventive strategies. However, atherosclerosis develops in an underlying way and early diagnosis and effective prediction are difficult. For this reason, one of the great challenges of cardiovascular medicine is to find a way to predict individual's risk of suffering a cardiovascular accident and to detect the presence of subclinical atherosclerosis.

Conventional lipid analysis only provides information on the total amount of cholesterol in each of the lipid fractions. However, they do not report on individual characteristics of lipid-carrying lipoproteins. As the lipoprotein profile reflects part of the complexity of the metabolism, it is necessary to learn beyond the lipid content. Advanced lipoprotein test adds information about the etiology of lipoprotein metabolism and function, helps to properly characterize the patient's dyslipidemic phenotype, aids clinical decisions and can guide appropriate therapy<sup>15</sup>.

Nuclear magnetic resonance (NMR) spectroscopy is a technique that allows the characterization of complete lipoprotein profile (VLDL, LDL and HDL), including the particle number, size and lipidic content, in a high throughput way, necessary to be used in clinics<sup>15</sup>.

## Chapter 1

Therefore the exhaustive analysis of the profile of lipoproteins by NMR, an advanced lipoprotein test, results in a promising tool for early diagnosis of these diseases.

Different scientific publications support this fact: recent cost-effectiveness studies conducted in the clinical practice in the USA have concluded that the inclusion of these tests for the risk evaluation and the LDL-lowering therapy guidance by using the LDL-P parameter (and not the LDL-C) have demonstrated to be cost effective, with greater clinical and economic benefit seen over longer time horizons and with increased use of generic statins<sup>45,46</sup>.

Recently, the research group in which the present thesis has been developed has patented and validated the Liposcale test, an advanced lipoprotein test based on diffusion ordered NMR spectroscopy (DOSY-NMR) that measures the size, the lipid content and the number of the particles of the main types of lipoprotein (VLDL, LDL and HDL) and the concentration of particles of nine subtypes (large, medium and small of each main type). The Liposcale test is technologically innovative because it is based on the physical sizes of the particles thanks to 2D nuclear magnetic resonance spectroscopy. This approach allows to directly measure the size of the lipoproteins providing more accurate results than the commercial alternatives<sup>27</sup>.

## **1.2 Motivation**





The doctoral thesis presented in this document is the result of the research conducted in the Department of Electronic, Electrical and Automation Engineering at the Rovira i Virgili University (URV) in collaboration with the Metabolomics Platform of the same university, the Research Unit of Lipids and Atherosclerosis (URLA) of Sant Joan University Hospital from Reus (HUSJR), the CIBER of Diabetes and Metabolic Diseases (CIBERDEM), the Institut d'Investigació Sanitària Pere Virgili (IISPV) and the Spin-off company Biosfer Teslab, co-founded and lead (since 2015) by the PhD candidate. Complementary, part of the research presented in this document was conducted in the Cardiovascular Disease Unit of the Division of Preventive Medicine of the Brigham and Women's Hospital, a Harvard Medical School Affiliate.

Thanks to this collaboration it was possible to develop and consolidate a methodology to get insight the lipoprotein metabolism through the whole and fractioned human plasma analysis by using NMR. In particular, the study of the metabolism by the Liposcale test, an advanced lipoprotein test based on NMR spectroscopy patented and developed by our research group. The use of NMR for the human plasma analysis is aimed at obtaining a better characterization of plasma lipoproteins, i.e. lipid content, size, particle number and particle distribution, in order to improve cardiometabolic characterization for cardiovascular risk assessment.

As a consequence of developing the Liposcale test, opportunity and need of constituting a company arise to, firstly, finish the industrialization process of the test; secondly, to construct the regulatory and quality environment in order to make it available to

## Chapter 1

society through the commercialization and; finally, to collaborate with other research institutions to generate scientific evidences to facilitate the incorporation of the advanced lipoprotein test for clinical applications. Thus, Biosfer Teslab S.L., a spin-off of the Rovira i Virgili University (URV) and the Pere Virgili Health Research Institute (IISPV) was founded in December 2013 in Reus (Tarragona). Its creation comes from the results obtained during the research of Dr. Roger Mallol Parera and part of the results presented in this thesis in relation of the lipoprotein characterization by NMR.

It is remarkable how far the company has come since created. In three years, the Biosfer team has achieved industrial development of the first test (Liposcale) created in a pure research framework. It has also overcome regulatory barriers to achieve CE certification for the current Liposcale lipoprotein test and the approval by the Spanish Agency of Medicine and Medical Devices (AEMPS) for manufacture of medical software for *in-vitro* diagnostic applications. Finally, Biosfer has establish solid research collaborations which have generated different research articles summarized in this doctoral thesis.

Despite being a newly created company, Biosfer Teslab has obtained a good evaluation in four competitive tenders for its projects in Innovation and Development:

- Two Torres Quevedo grants from the Ministry for recruitment of Doctors in private enterprise (2014 and 2017).
- ENISA loan guaranteeing the company's structural capacity (December 2015).

- Aid for development of a project at the territorial level by the Government of Catalonia (NUCLIS, financed by Acció10, Generalitat de Catalunya, January 2016).
- Neotec-CDTI Aid, financed by CDTI (Ministry of Economy, Spain) for development of new *in-vitro* diagnostic tests based on NMR for early detection of cardiometabolic disease (February 2017).

Biosfer Teslab has also been awarded by an international business acceleration program, The Big Booster, during which the PhD candidate took part in a prestigious MassChallenge program in the R&D capital of the health sector in USA (Boston).

Reinforcing the innovative value of the company, since August 2014, Products and Technology (P&T) (a subsidiary of the Catalan pharmaceutical company Laboratorios Rubió) had become part of Biosfer's capital stock, enabling the industrial development and the introduction of new diagnostic tests in the clinic through a more consolidated business infrastructure, knowledge of the market and an extensive commercial network.

Biosfer Teslab signed also different agreements of clinical and scientific collaboration. Biosfer collaborates with the Spanish Nephrology Society, with the Spanish Arteriosclerosis Society and with the Institute of Health Research (INCLIVA) of Valencia, with the will to continue innovating and allowing the NMR to be a clinical tool of value for the improvement of personalized medicine.

This thesis has generated different scientific publications which will be detailed in the next sections regarding to lipoprotein profiling and monitoring by using, mainly, the NMR technology complemented by

## Chapter 1

other biophysical techniques -Atomic Force Microscopy (AFM) and spectrofluorimetry- as well as two patents that have been filled in 2014 to the European Patent Office (EPO) and, recently, to Patent Cooperation Treaty (PCT).

### **1.3 Hypothesis and objectives**



The constant growth of analytical techniques applied in the medical field over the last years is an undeniable fact that indicates the importance of collaborating between interdisciplinary projects, as an ideal environment to provide clinicians with better tools for clinical diagnostics. In particular, determination of lipoprotein particle size and number using advanced lipoprotein tests (ALTs) is of particular importance to improve cardiovascular risk prediction and evaluation of the metabolic state.

The research presented in this thesis is based, mainly, on the lipoprotein characterization by NMR spectroscopy for cardiometabolic risk evaluation and monitoring.

The application of the NMR lipoprotein profile characterization has allowed to explore lipoprotein properties beyond lipid content from complementary perspectives: NMR allows advancement of knowledge of the molecular lipoprotein structure favoring to understand their functionality in processes that deal with metabolic disorders; makes possible the evaluation of different types of interventions, both pharmacological and nutritional; and, finally, provides analysis of large sets of samples enabling epidemiological study of the lipoprotein profile associated with concrete life habits.

In this context, the objectives of this thesis have been:

1. Mastering of the use of Nuclear magnetic field (NMR) for lipoprotein characterization beyond lipid content and its application in the characterization of cardiometabolic risk.

2. Approaching the Lipoprotein structure and lipid composition. Application of biophysical techniques to explore abnormal lipoprotein

## Chapter 1

subclasses altered in diseases, such as size, particle lipid distribution and surface properties.

3. Evaluating pharmacological and nutritional interventions through the lipoprotein profile and assessment of changes in metabolism.



## **1.4 Organization of the document**



This chapter has provided a general overview of the background and motivation for the realization of this thesis. The need for better predictors of cardiovascular disease is increasing due to the pandemic levels which metabolic disorders are achieving. One of the main areas where new biomarkers can be looked for is the area of lipids and lipoproteins. For this purpose, NMR spectroscopy appears to be a suitable analytical tool to develop novel methodologies, which will aid in the assessment and management of cardiovascular events.

**Chapter 2** presents a state of the art of the lipoprotein characterization by NMR, from a research framework to the clinical practice. In the first section of the chapter, the lipoprotein classification and metabolism are described as well as the standard methods for lipoprotein quantification. In the second section, different strategies for the lipoprotein characterization by using 1 and 2-dimensional NMR methodologies are briefly explained. The third section includes the patent of the Liposcale lipoprotein characterization. Finally, the final two sections include the industrial development that the company Biosfer has carried out for the implementation of the Liposcale test into the clinical practice and the main studies in which the PhD candidate has participated since the creation of the company.

**Chapter 3** focuses on the use of lipoproteins as biomarkers beyond their lipidic content for the evaluation and monitoring of the HDL subclass in the diabetic dyslipemia. By using NMR and complementary biophysical techniques -such as AFM and spectrofluorimetry- a new mathematical model for HDL structure is stated accordingly to the NMR derived parameters and biochemical

## Chapter 1

composition. The HDL size determines the structure which modulates the final function of lipoproteins particles.

**Chapter 4** describes how nutrition and, in particular, the fish consumption and total n-3, and the main n-3 subtypes: eicosapentaenoic (EPA), docosahexaenoic (DHA) and alpha-linolenic (ALA) fatty acids, modulates the lipoprotein profile in an epidemiological association study and two nutritional interventions.

**Chapter 5** discusses the current use of the DOSY  $^1\text{H}$ -NMR based on lipoprotein characterization for clinical applications and the perspectives for its use in the near future in different contexts and, particularly, for the study of the structure and composition of the HDL subfraction. Finally, the chapter summarizes the main results and conclusions derived from the NMR experiments for the study of metabolism presented in this thesis.

## **1.5 References**



1. Go, A. S. *et al.* Heart Disease and Stroke Statistics--2013 Update: A Report From the American Heart Association. *Circulation* **127**, e6--e245 (2013).
2. Gerszten, R. E. & Wang, T. J. The search for new cardiovascular biomarkers. *Nature* **451**, 949–952 (2008).
3. Brunzell, J. D. *et al.* Lipoprotein Management in Patients With Cardiometabolic Risk. *J. Am. Coll. Cardiol.* **51**, 1512–1524 (2008).
4. Gupta, A. *et al.* Carotid plaque MRI and stroke risk: a systematic review and meta-analysis. *Stroke* **44**, 3071–3077 (2013).
5. Honda, O. *et al.* Echolucent carotid plaques predict future coronary events in patients with coronary artery disease. *J. Am. Coll. Cardiol.* **43**, 1177–1184 (2004).
6. Sachdeva, A. *et al.* Lipid levels in patients hospitalized with coronary artery disease: An analysis of 136,905 hospitalizations in Get With The Guidelines. *Am. Heart J.* **157**, 111--117.e2 (2009).
7. Jiang, R. *et al.* Non-HDL cholesterol and apolipoprotein B predict cardiovascular disease events among men with type 2 diabetes. *Diabetes Care* **27**, 1991–1997 (2004).
8. Mallol, R., Rodriguez, M. A., Brezmes, J., Masana, L. & Correig, X. Human serum / plasma lipoprotein analysis by NMR : Application to the study of diabetic dyslipidemia. (2012). doi:10.1016/j.pnmrs.2012.09.001
9. Otvos, J. D. *et al.* Low-Density Lipoprotein and High-Density Lipoprotein Particle Subclasses Predict Coronary Events and Are Favorably Changed by Gemfibrozil Therapy in the Veterans Affairs High-Density Lipoprotein Intervention Trial. *Circulation* **113**, (2006).
10. Cromwell, W. C. *et al.* LDL Particle Number and Risk of Future Cardiovascular Disease in the Framingham Offspring Study - Implications for LDL Management. *J. Clin. Lipidol.* **1**, 583–92 (2007).
11. Mora, S. *et al.* LDL particle subclasses, LDL particle size, and carotid atherosclerosis in the Multi-Ethnic Study of Atherosclerosis (MESA). *Atherosclerosis* **192**, 211–217 (2007).
12. Reiner, Z. *et al.* ESC/EAS Guidelines for the management of dyslipidaemias: The Task Force for the management of dyslipidaemias of

## Chapter 1

the European Society of Cardiology (ESC) and the European Atherosclerosis Society (EAS). *Eur. Heart J.* **32**, 1769–1818 (2011).

13. Piepoli, M. F. *et al.* 2016 European Guidelines on cardiovascular disease prevention in clinical practice. *Eur. J. Prev. Cardiol.* **23**, NP1--NP96 (2016).

14. Kontush, A. HDL particle number and size as predictors of cardiovascular disease. *Front. Pharmacol.* **6**, 218 (2015).

15. Mora, S. *et al.* Lipoprotein Particle Profiles by Nuclear Magnetic Resonance Compared With Standard Lipids and Apolipoproteins in Predicting Incident Cardiovascular Disease in Women. *Circulation* **119**, 931–939 (2009).

16. Mackey, R. H. *et al.* High-Density Lipoprotein Cholesterol and Particle Concentrations, Carotid Atherosclerosis, and Coronary Events. *J. Am. Coll. Cardiol.* **60**, 508–516 (2012).

17. Mora, S., Glynn, R. J. & Ridker, P. M. HDL cholesterol, size, particle number, and residual vascular risk after potent statin therapy. *Circulation* (2013).

18. The Emerging Risk Factors Collaboration. Diabetes mellitus, fasting blood glucose concentration, and risk of vascular disease: a collaborative meta-analysis of 102 prospective studies. *Lancet* **375**, 2215–2222 (2010).

19. Lind, M. *et al.* Glycemic Control and Excess Mortality in Type 1 Diabetes. *N. Engl. J. Med.* **371**, 1972–1982 (2014).

20. Malmberg, K. *et al.* Impact of Diabetes on Long-Term Prognosis in Patients With Unstable Angina and Non-Q-Wave Myocardial Infarction. *Circulation* **102**, (2000).

21. Burke, A. P. *et al.* Morphologic Findings of Coronary Atherosclerotic Plaques in Diabetics. *Arterioscler. Thromb. Vasc. Biol.* **24**, (2004).

22. Coleman, R. L., Stevens, R. J., Retnakaran, R. & Holman, R. R. Framingham, SCORE, and DECODE Risk Equations Do Not Provide Reliable Cardiovascular Risk Estimates in Type 2 Diabetes. *Diabetes Care* **30**, (2007).



23. Colhoun, H. M. *et al.* Lipoprotein Subclasses and Particle Sizes and Their Relationship With Coronary Artery Calcification in Men and Women With and Without Type 1 Diabetes. *Diabetes* **51**, (2002).
24. Soedamah-Muthu, S. S., Chang, Y.-F., Otvos, J., Evans, R. W. & Orchard, T. J. Lipoprotein subclass measurements by nuclear magnetic resonance spectroscopy improve the prediction of coronary artery disease in Type 1 Diabetes. A prospective report from the Pittsburgh Epidemiology of Diabetes Complications Study. *Diabetologia* **46**, 674–682 (2003).
25. Mooradian, A. D. Dyslipidemia in type 2 diabetes mellitus. *Nat. Rev. Endocrinol.* (2009).
26. Chapman, M. J. *et al.* Triglyceride-rich lipoproteins and high-density lipoprotein cholesterol in patients at high risk of cardiovascular disease: evidence and guidance for management. *Eur. Heart J.* **32**, 1345–61 (2011).
27. Mallol, R. *et al.* Liposcale: a novel advanced lipoprotein test based on 2D diffusion-ordered <sup>1</sup>H-NMR spectroscopy. *J. Lipid Res.* **56**, 737–746 (2015).
28. National Cholesterol Education Program (NCEP) Expert Panel on Detection, Evaluation, and Treatment of High Blood Cholesterol in Adults (Adult Treatment Panel III). Third Report of the National Cholesterol Education Program (NCEP) Expert Panel on Detection, Evaluation, and Treatment of High Blood Cholesterol in Adults (Adult Treatment Panel III) final report. *Circulation* **106**, 3143–421 (2002).
29. Smith, S. C. *et al.* AHA/ACCF Guideline AHA/ACCF Secondary Prevention and Risk Reduction Therapy for Patients With Coronary and Other Atherosclerotic Vascular Disease: 2011 Update A Guideline From the American Heart Association and American College of Cardiology Foundation. *Circulation* **124**, 2458–73 (2011).
30. Perk, J. *et al.* European Guidelines on cardiovascular disease prevention in clinical practice (version 2012): The Fifth Joint Task Force of the European Society of Cardiology and Other Societies on Cardiovascular Disease Prevention in Clinical Practice (constituted by representatives of nine societies and by invited experts) \* Developed

## Chapter 1

with the special contribution of the European Association for Cardiovascular Prevention & Rehabilitation (EACPR). *Eur. Heart J.* **33**, 1635–1701 (2012).

31. Waters, D. D. *et al.* Lipid Treatment Assessment Project 2: A Multinational Survey to Evaluate the Proportion of Patients Achieving Low-Density Lipoprotein Cholesterol Goals. *Circulation* **120**, 28–34 (2009).

32. Noto, D., Cefalù, A. B. & Averna, M. R. Beyond Statins: New Lipid Lowering Strategies to Reduce Cardiovascular Risk. *Curr. Atheroscler. Rep.* **16**, 414 (2014).

33. Investigators, T. A.-H. Niacin in Patients with Low HDL Cholesterol Levels Receiving Intensive Statin Therapy. *N. Engl. J. Med.* **365**, 2255–2267 (2011).

34. Group, T. A. S. Effects of Combination Lipid Therapy in Type 2 Diabetes Mellitus. *N. Engl. J. Med.* **362**, 1563–1574 (2010).

35. Carmena, R., Duriez, P. & Fruchart, J.-C. Atherogenic Lipoprotein Particles in Atherosclerosis. *Circulation* **109**, III-2-III-7 (2004).

36. Li, Z. *et al.* Human Nutrition and Metabolism Fish Consumption Shifts Lipoprotein Subfractions to a Less Atherogenic Pattern in Humans 1. *J. Nutr* **134**, 1724–1728 (2004).

37. Bogl, L. H. *et al.* Association between habitual dietary intake and lipoprotein subclass profile in healthy young adults. *Nutr. Metab. Cardiovasc. Dis.* **23**, 1071–8 (2013).

38. Ahmed, H. M., Blaha, M. J., Nasir, K., Rivera, J. J. & Blumenthal, R. S. Effects of Physical Activity on Cardiovascular Disease. *Am. J. Cardiol.* **109**, 288–295 (2012).

39. Kien, C. L. *et al.* A Lipidomics Analysis of the Relationship Between Dietary Fatty Acid Composition and Insulin Sensitivity in Young Adults.

40. Reiffel, J. A. & McDonald, A. Antiarrhythmic Effects of Omega-3 Fatty Acids. *Am. J. Cardiol.* **98**, 50–60 (2006).

41. Geleijnse, J. M., Giltay, E. J., Grobbee, D. E., Donders, A. R. T. & Kok, F. J. Blood pressure response to fish oil supplementation:

- metaregression analysis of randomized trials. *J. Hypertens.* **20**, 1493–9 (2002).
42. Goodfellow, J., Bellamy, M. F., Ramsey, M. W., Jones, C. J. & Lewis, M. J. Dietary supplementation with marine omega-3 fatty acids improve systemic large artery endothelial function in subjects with hypercholesterolemia. *J. Am. Coll. Cardiol.* **35**, 265–70 (2000).
43. Saravanan, P., Davidson, N. C., Schmidt, E. B. & Calder, P. C. Cardiovascular effects of marine omega-3 fatty acids. *Lancet* **376**, 540–550 (2010).
44. Okuda, Y. *et al.* Eicosapentaenoic Acid Enhances Nitric Oxide Production by Cultured Human Endothelial Cells. *Biochem. Biophys. Res. Commun.* **232**, 487–491 (1997).
45. Rizzo, J. A. *et al.* Managing to low-density lipoprotein particles compared with low-density lipoprotein cholesterol: a cost-effectiveness analysis. *J. Clin. Lipidol.* **7**, 642–52 (2006).
46. Grabner M, Winegar DA, Punekar R, Quimbo RA, Cziraky M, Cromwell W. Cost Effectiveness of Achieving Targets of Low-Density Lipoprotein Particle Number Versus Low-Density Lipoprotein Cholesterol Level. *Am J Cardiol.* 2017;119(3):404-409.



**Chapter 2. State of the art. Lipoprotein analysis by  $^1\text{H}$ -NMR and its clinical relevance**



## **2.1 Lipoproteins, metabolism and standard quantification methods**





Lipoproteins are important constituents of the lipid fraction of the human body, which function as carriers for water-insoluble lipids through the aqueous bloodstream. Lipoproteins vehicles provide the active mobilization of endogenous and exogenous (dietary) lipids through the aqueous compartments within the cells, as well as in the blood and body tissues where lipid molecules can be either stored (i.e. adipose tissue) or used as energy source<sup>1</sup>.

The general structure of lipoprotein molecules is spherical and they are synthesized within the liver and intestines. Non-polar lipids (triacylglycerols and cholesterol esters) are mainly found within the core, while polar lipids (phospholipids and free cholesterol) are distributed through a surface monolayer together with the protein component (named as apolipoproteins or apoproteins), a group of proteins of immense structural diversity, that define the structure, metabolism and functionality of a given lipoprotein class, as well as its interaction with receptor molecules or different enzymes in the liver and peripheral tissues<sup>1</sup>.

Based on their buoyant densities, lipoproteins can be classified in five major groups: Chylomicrons (CM), Very Low Density Lipoproteins (VLDL), Intermediate Density Lipoproteins (IDL), Low Density Lipoproteins (LDL), and High Density Lipoprotein (HDL) with CM being the biggest and least dense lipoproteins particle.

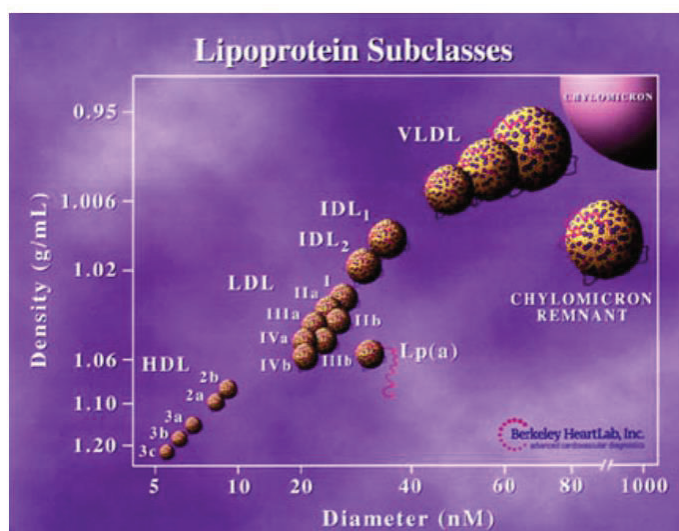


**Figure 1.** Lipoprotein subclasses<sup>2</sup>.

Each of these lipoprotein classes can be further divided into several subclasses, but the number and nomenclature is method-dependent, since the density of lipoproteins is really a continuum, not discrete values corresponding to a finite number of classes.

Chylomicrons transport triglycerides and esterified cholesterol formed by dietary lipids (such as free fatty acids, monoglycerides and free cholesterol) being processed. In addition to cholesterol absorbed from the diet, they may also receive new cholesterol synthesized in the gut and cholesterol transferred from other lipoproteins. Chylomicrons are rich in triglycerides. However, while tissues take up fatty acids and glycerol from released and hydrolyzed core triglycerides, as the circulating chylomicrons become progressively smaller, their triglyceride content decreases and they become relatively richer in cholesterol and protein. They become what is known as a chylomicron remnant. VLDLs are secreted by the liver to supply triglycerides to tissues in the fasting or postprandial state. VLDL particles are slightly smaller than

chylomicrons and they undergo exactly the same lipid release process described for chylomicrons. The loss of triglycerides converts some VLDL into IDL and LDL, which are the main cholesterol transporters<sup>2</sup>.

HDL are the most diverse lipoproteins. They are synthesized in the liver and small intestine as protein-rich, disc-shaped particles containing ApoA1 and phospholipids. These particles mature by the acquisition of cholesterol from peripheral tissues and the action of several esterifying enzymes (LCAT)<sup>3</sup>.

The HDL particles make it possible for cholesterol to flow out of the cells, esterify in plasma, transfer to other lipoproteins and return to the liver for excretion, a process known as reverse cholesterol transport. The HDL mediation of the transfer of lipids and apolipoproteins between lipoprotein classes also plays a key role in the overall lipoprotein metabolism.

**Table 1:** List of the origin, function and composition of the main lipoproteins<sup>2</sup>.

	Origin	Density	APO	Percentage %				Function
				Chol	TG	Prot	PL	
<b>CM</b>	Intestine	<0.950	A, B, C, E	4	90	1	5	Exogenous lipids transport (from intestine to cells)
<b>VLDL</b>	Liver	0.950-1.006	B, C, E	25	55	8	12	Endogenous lipids transport (from liver to cells)
<b>LDL</b>	VLDL via IDL	1.019-1.063	B	55	5	20	20	Cholesterol transport to cells
<b>HDL</b>	Intestine, liver	1.063-1,210	A, C, E, J...	20	5	50	25	Cholesterol transport from cells to liver

## Chapter 2

Lipoproteins fractionation and quantification is a matter of primary interest in the field of clinical medicine since elevated concentrations of cholesterol and triglycerides, in specific lipoproteins, have been associated with significantly increased occurrence of cardiovascular diseases (CVDs)<sup>4</sup>.

Studies on lipoprotein metabolism have shown a highly consistent and direct correlation between plasma LDL and the development of atherosclerosis<sup>4</sup>. Even though such epidemiological investigations have shown a positive correlation between total cholesterol concentrations in LDL and Coronary Heart Disease (CHD) mortality, total LDL cholesterol does not accurately predict the risk of CHD in many patients<sup>5</sup>. The LDL/HDL cholesterol ratios, the LDL particle number or the Non-HDL cholesterol are nowadays considered risk indicators with greater predictive value than single parameters, such as LDL<sup>6</sup> cholesterol. Due to their role on reverse cholesterol transport, HDL prevent the formation of atherosclerotic plaques that may derive from LDL metabolism and thus represent a non-casual integrative marker of CVDs<sup>7</sup>. Moreover, it has been proven that individuals with predominantly small LDL particles experience greater CHD risk than those with large-size LDL<sup>8</sup>, making accurate quantification of the lipoproteins subfractions an essential screening tool for CVDs prevention and diagnosis.

Several analytical approaches can be used for accurately measuring blood lipoproteins, such as gel electrophoresis and Gel-Permeation High Performance Liquid Chromatography (GP-HPLC), but density gradient Ultra-Centrifugation (UC) represents the “gold standard

method” for lipoproteins isolation and quantification. A brief description of standard quantification methods is detailed below:

*Ultracentrifugation.* The UC technique is often described as the benchmark method for lipoproteins measurement which has become a routine method for lipoproteins separation<sup>9</sup>. Separation of CM, VLDL, LDL, and HDL is obtained by adjusting the density of the medium at each centrifugation step in order to allow sequential floatation of the individual lipoprotein fractions. A discontinuous gradient is then created and layers of solvents with different densities will cause the lipoproteins of different densities to be isolated in a cumulative fashion. The main disadvantage is that, due to long spin times, complete separation of all lipoprotein fractions may require from 2 to 5 days of centrifugation time which seriously limits the applicability of the method as a rapid individualized monitoring tool and naturally in large epidemiological studies<sup>10</sup>.

In order to reduce the experiment time, several improvements in the UC equipment have been introduced. Amongst these, the Vertical Auto Profiling (VAP) method allows lipoproteins to be separated in a single spin by using high centrifugal speeds (65,000 rpm, 1 hour)<sup>11</sup>. This is achieved by using a vertical rotor in which the centrifuge tube remains perpendicular to the x-axis (ground) during centrifugation. This set-up will allow the lipoproteins separation across the shorter horizontal axis of the centrifuge. After centrifugation, all five lipoprotein fractions are analyzed for cholesterol content using the continuous flow VAP analyzer: every lipoprotein layer is mixed with a specific reagent for cholesterol connected to a spectrophotometric cholesterol detector.

## Chapter 2

*Gel-Permeation High Performance Liquid Chromatography.* GP-HPLC is used to separate lipoproteins on the basis of the particle diameter, with small particles exhibiting a longer elution time than the big ones. The particle diameter of the lipoproteins is calibrated using stained lipoprotein standards with a known diameter whose size can be determined by gel gradient electrophoresis, dynamic light scattering or electron microscopy<sup>12</sup>. The elution position of the lipoproteins is derived from the relationship of calibration standards and its retention time. GP-HPLC can be coupled with enzymatic assays for lipid quantification<sup>12</sup>.

*Gel Electrophoresis.* Gel electrophoresis is a method for macromolecules separation and analysis based on their size and charge. The lipid concentrations per main lipoprotein class are calculated using peak integration. Gradient GE using nondenaturing conditions is commonly used to characterize the distribution of particles with very small differences in size<sup>13</sup>.

Nevertheless, lipoproteins analysis by the previous standard techniques are time consuming and labour intensive as they require numerous sample handlings, and specific enzymatic assays are needed to further estimate their composition<sup>10</sup>.

High-field proton Nuclear Magnetic Resonance (<sup>1</sup>H-NMR)-based lipoprotein profiling has proven to be a valuable alternative to the standard lipoprotein quantification methods. <sup>1</sup>H-NMR, which is normally used for structure elucidation and chemical mixture quantifications, has one more advantage, namely that it is sensitive to the size (rotational diffusion), density of macromolecules and supramolecular aggregates as well as the lipid concentration<sup>14</sup>. This makes NMR a unique platform for

investigating lipoprotein particle profiles because different lipoproteins fractions and subfractions have different magnetic susceptibilities which will broadcast different signals whose amplitude reflects particles concentration. On the other hand, minimum sample handling, non-destructive, fast and automatable features make  $^1\text{H-NMR}$  spectroscopy a preferable/valuable screening tool for clinical practice as well as for large scale epidemiological investigation.





## **2.2 Serum/Plasma lipoprotein analysis by $^1\text{H}$ -NMR spectroscopy**



$^1\text{H}$ -NMR spectroscopy has become an indispensable technique for characterization of complex biological samples such as tissues and body fluids<sup>15</sup>. In particular, due to the possibility of conducting phase transitional studies, the use of  $^1\text{H}$ -NMR spectroscopy has emerged as a valuable screening tool for lipoproteins in plasma and serum samples<sup>16-18</sup>. The lipids inside the lipoproteins exist as liquid crystals of triglycerides and cholesterol esters whose limited mobility gives rise to the broadening of the NMR signals of the methyl ( $-\text{CH}_3$ ) and methylene ( $-\text{CH}_2-$ ) groups centered around 0.8 and 1.2 ppm, respectively.

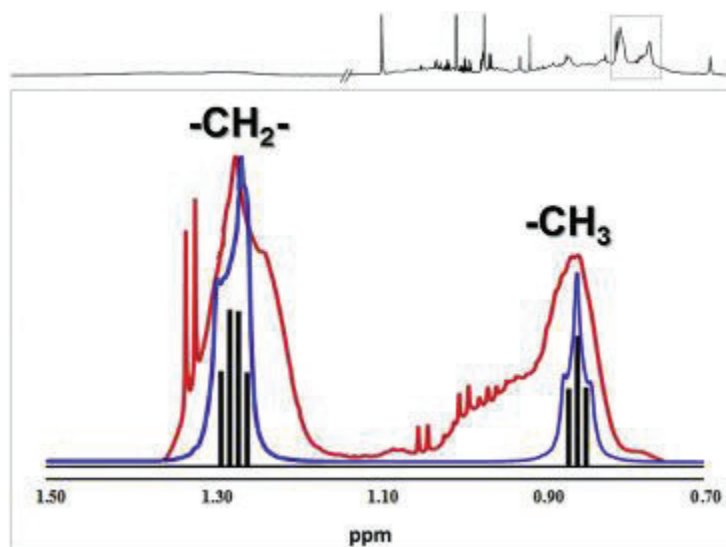


**Figure 1.** Methyl and methylene regions of the NMR plasma spectrum<sup>19</sup>.

The previous figure illustrate the broadening of the pure isolated methyl and methylene signal  $\text{CH}_2\text{-CH}_3$  (black line), pure fat with conformational freedom (blue line) and from the interior of the lipoproteins in a blood plasma sample (red line)<sup>19</sup>.

The main advantage of using NMR spectroscopy for the identification and quantification of lipoproteins is due to the fact that different lipoprotein fractions and subfractions have different chemical

## Chapter 2

compositions and sizes and therefore experience slightly different magnetic susceptibilities. This gives rise then to distinctive NMR signals whose chemical shift is mainly determined by the local electron density, and rotational diffusion of the lipoprotein vehicles. In particular, the methyl (-CH<sub>3</sub>) signals arising from large and less dense lipoproteins particles (i.e. VLDL and LDL) are different in shape and resonate at lower field strength (higher frequency) than the lipid signals emitted by smaller lipoproteins (i.e. HDL)<sup>20</sup>.

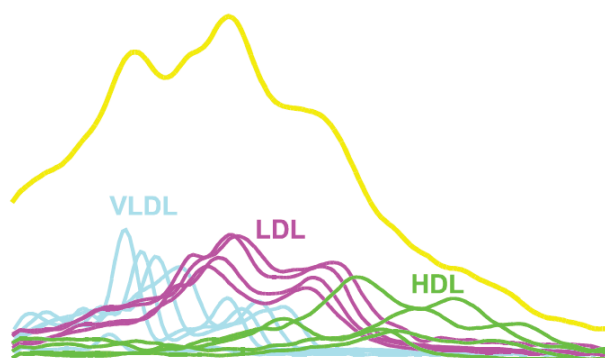


**Figure 2.** Size depending chemical shift. Adapted from: Spectroscopic Approach to Lipoprotein Subclass Analysis. J. Otvos et al., **JCLA**, 1996.

A typical NMR spectrum of plasma/serum is characterized by the presence of numerous metabolites (i.e. amino acids, organic acids), macromolecules (i.e. proteins) and lipoproteins whose signals are heavily overlapped. The entire up-field signal from about 0.6 to 1.4 ppm can be used for lipoprotein quantifications, but in many cases only the methyl signal envelope at approximately 0.8 ppm is used<sup>21,22</sup>. The latter band contains the distinctive signals emitted by the terminal methyl group protons of phospholipids, cholesterol, cholesterol esters and triglycerides from the different lipoprotein main fractions and all the subfractions. The individual amplitudes of the NMR signals are directly

proportional to the concentration of the lipoprotein particles giving NMR spectroscopy the unique capability of identifying and quantifying blood lipoproteins.

Several  $^1\text{H-NMR}$  based protocols for lipoproteins fractions and subfractions identification and measurement have been developed. Amongst these, the commercial assays NMR LipoProfile<sup>®</sup> (LipoScience Inc., now Labcorp)<sup>21</sup>, AXINON<sup>®</sup> lipoFIT<sup>®</sup> (Numares AG, Regensburg, Germany)<sup>23</sup>, Brainshake-Nightingale Ltd.<sup>24</sup> and the Liposcale test (Biosfer Teslab SL)<sup>25</sup> are considered the pioneers for driving “the lipoprotein analysis by NMR” interest of the clinical and epidemiological community<sup>19</sup>.

### **2.2.1 Sample Handling procedures**

Lipoproteins are heterogeneous particles whose distribution in the blood depends on genotype-specific properties and reflects the dynamic response of the human body to changes in the external conditions (e.g. diet, lifestyle and environment)<sup>26</sup>. The sample handling and preparation steps required before lipoprotein quantification, such as sample collection, storage and sample preparation, can alter the lipoprotein structure by destroying the natural equilibrium of the sample. For this reason, high-throughput protocols and Standard Operating Procedures (SOPs) and Quality Control (QC) criteria have been developed for minimizing as such as possible the inherent variability.

#### **Measurement matrix: serum vs plasma**

Serum and plasma samples are routinely used for lipoprotein measurements. Both fractions derive from blood samples that have

## Chapter 2

undergone different biochemical treatments after collection. In the serum case, coagulation factors (i.e. fibrinogen) along with blood cells are removed by centrifugation, while plasma is typically obtained from blood samples to which an anticoagulant agent (i.e. heparin, citrate or EDTA) is added before the removal of blood cells. The choice of the most appropriate matrix and anticoagulant agent is a crucial point in lipoprotein studies. If the analysis contemplates the use of automated robots for the sample preparation step, the serum samples are the preferred specimens, as its use improves the reliability of the production process eliminating undesired stoppages (as the presence of fibrinogen increases the probability of clogging the robot's injection syringe).

### **Sample handling and storage**

Standardized sample handling and storage conditions are highly important in order to obtain blood samples with stable physical lipoprotein characteristics (i.e. density and size). Due to the rapid increase in the number of studies aimed at biomarker discovery by profiling technologies (i.e. HPLC and NMR spectroscopy) detailed standardized procedures for sample handling and storage have been developed whose analytical and experimental bias have been carefully assessed<sup>27,28</sup>. In particular, in the case of NMR spectroscopy, storage conditions have been shown to be critical and special attention has been paid to address the effect of common sources of analytical bias on serum and plasma profiles in terms of reproducibility and reliability of the obtained results<sup>29</sup>. According to the most recently developed SOPs,

blood serum and plasma samples can be stored for 9 months at  $-80\text{ }^{\circ}\text{C}$  without leading to any significant differences when analyzed<sup>28</sup>.

### **2.2.2 Serum/plasma lipoprotein analysis by 1D $^1\text{H}$ -NMR spectroscopy**

As it was mentioned before, lipoprotein analysis with NMR spectroscopy is based on the depending magnetic susceptibility of the molecules to the particle size: the methyl groups of the lipids traveling within the lipoprotein resonate at a slightly different frequency according to the lipoprotein size, being the lipids carried in smaller particles resonating at lower frequencies as from the internal space (in which the lipids are distributed unstructured) to the particle membrane (in which the lipids are arranged in a radial order) and, therefore, it manifests itself in a general directional dependency of the magnetizability existing a size-depending shield. For larger particles, this results in a lower shielding and consequently a higher chemical shift than for smaller particles. This magnitude is different enough and, therefore, lipoproteins can be quantified through the signal decomposition of the methyl group from the 1-D NMR spectrum into individual signals using basically two different strategies:

The Curve Fitting method and multivariant Partial Least Squares (PLS) regressions<sup>30</sup>. In curve fitting methods, two different approaches have been applied: in the first one, the NMR spectra are fitted with individual lorentzian line shapes while, in the second one, the NMR spectra are fitted with pure line profiles from predetermined lipoprotein subclass spectra. Alternatively, in the case of multivariate PLS

## Chapter 2

regression, it has been applied either in the full spectral version - normally restricted to be from 0.6 to 1.4 ppm- or in the interval based version (*i*PLS) -where the same region is divided into a number of small intervals- which are to be regressed towards the response values of triglycerides and cholesterol, respectively<sup>31</sup>.

The above mentioned methods are outlined in the following figure:

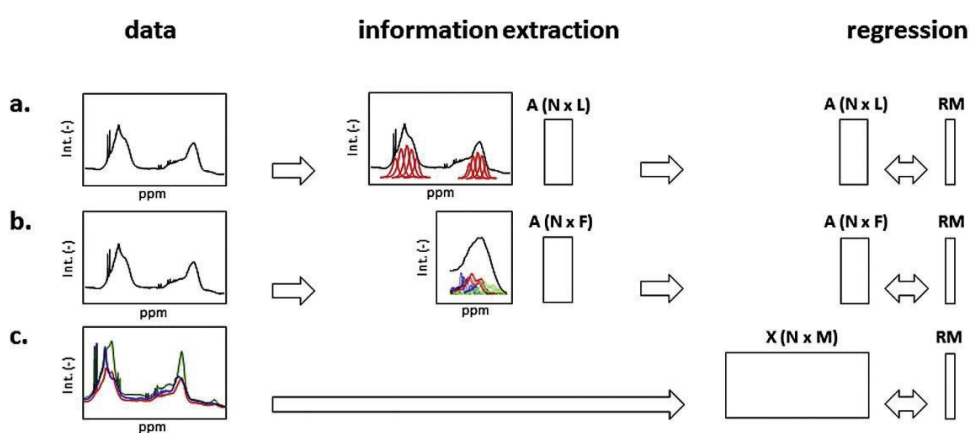


**Figure 3.** Strategies for lipoprotein quantification from 1-D <sup>1</sup>H-NMR Spectra a) Curve fitting using Lorentzian functions; b) Curve fitting using isolated lipoprotein subfractions functions c) PLS regression models. Adapted from Aru *et al.*<sup>19</sup>

The most relevant groups that have developed and applied successfully the previous mentioned strategies to introduce the current commercially available advanced lipoprotein tests will be described below:

### The NMR LipoProfile test

Since the beginning of the 1990s the group led by Professor James Otvos created and perfected the LipoProfile<sup>®</sup> test, which was made commercially available in 1997 by Liposcience Inc (from 2014, acquired by Labcorp). In the first studies reported by Otvos and



colleagues, they described a curve fitting method using isolated lipoprotein subfractions functions for quantifying the particle concentration and mean particle size of different lipoprotein subclasses. First, the main lipoprotein fractions (chylomicrons, VLDL, IDL, LDL and HDL) obtained by sequential ultracentrifugation<sup>32</sup> were used to obtain highly purified lipoprotein subfractions with a range of particle diameters as homogeneous as possible. Agarose gel filtration chromatography was used in combination with ultracentrifugation. The lipid content (cholesterol and triglycerides) of lipoprotein subfractions was measured by standard biochemistry methods and the particle size for the purified VLDL and LDL subclasses were assessed by Transmission Electron Microscopy (TEM). Additionally, non-denaturing gradient gel electrophoresis<sup>33</sup> was used to measure the particle sizes of the LDL<sup>34,35</sup> and HDL<sup>36-38</sup> subfractions. Then, <sup>1</sup>H-NMR spectra were acquired of all plasma and isolated lipoprotein samples on a 400 MHz NMR spectrometer equipped with a flow probe and a sample volume of 120  $\mu$ l. All NMR measurements for lipoprotein analyses were performed at 47 °C, a temperature at which the molecules in the core of the particles have an NMR-isotropic behavior. The basic principle of the method is the specific magnetic behavior of lipoproteins: i.e. lipids in smaller lipoproteins broadcast signals at lower frequencies than lipids in larger ones resulting from the different compositions of the lipoproteins<sup>39,40</sup>. Particle concentrations are obtained by fitting the methyl envelope arising at around 0.8 ppm of the <sup>1</sup>H-NMR spectra of plasma samples. The adjusted curve is calculated using a linear combination of <sup>1</sup>H-NMR spectra from individual lipoprotein subfractions taken from a reference

## Chapter 2

library<sup>20,40</sup> in a linear least squares process<sup>41</sup>. This spectral library of lipoprotein subfractions, measured by <sup>1</sup>H-NMR, is representative of the different subfractions which can be found in human plasma samples of patients with either normolipidemia or dyslipidemia. It is worth mentioning that the area of the methyl envelope is proportional to the number of protons (3) for every methyl termination of the core lipids (i.e. 3 for TG and CE). This means that the amplitude is insensitive to compositional variability in subclasses (cholesterol ester–triglyceride exchange mediated by cholesterol ester transport protein, CETP)<sup>42</sup>.

The mean particle sizes estimated by LipoProfile<sup>®</sup> have been compared with those measured by TEM (VLDL and LDL fractions)<sup>43</sup> and GGE (LDL and HDL fractions)<sup>34–38</sup>. Agreement with GGE was excellent, although some offset differences in mass estimation were found between LDL sizes measured by NMR and TEM. Nowadays, the LipoProfile<sup>®</sup> test is the most commercially spread method which can quickly and accurately give information about the size and particle number of several lipoprotein fractions in plasma (or serum) samples<sup>20,40</sup>. The NMR LipoProfile<sup>®</sup> test<sup>44</sup> has been available in United States hospitals since 1997 for clinical analysis. Since then, millions of analyses have been performed in the LipoScience laboratory in North Carolina, and more than 250 clinical studies have been completed.

### **The Mika Ala-Korpela methodologies**

During the first half of the 1990s, Ala-Korpela and colleagues set up a curve fitting model by using lorentzian functions for deconvoluting the overlapping information in the methyl and methylene peaks of <sup>1</sup>H-NMR spectra of plasma samples<sup>45–47</sup>, measured at the physiological

temperature of 37 °C. In these studies, VLDL, LDL and HDL fractions were modeled by adding three lorentzian components for VLDL and LDL fractions and one for HDL. The approach used for this curve fitting analysis was an in-house algorithm, named as FITPLAC, that mathematically optimized the half-line width, the resonance frequency and the intensity for each lorentzian function, in order to characterize the lipoprotein profile. The model also included background resonances related to residual water, and albumin-bound immobile fatty acids or proteins<sup>46,48</sup>.

The curve fitting analysis of the methyl peak using the FITPLAC algorithm confirmed that the parameters of the lorentzians functions for every fraction were very similar for all the individuals, so the half linewidth and position of every lorentzian was set at a constant value. This indicated that the main variable in the <sup>1</sup>H-NMR spectra of the lipoprotein fractions of different people was the intensity for each lorentzian function (i.e. the fraction concentration). The linear correlation between the fraction areas found by NMR and the concentration values of triglycerides, phospholipids, total cholesterol, free cholesterol, esterified cholesterol, total proteins and total masses of the VLDL, LDL and HDL fractions by biochemistry methods made it possible to estimate their concentration using statistical methods. In particular, correlation coefficients were found to be high (e.g. 0.98, 0.88, and 0.93) in the VLDL triglycerides, LDL cholesterol, and HDL cholesterol, respectively, in plasma samples.

However, curve fitting with multiple lorentzians is an ill-posed problem which is easily influenced by the shapes of the spectra, strongly

## Chapter 2

overlapping peaks and the number of curves to be fitted. In recent applications, the same group solved this problem by applying a Bayesian approach for lipoproteins quantification from  $^1\text{H-NMR}$  spectra<sup>39,49</sup>. By using this methodology, the total concentration of TG and C in serum, as well as VLDL-TG, IDL-C, LDL-C and HDL-C can be quantified. They also reported that they were able to quantify total lipid content, and particle concentrations and size in 14 lipoprotein subclasses, distributed in chylomicrons, 5 VLDL, 1 IDL, 3 LDL and 4 HDL. The lipoprotein size of these subclasses was calibrated with High Performance Liquid Chromatography<sup>50</sup>, although no details about the calibration process were given.

From 2014, the Finnish company Brainshake (since 2017 known as Nightingale Health Ltd.) was established as a serum NMR metabolomics platform that measures more than 200 metabolic measures in a highly automated way. Among their products, they commercialize the lipoprotein profile characterization developed by Ala-Korpela and colleagues.

### **PLS regression models**

PLS regression represents an effective alternative to curve fitting and was first applied to quantification of lipoproteins by Bathen et al. (2000) where PLS and Neuronal Network (NN) analysis were combined<sup>51</sup>. In this approach, a PLS regression model is built to find the best linear association between the NMR spectra and the measured data from a reference method (i.e. UC). In contrast to the curve fitting approach, overlapping signals do not need to be deconvoluted directly since the PLS models focus on the relation between the NMR spectra

and the reference UC data. PLS regression is an effective method for quantification, and most modern lipoprotein quantifications are based on this method. Since PLS models are based on correlation (or covariance in the unscaled version), special care has to be taken to interpret the models in order to limit the effect of the so-called cage of covariance<sup>52</sup>.

*Interval* PLS. In order to develop a more parsimonious regression model, *i*PLS has been proposed for lipoproteins quantification. *i*PLS allows localization of relevant spectral regions that are correlated with the response variable (i.e. cholesterol and/or triglycerides concentrations as measured by a reference method) in the regression equation. This approach, which combines PLS with regional/interval variable selection, has proven to be successful for the prediction of postprandial chylomicrons<sup>53</sup> as well as for the determination of cholesterol in rodent plasma lipoprotein fractions<sup>54</sup>. However, in principle many other variable selection methods could be used for improving the parsimony, interpretability and performance of the prediction methods.

### **2.2.3 Serum/plasma lipoprotein analysis by 2D <sup>1</sup>H-NMR spectroscopy**

Despite of the great technological advances and efforts made by the pioneers in the field of advanced lipoprotein testing (ALT) by NMR, there is still some controversy about the introduction of NMR-based ALTs into clinical practice, partly because current methods do not provide a direct measure of lipoprotein sizes. As an alternative to current NMR methods, there has been increasing interest in 2D

## Chapter 2

diffusion-edited  $^1\text{H}$  NMR spectroscopy for the analysis of plasma samples<sup>18</sup>. Briefly, by applying a gradient strength iteratively, different NMR spectra are acquired while their intensities are attenuated. Changes in the NMR intensity of a given peak depend not only on the strength of the gradient applied, but also on the diffusion coefficient of the metabolite from which such resonance originates. Thus, using diffusion NMR experiments it is possible to obtain estimated diffusion coefficients of the lipoproteins within a plasma sample. Once the diffusion coefficients have been derived, they can be entered into the Stokes–Einstein equation to assess the hydrodynamic radius.

Several prior works have used diffusion experiments:

Liu et al. mathematically<sup>55</sup> deconvoluted the methyl and methylene peaks in the diffusion-edited  $^1\text{H}$ -NMR spectra of one plasma sample into six lorentzian functions, each one of which was characterized by amplitude, position, width and a diffusion coefficient. They demonstrated that the hydrodynamic radii estimated from the diffusion coefficients for every function has a good correlation with the radii of the conventional subfractions. The measurements were made at 25 °C, a temperature at which some lipid fractions have reduced visibility in the NMR spectra. The same group shown that the use of diffusion-edited experiments improved their assessments of hepatotoxicity in rat blood serum compared to assessments derived from traditional  $^1\text{H}$ -NMR spectra<sup>55</sup>.

Dyrby et al.<sup>56</sup> applied multi-way calibration by N-PLS and multi-way curve resolution using PARAFAC to 2D diffusion-edited  $^1\text{H}$ -NMR spectra of human blood samples. The application of PARAFAC with four

components extracted from the methylene peak revealed that these components correspond well with the four main lipoprotein groups (VLDL, IDL, LDL and HDL) because the diffusion coefficients (and hence their derived radii) that represent the extracted coefficients correspond quite well with the size characteristics of each fraction. However, the correlation between them and the concentration of the fractions was poor, probably because of the limited number of samples ( $n = 17$ ). N-PLS calibration led to better lipoprotein lipid correlations for the four main fractions, and the 11 subfractions considered (the correlation coefficient  $r$  had values between 0.75 and 0.98)<sup>56</sup>.

Numares, a German company (<http://www.numares-health.com/quicklinks-oben-health/home.html> -consulted 15.08.2017-), has described a procedure for determining the concentration and size of lipoprotein subclass particles, and a patent application for the invention. The serum/plasma samples are measured at different temperatures (typically 278 K, 298 K, 308 K and 318 K). As the temperature rises, the relaxation times  $T1$  and  $T2$  increase and the lineshape narrows. These measuring conditions, combined with three Diffusion weighted  $^1\text{H-NMR}$  measurements carried out with a modified STE-LED (stimulated echo and longitudinal eddy-current delay) pulse sequence, produce a range of different spectra, which depend on the attenuation of the lipoprotein fractions under each of the measuring conditions. Previously, the different lipoprotein classes were characterized individually and their characteristic parameters (chemical shift, shape of NMR signal intensities, signal width and line form) extracted for each temperature and gradient strength. Then, the simulated NMR spectrum is calculated

## Chapter 2

and adjusted to the experimental spectrum by means of multidimensional optimization processes. The lipoprotein size limits of the different fractions are calculated once the particle density is known through their lipid contents. This method makes it possible to determine 15 different fractions – including CM, VLDL, IDL, LDL, HDL fractions – and Lp(a) proteins. The determination of the latter is clinically very relevant because of the high health risk associated with this lipoprotein<sup>57</sup>.

In our research group, Mallol et al.<sup>58</sup> used a mathematical deconvolution of the 2D diffusion edited spectra of plasma samples into 8 lorentzian functions to demonstrate that the extracted areas and diffusion coefficients in a set of 26 plasma samples separate the different lipoprotein profiles (normal, high triglycerides, low HDL/LDL ratio, and both risk factors) in a PCA score plot much better than the original spectra. They also showed that the relationship between the shift position of the lorentzian functions and the lipoprotein radii calculated from the experimental diffusion coefficient agrees with results found by other authors<sup>39,40</sup>, particularly in normolipidemic samples.

The latter study, established the bases for the development and refinement of the advanced lipoprotein test, named Liposcale test. The Liposcale test is a novel method for characterizing lipoprotein particles based on 2D diffusion-ordered <sup>1</sup>H-NMR spectroscopy (DOSY). DOSY allows measuring the diffusion coefficients and directly calculating lipoprotein sizes through the Stokes-Einstein equation<sup>59</sup>. It should be noted that the direct measurement of lipoprotein size is of particular importance since it is used to calculate the number of lipoprotein



particles by dividing the spatial volume of the total lipid molecules by the mean volume (i.e. size) of the lipoprotein particles. Thus, the development of the Liposcale test, based on DOSY NMR experiments, enables direct measurement of lipoprotein sizes producing more accurate determinations of lipoprotein particle concentrations than 1D NMR-based methods, and has originated a patent application and several research application studies that will be presented in the next section as part of the research of the PhD candidate.



## **2.3 The Liposcale test**



As a Metabolomic Platform, the research group in which the present thesis has been conducted, has closely collaborate with several research clinical teams to provide NMR-based on technologies and software development solutions for biomarker research discovery and disease assessment, including the DOSY-NMR-based on Liposcale test.

The analysis of plasma by means of DOSY-NMR generates a complex resonance spectrum from which a superior degree of information compared to that obtained in the traditional analyses.

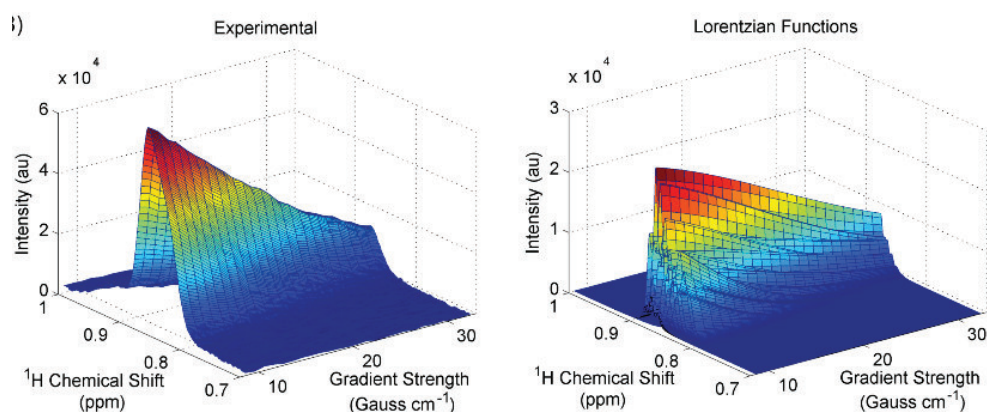


**Figure 1.** DOSY-NMR experimental spectrum, mathematical reconstruction with Lorentzian function. Mallol R. et al., Journal of Lipid Research, 2015.

The DOSY-NMR plasma spectrum is characterized by the appearance of peaks in different areas, the intensity of which is proportional to the concentration of molecular families that resonate at characteristic frequencies. The complexity of this spectrum is at the same time an opportunity to identify new patterns, profiles or markers associated with certain diseases.

## Chapter 2

As a consequence of the development of this test, the opportunity and need arise of intellectually protecting, refining and adapting it to the clinical and commercial requirements with the final objective to translate the basic research to a useful tool for clinicians and patients. With this specific purpose, the spin-off company Biosfer Teslab was created as an independent institution to carry out these tasks.

This section describes the patented technology, the industrial development process and the clinical application studies in which the PhD candidate, as the scientific responsible and current CEO of the company (from 2015), has participated.

### 2.3.1 The technology

#### METHOD FOR THE CHARACTERIZATION OF LIPOPROTEINS

(12) INTERNATIONAL APPLICATION PUBLISHED UNDER THE PATENT COOPERATION TREATY (PCT)

(19) World Intellectual Property  
Organization  
International Bureau



(10) International Publication Number  
**WO 2015/079000 A1**

(43) International Publication Date  
4 June 2015 (04.06.2015)

- (51) International Patent Classification:  
*G01N 33/92* (2006.01)      *G01N 24/08* (2006.01)  
*G01R 33/465* (2006.01)
- (21) International Application Number:  
PCT/EP2014/075873
- (22) International Filing Date:  
27 November 2014 (27.11.2014)
- (25) Filing Language: English
- (26) Publication Language: English
- (30) Priority Data:  
13382478.9 27 November 2013 (27.11.2013) EP
- (71) Applicants: INSTITUT D'INVESTIGACIÓ SAN-  
ITÀRIA PERE VIRGILI [ES/ES]; Escorxador, s/n, E-  
43003 Tarragona (ES). UNIVERSITAT ROVIRA I VIR-  
GILI [ES/ES]; Escorxador, s/n, E-43003 Tarragona (ES).
- (72) Inventors: MALLOL PARERA, Roger; Avenida de Tar-  
ragona, 1 - Escalera 4, 6e B, E-43204 Reus - Tarragona  
(ES). AMIGÓ GRAU, Núria; Duesaigües, 3A, 1r 2a, E-  
43203 Reus - Tarragona (ES). CORREIG BLANCHAR,  
Xavier; Escornalbou, 22, E-43203 Reus - Tarragona (ES).  
MASANA MARÍN, Lluís; Cases de Müller, 20, E-43005  
Tarragona (ES). RODRÍGUEZ MARTÍNEZ, Miguel  
Àngel; Ausiàs March, 14 - Escalera A2, 1r 3a, E-43480  
Vilaseca, Tarragona (ES). HERAS IBÁÑEZ, Mercedes;  
Àngel Guimerà, 25 - 3ºB, E-43202 Reus - Tarragona (ES).  
PLANA GIL, Núria; La Selva, 9, Urbanización La Mora,
- E-43008 Tarragona (ES). RIBALTA VIVES, Josep; Es-  
pronceda 17, Àtic B, Reus, Tarragona E-43202 (ES).
- (74) Agent: DE LA VEGA VELÁZQUEZ, Laura; ABG Pat-  
entes, S.L., Avenida de Burgos, 16D, Edificio Euromor, E-  
28036 Madrid (ES).
- (81) Designated States (*unless otherwise indicated, for every  
kind of national protection available*): AE, AG, AL, AM,  
AO, AT, AU, AZ, BA, BB, BG, BH, BN, BR, BW, BY,  
BZ, CA, CH, CL, CN, CO, CR, CU, CZ, DE, DK, DM,  
DO, DZ, EC, EE, EG, ES, FI, GB, GD, GE, GH, GM, GT,  
HN, HR, HU, ID, IL, IN, IR, IS, JP, KE, KG, KN, KP, KR,  
KZ, LA, LC, LK, LR, LS, LU, LY, MA, MD, ME, MG,  
MK, MN, MW, MX, MY, MZ, NA, NG, NI, NO, NZ, OM,  
PA, PE, PG, PH, PL, PT, QA, RO, RS, RU, RW, SA, SC,  
SD, SE, SG, SK, SL, SM, ST, SV, SY, TH, TJ, TM, TN,  
TR, TT, TZ, UA, UG, US, UZ, VC, VN, ZA, ZM, ZW.
- (84) Designated States (*unless otherwise indicated, for every  
kind of regional protection available*): ARIPO (BW, GH,  
GM, KE, LR, LS, MW, MZ, NA, RW, SD, SL, ST, SZ,  
TZ, UG, ZM, ZW), Eurasian (AM, AZ, BY, KG, KZ, RU,  
TJ, TM), European (AL, AT, BE, BG, CH, CY, CZ, DE,  
DK, EE, ES, FI, FR, GB, GR, HR, HU, IE, IS, IT, LT, LU,  
LV, MC, MK, MT, NL, NO, PL, PT, RO, RS, SE, SI, SK,  
SM, TR), OAPI (BF, BJ, CF, CG, CI, CM, GA, GN, GQ,  
GW, KM, ML, MR, NE, SN, TD, TG).
- Published:  
— with international search report (Art. 21(3))

#### OBJECT OF THE INVENTION

The present invention relates to a method for the characterization of lipoproteins and is applicable in the field of biomedicine.

#### PRIOR ART

Lipids are mainly present in the blood in the form of lipoproteins, which are particles synthesized in the liver and intestines that transport cholesterol, triglycerides and other lipids through the blood stream into

## Chapter 2

peripheral tissues. Abnormal levels of blood lipids may be indicative of cardiovascular diseases. To assess cardiovascular risk, a standard lipid panel is generally used, which includes the concentration of plasma triglycerides, total cholesterol, LDL cholesterol and HDL cholesterol. All these parameters are measured experimentally except for the LDL cholesterol, which is estimated using the Friedewald formula. A critical limitation of this formula is its inaccuracy under certain conditions. Also, the measure of the amount of cholesterol in HDL and LDL lipoprotein fractions does not suffice to predict cardiovascular risk in every case, since also the size and particle number of lipoprotein particles may be relevant for a correct diagnosis of lipid-related diseases. Thus, lipoprotein particles play a main role in cardiovascular diseases and metabolic disorders<sup>60,61</sup>.

Lipoproteins are divided into five main fractions or classes depending on their size and density: chylomicrons (Q; radii 400-2500 Å), very low density lipoproteins (VLDL; radii 150-400 Å), intermediate density lipoproteins (IDL; radii 125-175 Å), low density lipoproteins (LDL; radii 90-140 Å) and high density lipoproteins (HDL; radii 25-60 Å). These main fractions or classes can be further divided into different subclasses to obtain a more detailed lipoprotein profile.

It is generally accepted that the structure of a lipoprotein particle is substantially spherical and comprises an inner core and an outer shell, wherein non-polar lipids (triacylglycerols and cholesteryl esters) are found within the core, while polar lipids (phospholipids and free cholesterol) are distributed through a surface monolayer (shell). The



protein components of lipoproteins (called apolipoproteins or apoproteins) are located on the shell together with the polar lipids.

Advanced lipoprotein testing (ALT) aims to provide the most detailed information on lipoprotein particles. Among the analytical techniques for advanced lipoprotein testing currently used the following may be mentioned:

- Density Gradient Ultracentrifugation, which allows measuring the relative cholesterol distribution for different lipoprotein subclasses (K.R. Kulkarni et al., Quantification of cholesterol in all lipoprotein classes by the VAP-II method, *Journal of Lipid Research* 35 (1994) 159–168)<sup>11</sup>. However, it does not provide either the concentration of triglycerides, or the numbers and sizes of the lipoprotein particles.
- Gradient Gel Electrophoresis, which can fractionate LDL and HDL subclasses directly from plasma according to their size (G.R. Warnick et al., Polyacrylamide gradient gel electrophoresis of lipoprotein subclasses, *Clinics in Laboratory Medicine* 26 (2006) 803)<sup>62</sup>. This method requires custom-made gels and strict attention to laboratory quality control since small variations in gel quality and laboratory conditions may affect accuracy.
- High Performance Liquid Chromatography measures the cholesterol and triglyceride content as well as the size of the major lipoproteins and their subclasses (M. Okazaki et al., Component analysis of HPLC profiles of unique lipoprotein subclass cholesterol for detection of coronary artery disease, *Clinical Chemistry* 52 (2006) 2049–2053)<sup>63</sup>.

## Chapter 2

- Ion Mobility Analysis relies on differences in electrophoretic mobility of gas-phased lipoprotein particles and allows measuring the size and concentration of some lipoprotein subclasses (M.P. Caulfield et al., Direct determination of lipoprotein particle sizes and concentrations by ion mobility analysis, *Clinical Chemistry* 54 (2008) 1307–1316)<sup>64</sup>.
- <sup>1</sup>H-NMR Spectroscopy for quantifying lipoprotein subclasses based on sophisticated line-shape fitting techniques (M. Ala-Korpela et al., <sup>1</sup>H-NMR-based absolute quantification of human lipoproteins and their lipid contents directly from plasma, *Journal of Lipid Research* (1994) 2292-2304)<sup>46</sup>. However, said techniques require the use of a library of spectra previously characterized and have the disadvantage of extensive lipoprotein signal overlap in the analysis of the spectra of plasma.
- Diffusion-Ordered NMR Spectroscopy of lipoprotein fractions, which uses the methyl peak of isolated lipoproteins to calculate the diffusion coefficient of the lipoproteins and estimate their size from this value (R. Mallol et al., Particle size measurement of lipoprotein fractions using diffusion ordered NMR spectroscopy, *Analytical and Bioanalytical Chemistry* 402 (2012) 2407–2415)<sup>65</sup>. However, this method requires a previous step of ultracentrifugation of the sample in order to obtain the different lipoprotein fractions and cannot be used directly in a blood serum or blood plasma sample.  
Analytical methods which physically separate the different

lipoprotein fractions and subclasses, such as ultracentrifugation, are laborious and time-consuming. Moreover, samples suffer a high degree of manipulation and they might remain at 4°C for days.

Also, ALT methods are not yet ready for routine clinical use, some of their limitations being the lack of standardization and the varying approaches. Thus, there is a need for a method which allows reliable characterization of different lipoprotein fractions and subclasses directly from a blood serum or a blood plasma sample, using a single analysis and without the processing or destruction of the sample. This will be useful for developing and monitoring diet and drug therapies and getting insight into the pathophysiology of cardiovascular diseases.

#### **SUMMARY OF THE INVENTION**

The present invention overcomes the above problems by the provision of a method according to claim 1. The dependent claims define preferred embodiments of the invention.

Currently, LDL and HDL cholesterol are two factors for cardiovascular risk that are routinely used to assess the cardiovascular risk of an individual. However, a high percentage of individuals suffering a cardiovascular event have normal levels of LDL cholesterol. Patients with metabolic disorders such as diabetes tend to have LDL lipoproteins which are smaller, poorer in cholesterol content and more atherogenic. This smaller size is associated with a greater number of particles, thus resulting in a cholesterol concentration similar to that of a pattern with a smaller concentration of larger less atherogenic particles. That is the reason why there is interest in determining the size and number of LDL

## Chapter 2

lipoprotein particles, beyond their lipid load, to assess cardiovascular risk of a patient. Moreover, there are studies which indicate that the size and number of HDL particles are better predictors of cardiovascular risk than HDL cholesterol. The present invention allows exhaustive characterization of lipoprotein particles, providing in a fast and reliable way the size and number of particles of the main lipoproteins classes and subclasses without physical separation of the different lipoprotein fractions and subfractions in the sample.

The method according to the invention comprises the following steps:

- obtaining a 2D diffusion-ordered  $^1\text{H}$ -NMR spectrum of a sample;
- performing a surface fitting of a portion of the spectrum corresponding to the methyl signal using a plurality of model functions, each model function corresponding to a given particle size associated to a lipoprotein fraction and subclass and including at least one model parameter to be estimated during the fitting, the estimated model parameters being the set of model parameters for which the difference between the NMR signal and the model signal built as a linear combination of the model functions is minimized,

wherein each model function is a triplet of lorentzian functions having the form:

$$\begin{aligned} \text{Triplet}_j = & \text{Lorentzian}(h_{1j}, f_j - f_{0j}, w_j, D_j) \\ & + \text{Lorentzian}(h_{2j}, f_j, w_j, D_j) \\ & + \text{Lorentzian}(h_{3j}, f_j + f_{0j}, w_j, D_j), \end{aligned}$$

where  $h_{ij}$ (au),  $f_j$ (ppm),  $w_j$ (ppm), and  $D_j$ ( $\text{cm}^2\text{s}^{-1}$ ) are the intensities, chemical shift, width, and diffusion coefficient, respectively, associated to a lipoprotein particle size  $j$ .

The side lorentzian functions are equally spaced in the chemical shift axis relative to the central lorentzian function, namely in an amount  $f_0$ .

The model parameters to be determined for a lipoprotein particle size are one or several from:  $f$ ,  $f_0$ ,  $h_1$ ,  $h_2$ ,  $h_3$ ,  $w$  and  $D$ .

Advantageously, the use of triplets of lorentzians as the model functions associated to each lipoprotein particle size results in a more accurate fitting of the NMR signal, when compared to other methods.

The sample is preferably a blood plasma sample or a blood serum sample, but samples of other biological fluids may be also used, such as cerebrospinal fluid, encephalorachidian fluid or amniotic fluid.

Thus, the NMR methyl signal is decomposed as a number of model functions, each model function corresponding to a lipoprotein particle size. Each model function is thus associated with a given lipoprotein fraction and subclass according to its lipoprotein particle size. Not all the model functions included in the fitting will necessarily contribute to the model signal built, since not all the lipoprotein particle sizes included in the fitting are necessarily present in the sample.

According to the method of the invention, the lipoproteins present in the sample are identified and characterized by determining the intensity, chemical shift, width, and diffusion coefficient of the associated lipoprotein signals. For further characterization of the lipoproteins present in the sample, additional lipoprotein parameters

## Chapter 2

may be determined in subsequent steps based on the model functions and on the estimated model parameters.

Preferably, the lorentzian functions of the triplet associated to each lipoprotein particle size  $j$  have the form

$$\text{Lorentzian}_j(h_j, f_j, w_j, D_j) = \frac{h_j}{1 + \left(\frac{f - f_j}{w_j}\right)^2} e^{-k \cdot D_j \cdot G^2}$$

where  $k$  is the Boltzmann constant and  $G$  is the gradient strength applied (Gauss  $\text{cm}^{-1}$ ). The first quotient part of the lorentzian corresponds to a 1D lorentzian, whereas the exponential part includes the attenuation effect by means of the diffusion gradient. This preferred form of the lorentzian functions is applicable to each embodiment of the invention.

In a preferred embodiment, the method comprises identifying the lipoproteins present in the sample as those associated to the model functions having a nonzero contribution to the theoretical model signal resulting from the fitting and determining at least one and preferably all of: average size of lipoprotein particle classes, average size of lipoprotein particle subclasses, class and/or subclass lipoprotein particle concentration, lipid concentration of at least one lipoprotein particle class and/or lipid concentration of at least one lipoprotein particle subclass.

In a preferred embodiment, for the model function associated to each lipoprotein particle size  $j$  the intensities of the side lorentzian functions are made proportional to the intensity of the central lorentzian function:

$$h_{1j} = \alpha_j \cdot h_{2j}, \text{ with } \frac{1}{4} \leq \alpha_j \leq \frac{3}{4}, \text{ and}$$

$$h_{3j} = \beta_j \cdot h_{2j}, \text{ with } \frac{1}{4} \leq \beta_j \leq \frac{3}{4}.$$

In an embodiment, the proportionality factor  $\alpha_j$  is made the same for all lipoprotein particle sizes and/or the proportionality factor  $\beta_j$  is made the same for all lipoprotein particle sizes.

In a preferred embodiment, the intensities of the side lorentzian functions are taken to be equal, i.e.  $h_{1j} = h_{3j}$ .

In a preferred embodiment,

$h_1 = \frac{h_2}{2}$ , i.e. the intensities of the side lorentzian functions are approximately half the intensity of the central lorentzian function, and/or

$f_0 = 0.01$  ppm, i.e. the side lorentzian functions are spaced approximately 0.01 ppm in the chemical shift axis relative to the central lorentzian function.

In a preferred embodiment, the number of model functions used is greater than or equal to 9, each model function corresponding to a lipoprotein particle size.

In a preferred embodiment, the lipoprotein particle sizes used in the fitting are defined based on experimental results obtained for example by NMR, HPLC, Gradient Gel Eletrophoresis, or Atomic Force Microscope. The lipoprotein particle sizes used in the method may be selected based on any other technique.

Preferably, lipoprotein particle sizes corresponding to several lipoprotein classes and/or subclasses are used in the method.

The surface fitting may be performed taking all the model parameters as free parameters to be determined during the fitting. However, in a preferred embodiment, the surface fitting is performed

## Chapter 2

fixing a number of model parameters and using at least one other model parameter as a free parameter to be determined. More preferably, at least the signal intensity of the central lorentzian ( $h_2$ ) is used as a free parameter and at least one of the chemical shift, width, and diffusion coefficient are fixed.

Where the number of model parameters to be estimated in the surface fitting is high, multiple solutions for the fitting appear, many of them having no biological meaning. Advantageously, fixing parameters by establishing relations between pairs of model parameters allows reducing the dimensionality of the problem and avoids the appearance of solutions with no biological relevance.

The shift of the side lorentzian functions relative to the central lorentzian function may be estimated during the surface fitting or may be taken as a given value. Similarly, the intensities of the side lorentzian functions may be estimated during the surface fitting or may be taken to be related to the intensity of the central function, preferably to be half the intensity of the central lorentzian function.

In a preferred embodiment, the fixed model parameters used in the surface fitting are determined based on the lipoprotein particle size and on regression models, the regression models relating pairs of fixed model parameters and/or a model parameter and the lipoprotein particle size.

In a preferred embodiment, the regression models used for the fixed parameters are obtained from the deconvolution of the methyl signal of a plurality of NMR spectra using a plurality of model lorentzian functions with the intensity, chemical shift, width, and diffusion



coefficient being free model parameters estimated to minimize the difference between the NMR methyl signal and the model signal built as a linear combination of the model functions, the regression models respectively relating at least (i) the chemical shift and the lipoprotein particle size, and/or (ii) the width and the lipoprotein particle size.

In a preferred embodiment, the regression models relating pairs of model parameters are built according to the following steps:

- obtaining a 2D diffusion-ordered  $^1\text{H}$ -NMR spectrum for a plurality of samples;
- for each sample, performing a surface fitting of a portion of the spectrum corresponding to the methyl signal using a plurality of model functions, each model function being dependent on the model parameters to be fixed, wherein all the model parameters to be fixed are estimated during the surface fitting as the set of model parameters for which the difference between the NMR signal and the model signal built as a linear combination of the model functions is minimized, and
- using the model parameters estimated in the previous step to build regression models relating pairs of model parameters.

Preferably, the regression models respectively relate at least (i) the chemical shift and the lipoprotein particle size, and/or (ii) the width and the lipoprotein particle size.

The plurality of samples used to build the regression models includes different lipids profiles and the number of samples considered is sufficiently high to be statistically meaningful. Preferably, the number of samples is equal to or greater than 100 and includes samples taken

## Chapter 2

from healthy subjects and samples corresponding to different profiles of atherogenic dyslipidaemia.

Preferably, the model functions used to build the regression models are lorentzian function triplets of the form:

$$\begin{aligned} \text{Triplet}_j &= \text{Lorentzian}(h_{1j}, f_j - f_{0j}, w_j, D_j) \\ &+ \text{Lorentzian}(h_{2j}, f_j, w_j, D_j) \\ &+ \text{Lorentzian}(h_{3j}, f_j + f_{0j}, w_j, D_j), \end{aligned}$$

In a preferred embodiment,  $h_1 = h_3 = h_2/2$ .

In a preferred embodiment, the triplets of lorentzian functions used to build the regression models have the form:

$$\begin{aligned} \text{Triplet}_j &= \text{Lorentzian}\left(\frac{h_j}{2}, f_j - 0.01, w_j, D_j\right) \\ &+ \text{Lorentzian}(h_j, f_j, w_j, D_j) \\ &+ \text{Lorentzian}\left(\frac{h_j}{2}, f_j + 0.01, w_j, D_j\right) \end{aligned}$$

Alternatively, the shift ( $f_0$ ) of the side lorentzian functions relative to the central lorentzian function may be determined during the fitting performed to build the regression models. A single value of the shift ( $f_0$ ) may be used for all the lipoprotein sizes. Similarly, the intensities of the side lorentzian functions may be estimated during the fitting performed to build the regression models.

In a preferred embodiment, the diffusion coefficient of the model functions is estimated from the lipoprotein particle size by means of the Einstein Stokes equation

$$D = \frac{kT}{6\pi\eta R_H}$$

$k$  (J K<sup>-1</sup>) being Boltzmann constant,  $T$  (K) temperature,  $\eta$  (Pa s) viscosity and  $R_H$  (Å) the lipoprotein particle size.

In a preferred embodiment, the method of the invention further includes correcting the estimated diffusion coefficients to take into account dilution effects, using a relation between the NMR area and the diffusion coefficient obtained for several dilutions of a sample wherein the sum of the concentration of total cholesterol and triglycerides of said sample is higher than 300 mg/dL. Advantageously, using a corrected diffusion coefficient to take into account dilution effects results in a more accurate surface fitting.

In a preferred embodiment, the NMR area associated to a lipoprotein function is corrected to consider only the contribution of the lipids included in the lipoprotein particle core.

In a preferred embodiment, the corrected NMR area ( $A'$ ) is determined using the following expression:

$$A' = A \cdot \frac{(9 \cdot (R - s)^3)}{[(9 \cdot (R - s)^3) + 6 \cdot p \cdot (R^3 - (R - s)^3)]}$$

with  $A$  (au) and  $R$ (Å) being respectively the area and lipoprotein particle size associated to each model function,  $s$ (Å) being the thickness of the lipoprotein particle shell and  $p$  being the ratio of apoprotein mass per unit volume (mg/ml) in the shell of the particle relative to the total mass per unit volume (mg/ml) in the particle shell (proteins, free cholesterol and phospholipids). The proteins in the shell of the lipoprotein particles are called apolipoproteins. The ratio  $p$  depends on the lipoprotein fraction. For HDL  $p$  is approximately 0.5. For other lipoprotein fractions  $p$  is smaller. Generally, the thickness of the lipoprotein particle core is estimated as  $s = 20 \pm 2$  Å.

## Chapter 2

As used herein, the term “apolipoproteins” or “apoproteins”, i.e. proteins in the shell of the lipoprotein particles, refer to proteins that bind lipids to form lipoproteins and transport lipids through the circulatory system. Apolipoproteins are amphipathic molecules that can surround lipids creating the lipoprotein particle that is itself water-soluble and can thus be carried through water-based circulation (i.e., blood). There are six classes of apolipoproteins (A-H) and several subclasses; in particular, Apo A-I (or Apo A1) is the major protein component of HDL particles wherein Apo A-II (or Apo A2) is also present in a minor concentration. Illustrative, non-limitative, methods for determination of apolipoprotein concentration include without limitation, colorimetric methods, Western blot or ELISA. If apolipoprotein concentration is determined in an isolated fraction of lipoproteins any method well-known in the art for determining protein concentrations may be used such as enzymatic methods, colorimetric methods (Biuret, Lowry, Bradford, etc.) or immunochemical techniques (Western blot, ELISA, etc.). If apolipoprotein concentration is determined in a plasma or serum sample immunochemical techniques are used in order to obtain a specific detection of apolipoproteins. Illustrative, non-limitative, immunochemical techniques for apolipoprotein detection include immunoturbidimetric techniques, immunonefelometric techniques, radial immunodiffusion, ELISA, electroimmunoanalysis, and radioimmunoanalysis.

The correction of the area is more important as the lipoprotein particle size decreases, i.e. the correction is greater for HDL particles than for LDL or VLDL particles, due to the smaller size of HDL particles.

In a preferred embodiment, the method additionally comprises determining at least one lipoprotein parameter selected from: average particle size of lipoprotein fractions, average particle size of lipoprotein subclasses, fraction lipoprotein particle concentration, subclass lipoprotein particle concentration and lipid concentration of at least one lipoprotein particle subclass and/or lipid concentration of at least one lipoprotein particle fraction.

In a preferred embodiment, the average size of a lipoprotein particle fraction is determined as:

$$Size (\text{\AA}) = \frac{\sum_{i=1}^n R_i \cdot PN_i}{\sum_{i=1}^n PN_i},$$

$n$  being the number of lipoprotein particle subclasses included in the lipoprotein particle fraction,  $R(\text{\AA})$  being the lipoprotein particle size and  $PN_i$  being the particle number for said lipoprotein particle size.

In a preferred embodiment, the particle number ( $PN$ ) for a lipoprotein is determined as:

$$PN_i \propto \frac{A_i}{R_i^3}$$

with  $A(\text{au})$  and  $R(\text{\AA})$  being respectively the area and lipoprotein particle size associated to a model function  $i$ . Throughout the document the size of the lipoprotein particle will be understood as the lipoprotein particle radius in Angstroms. The number of lipoprotein particles of a specific size is proportional to the ratio of the area associated to the model function corresponding to said lipoprotein between the volume associated to said lipoprotein, the proportionality factor being a calibration parameter of the equipment used. Preferably, in the determination of the particle number the area associated to a

## Chapter 2

lipoprotein function is the area  $A'$  corrected to consider only the contribution of the lipids included in the lipoprotein particle core, according to an embodiment of the invention.

The average size of a lipoprotein particle fraction, as used herein, refers to the average size of the radius of the lipoproteins forming part of a particular lipoprotein particle fraction.

In a preferred embodiment, the lipoprotein particle concentration of a lipoprotein particle fraction is calculated by dividing the lipid volumes by the lipoprotein particle volumes. Lipid volumes are determined by using common conversion factors to convert concentration units into volume units. Total lipoprotein particle concentrations of each main lipoprotein particle fraction are obtained by summing the concentrations of the corresponding lipoprotein particle subclasses.

In a preferred embodiment, the method comprises determining the lipid concentration of at least one lipoprotein particle fraction and/or at least one lipoprotein particle subclass. More preferably, the determination of the lipid concentration is performed using regression models. In a preferred embodiment, the regression models are calibrated with lipid concentrations measured in lipoprotein fractions obtained by ultracentrifugation in the following regions: from 5.4 to 5.15 ppm, from 3.28 to 3.14 ppm, from 2.15 to 1.85 ppm, from 1.45 to 1 ppm and from 1 to 0.7 ppm. Other methods may be used for calibration, such as ELISA, chromatography, NMR or enzymatic methods.

The determination of the lipid concentration of a lipoprotein particle fraction or subclass includes the determination of at least one of

a lipid selected from triacylglycerols, cholesteryl esters, free cholesterol and phospholipids.

All the features described in this specification (including the claims, description and drawings) and/or all the steps of the described method can be combined in any combination, with the exception of combinations of such mutually exclusive features and/or steps.

### **BRIEF DESCRIPTION OF (the patent) DRAWINGS**

To better understand the invention, its objects and advantages, the following figures are attached to the specification in which the following is depicted:

- Figure 1 shows the deconvolution of a methyl signal according to the method of the invention, where the model functions used in the fitting are shown in figure 1A and the model functions grouped according to their lipoprotein fractions are shown in figure 1B.
- Figure 2 shows two regression models, respectively relating (a) size and chemical shift and (b) width and chemical shift.
- Figure 3 shows the relation between the NMR area of the methyl signal and the diffusion coefficient.
- Figure 4 shows the regions of the spectrum used in an embodiment of the method of the invention to calibrate the regression models for the lipid determination.
- Figure 5 shows the deconvolution of the methyl signal of three samples.

## Chapter 2

**Figure 1.**

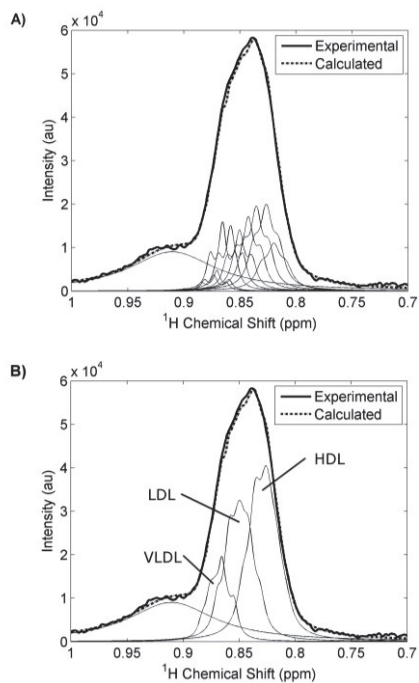


**Figure 2.**

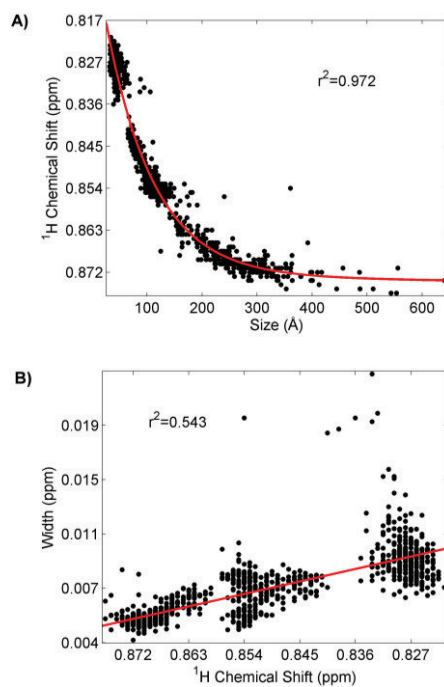


**Figure 3.**

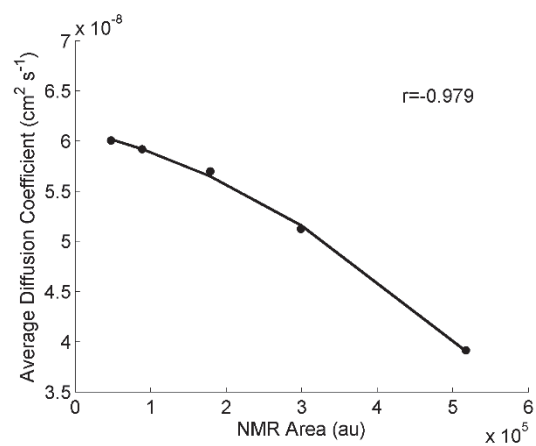




Figure 4.

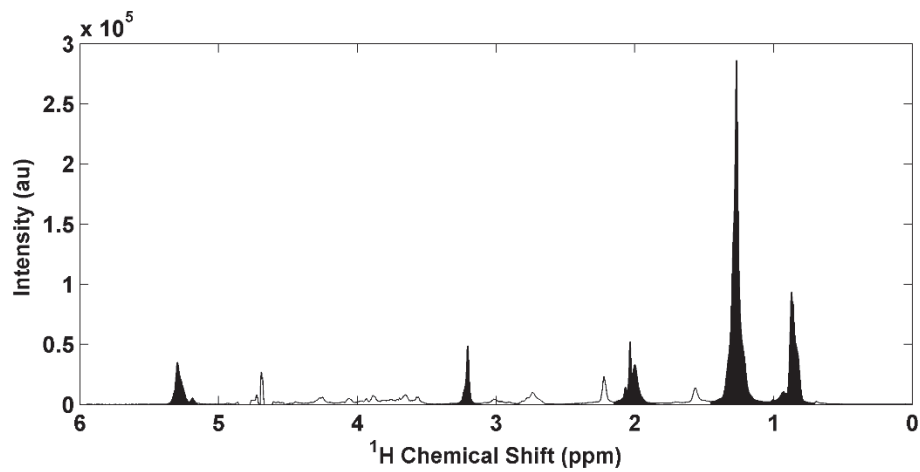
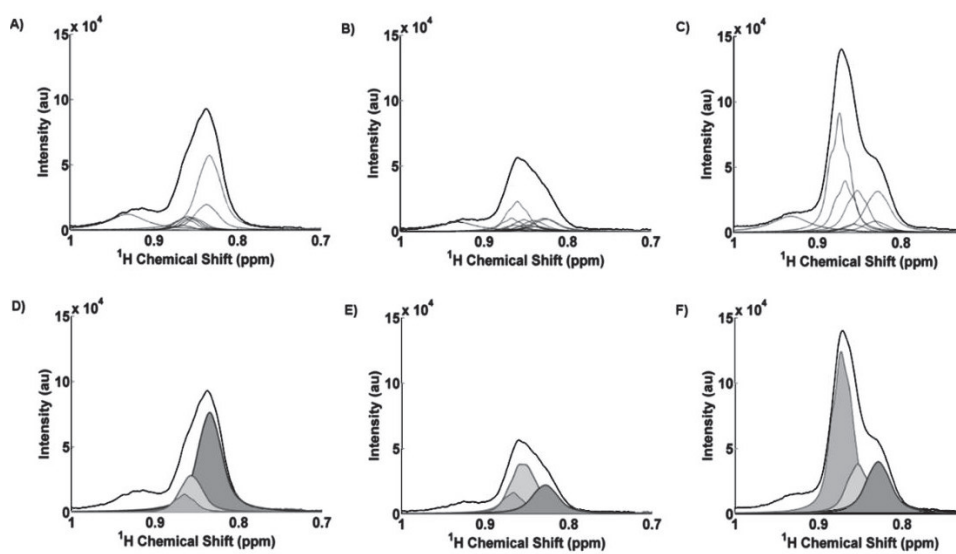


Figure 5.



### DETAILED DESCRIPTION OF THE INVENTION

In the *in vitro* method for the characterization of lipoprotein particles according to the invention, the samples are analysed by 2D diffusion-ordered  $^1\text{H-NMR}$  spectroscopy.

Once the 2D diffusion-ordered  $^1\text{H-NMR}$  spectrum has been obtained, a surface fitting is performed of the portion of the spectrum corresponding to the methyl signal. A plurality of model functions is used, each model function corresponding to a lipoprotein having a specific lipoprotein particle size and including a plurality of model parameters to be estimated during the fitting. The model function associated to each specific lipoprotein particle size is a triplet of lorentzian functions having the form:

$$\begin{aligned} \text{Triplet} = & \text{Lorentzian}(h_1, f - f_0, w, D) + \text{Lorentzian}(h_2, f, w, D) \\ & + \text{Lorentzian}(h_3, f + f_0, w, D), \end{aligned}$$

where  $h(\text{au})$ ,  $f(\text{ppm})$ ,  $w(\text{ppm})$ , and  $D(\text{cm}^2\text{s}^{-1})$  are the model parameters to be determined and are respectively the intensity, chemical shift, width, and diffusion coefficient associated to a lipoprotein signal.

The model parameters are estimated during the fitting as the set of model parameters for which the difference between the experimental NMR signal and the model signal built as a linear combination of the model functions is minimized.

Figure 1 shows the part of a spectrum corresponding to the methyl signal of a serum sample for a single gradient of a 2D diffusion-ordered  $^1\text{H-NMR}$  experiment and its fitting. In this case the fitting for a single gradient has been depicted for increased clarity, even if a surface fitting is performed for a plurality of diffusion gradients. Figure 1A

shows in thin trace a plurality of model functions used to fit an experimental NMR spectrum, which is also shown in thick trace. The theoretical model signal built from the fitting with model functions is depicted in dot line. Each model function can be associated to a given lipoprotein particle fraction according to its lipoprotein particle size. In Figure 1B thin lines correspond to the sum of the model signals associated to each corresponding lipoprotein fraction (in this example VLDL, LDL, HDL).

In this example, the surface fitting is performed fixing all parameters (chemical shift, width and diffusion coefficient) except the signal intensities, instead of estimating all parameters for each triplet of lorentzian functions. The following form is used for the triplet lorentzian functions:

$$\text{Triplet} = \text{Lorentzian}\left(\frac{h}{2}, f - 0.01, w, D\right) + \text{Lorentzian}(h, f, w, D) + \text{Lorentzian}\left(\frac{h}{2}, f + 0.01, w, D\right),$$

the two signals around the central signal being shifted 0.01 ppm relative to the central signal.

In order to fix the chemical shifts and widths associated to each model function, 300 spectra were previously deconvoluted using three triplet lorentzian functions with all their parameters free. Once the sets of parameters which best fit to the 300 experimental spectra have been obtained, they were used to fit two regression models to be used as predictors of the fixed parameters, a first regression model relating chemical shift and size (Figure 2a) and the second regression model relating width and chemical shift (Figure 2b). Figures 2a and 2b respectively show the chemical shift plotted as a function of size and the

## Chapter 2

width plotted as a function of chemical shift for the estimated parameters, from which corresponding relations relating both pair of parameters can be determined. Thus, at a fixed lipoprotein particle size, its NMR chemical shift and width can be estimated using the built regression models.

A third regression model may be built to relate the diffusion coefficient with another parameter. Alternatively, the diffusion coefficient may be obtained from the lipoprotein particle size using the Einstein Stokes equation:

$$D = \frac{kT}{6\pi\eta R_H}$$

Preferably, the lipoprotein particle sizes are selected based on experiments and corresponding to a number of different lipoprotein particle subclasses, which allows a more complete and reliable lipoprotein profile to be achieved.

Preferably, the determined diffusion coefficients are corrected in order to take into account possible dilution effects. To study the degree of correction needed, in a preferred embodiment of the invention a serum sample having high triglycerides levels (16 mmol/L) and various dilutions of the same sample (1:2, 1:4, 1:8 and 1:16) are analyzed (Figure 3). Then, the relation between NMR area and diffusion coefficient is used to predict the correction needed for each NMR signal:

$$D_0 = \frac{D}{1 - k_{S1} \cdot A - k_{S2} \cdot A}$$

where  $D_0$  is the average diffusion coefficient under dilution conditions,  $D$  and  $A$ (au) are the average diffusion coefficient and the total area of the methyl peak, respectively, and  $k_{S1}$ ,  $k_{S2}$  are the

regression coefficients.

To determine the average diffusion coefficient a number of spectra is obtained for each sample, each spectrum being obtained under a different gradient strength. The area under the methyl curve plotted as a function of the gradient decays exponentially with increasing gradients. The average diffusion coefficient is thus proportional to the slope of the line obtained when the logarithm of the signal attenuation  $A/A_0$  is plotted versus the square of the gradient:

$$\log(A/A_0) = -kDG^2$$

where  $A$  is the methyl signal area,  $A_0$  is the methyl signal area with zero gradient,  $k$  is a constant parameter and  $G$  is the gradient strength.

With the selected lipoprotein particle sizes and the chemical shift, width and diffusion coefficient determined for each lipoprotein particle size, the signal intensity is determined for each model function in order to minimize the difference between the experimental NMR signal and the model signal built from the plurality of model signals considered.

The fitting may be made by minimization of the normalized root mean squared errors (NRMSE) using the following equation:

$$NRMSE (\%) = \frac{\sqrt{\frac{\sum_i^n \sum_j^m (S_{exp} - S_{est})^2}{n \cdot m}}}{\max(S_{exp}) - \min(S_{exp})} \cdot 100$$

where  $S_{exp}$  and  $S_{est}$  are the experimental and estimated surfaces, respectively,  $n$  is the number of data points considered and  $m$  the number of gradients used.

## Chapter 2

Once the model parameters have been determined, particle-weighted lipoprotein sizes can be obtained by dividing the NMR area associated to each model function by their associated volume:

$$PN_i \propto \frac{A_i}{R_i^3}$$

where  $A_i$ ,  $R_i^3$  and  $PN_i$  are the area (au), volume ( $\text{\AA}^3$ ) and particle number (au/ $\text{\AA}^3$ ) of a given lipoprotein particle  $i$ . The proportionality factor relating the particle number with the ratio between area and volume can be easily obtained by known calibration standards, which directly relate the NMR area and the lipid concentration.

Then a mean particle size can be obtained for each lipoprotein particle fraction by multiplying the NMR lipoprotein particle sizes by their fractional particle concentration relative to the total particle concentration of a given fraction:

$$Z (\text{\AA}) = \frac{\sum_{i=1}^n R_i \cdot PN_i}{\sum_{i=1}^n PN_i}$$

where  $Z$  corresponds to mean lipoprotein particle size of a given lipoprotein particle fraction.

PLS regression models were calibrated to predict the cholesterol and triglyceride concentration of the main lipoprotein particle fractions (VLDL, LDL, and HDL). Regions from 5.4 to 5.15 ppm, from 3.28 to 3.14 ppm, from 2.15 to 1.85 ppm, from 1.45 to 1 ppm and from 1 to 0.7 ppm (shown in Figure 4) were used as X-Block and the cholesterol and triglyceride concentrations were used as Y-Block. Both blocks were mean-centered. The optimum number of latent variables (LV) and the validation performance of the PLS models, were assessed using venetian blinds cross-validation splitting the data 10 times. Coefficients of

determination between the predicted and reference concentrations ranged from 0.79 to 0.98 in the calibration step. The coefficients of determination of the validation step ranged from 0.81 to 0.98.

The determination of the lipid concentration of a lipoprotein particle fraction or subclass includes the determination of at least one of a lipid selected from triacylglycerols, cholesteryl esters, free cholesterol and phospholipids.

A triglyceride (or triacylglycerol) is an ester derived from glycerol and three fatty acids which can be found in a lipoprotein particle. Illustrative, non-limitative, fatty acids that can be found in lipoprotein triglycerides are palmitic acid, stearic acid, oleic acid, linoleic acid and araquidonic acid. Triglycerides are blood lipids that help enable the bidirectional transference of adipose fat and blood glucose from the liver. Illustrative, non-limitative, methods for determination of triglycerides concentration include enzymatic determination. Enzymatic determination of triglycerides is also possible because it is specific and sensitive. The principle of reaction is as follows: Triglycerides are hydrolyzed by a lipase in glycerol and free fatty acids. In the presence of glycerol kinase, glycerol is phosphorylated to glycerol-3-phosphate which is then oxidized with a glycerol phosphate oxidase with formation of hydrogen peroxide. In the presence of peroxidase, 4-chlorophenol and 4-aminoantipyrine with hydrogen peroxide yield a red-colored product, quinonimine. The staining intensity is directly proportional to the sample concentration of triglycerides.

Cholesterol is an amphipatic lipid. A cholesteryl ester is an ester of cholesterol wherein the ester bond is formed between the

## Chapter 2

carboxylate group of a fatty acid and the hydroxyl group of cholesterol. Illustrative, non-limitative, examples of cholesteryl esters present in a lipoprotein particle are cholesteryl palmitate, cholesteryl stearate, cholesteryl oleate, cholesteryl linoleate and cholesteryl araquidonate<sup>66</sup>. Cholesteryl esters have a lower solubility in water than cholesterol and are more hydrophobic. Numerous methods are available for determination of cholesterol concentration, e.g., gravimetric, nephelometric, turbidimetric, or photometric methods, among others. Commercially available kits for quantitative colorimetric/fluorimetric cholesterol and cholesteryl esters determination may be used. Usually, the concentrations of total and free cholesterol (esterified cholesterol being previously precipitated by, for example, digitonin) are determined, whereas the concentration of cholesteryl esters (esterified cholesterol) is calculated from the difference between these two concentrations. Enzymatic determination of cholesterol concentration is specific and sensitive. The principle of reaction is as follows: Cholesterol esterase catalyzes hydrolysis of cholesteryl esters to free cholesterol and free fatty acids. In the presence of cholesterol oxidase, cholesterol is oxidized to  $\delta$ -4-cholestanetriol to form hydrogen peroxide. In the presence of peroxidase, phenol and 4-aminoantipyrine with hydrogen peroxide yield a red-colored product, quinonimine. The staining intensity is directly proportional to the sample concentration of total cholesterol.

Phospholipids are a class of lipids that are present in the shell of lipoprotein particles and that are a major component of all cell membranes as they can form lipid bilayers. Most phospholipids contain



a diglyceride, a phosphate group, and a simple organic molecule such as choline. The structure of the phospholipid molecule generally consists of hydrophobic tails and a hydrophilic head. Illustrative, non-limitative, examples of phospholipids present in a lipoprotein particle are phosphatidylcholine, sphingophospholipids such as sphingomyelin, phosphatidylethanolamine, phosphatidylinositol and phosphatidylserine. Illustrative, non-limitative, methods for determination of phospholipids concentration, include commercially available assay kits for a quantitative colorimetric/fluorimetric phospholipid determination. The principle of reaction is as follows: phospholipids (such as lecithin, lysolecithin and sphingomyelin) are enzymatically hydrolyzed to choline which is determined using choline oxidase and a  $\text{H}_2\text{O}_2$  specific dye. The optical density of the pink colored product at 570 nm or fluorescence intensity (530/585 nm) is directly proportional to the phospholipid concentration in the sample.

**Example: 2D diffusion-ordered  $^1\text{H}$ -NMR spectroscopy (DOSY)**

Serum samples were analysed by NMR spectroscopy, recording  $^1\text{H}$ -NMR spectra on a BrukerAvance III spectrometer at 310 K. The double stimulated echo (DSTE) pulse program was used with bipolar gradient pulses and a longitudinal eddy current delay (LED). The relaxation delay was 2 s, the free induction decays were collected into 64K complex data points and 32 scans were acquired on each sample. The gradient pulse strength was increased from 5 to 95% of the maximum strength of 53.5 Gauss  $\text{cm}^{-1}$  in 32 steps, where the squared gradient pulse strength was linearly distributed.

Surface fitting:

## Chapter 2

In the present example, the lipoprotein NMR signals were modeled as triplets of Lorentzian functions, with the two signals around the central signal shifted 0.01 ppm:

$$\begin{aligned} \text{Triplet} = & \text{Lorentzian}\left(\frac{h}{2}, f - 0.01, w, D\right) \\ & + \text{Lorentzian}(h, f, w, D) \\ & + \text{Lorentzian}\left(\frac{h}{2}, f + 0.01, w, D\right) \end{aligned}$$

where  $h$  (au),  $f$  (ppm),  $w$  (ppm), and  $D$  ( $\text{cm}^2 \text{s}^{-1}$ ) are the intensity, chemical shift, width, and diffusion coefficient of a given lipoprotein signal, each lipoprotein signal corresponding to a lipoprotein particle size. 9 lipoprotein particle sizes and consequently also 9 model functions were used based on lipoprotein particle sizes obtained by HPLC.

The 9 model functions were associated with a given lipoprotein particle fraction (VLDL, LDL or HDL) according to their NMR size. Thus, functions F1-F3 were associated to VLDL, functions F4-F6 to LDL, and functions F7-F9 to HDL (Table 1 of the present section). Main lipoprotein particle fractions were defined as VLDL (193-409 Å), LDL (74-133 Å) and HDL (30-55 Å).

The surface fitting of the methyl signal was performed using 9 model functions with all parameters fixed (chemical shift, width and diffusion coefficient) except the signal intensity ( $h$ ). The fitting of each sample elapsed  $29.47 \pm 4.42$  seconds on average. The methyl signal was thus decomposed into individual lipoprotein signals to obtain the contribution of 9 lipoproteins with fixed NMR size. Figures 5A-C show the results of the surface fitting for three subjects, which are also summarized in Table 1. It must be noted that even using 9 model

functions to fit the spectra, not all of them are used to find the final solution. Figures 5D-F show the grouping of model functions according to their associated lipoprotein particle main fraction. Subject 1 shows a prominent HDL area (shown in dark grey in Figure 5D), subject 2 has increased LDL area (shown in light grey in Figure 5E), and subject 3 is characterized by a very high VLDL area (shown in medium grey in Figure 5F).

The uniqueness of the solutions was studied by fitting each sample ten times with randomly chosen initial values of the signal intensities. Because the dynamic range in signal intensity may be very high, the following formula was used to assess the coefficient of variation (CV) for each model function and sample across ten different fittings:

$$CV = \frac{SD(h)}{Max(h) - Min(h)} \cdot 100 (\%)$$

where  $h$  stands for signal intensity of a given model function. Maximum (Max), minimum (Min) and standard deviations (SD) values were assessed from the ten fittings in each sample. As a result, unique solutions were obtained for all samples after 10 runs.

In this case the coefficient of variation (CV) is determined for the signal intensity of the central lorentzian, since the other model parameters have been fixed during the fitting. The above expression for the calculation of the coefficient of variation may be generalized for the case where more than one free model parameters is used in the fitting.

Normalized root mean squared errors (NRMSE) of the fittings were calculated using the following equation

$$NRMSE (\%) = \frac{\sqrt{\frac{\sum_i^n \sum_j^m (S_{exp} - S_{est})^2}{n \cdot m}}}{\max(S_{exp}) - \min(S_{exp})} \cdot 100$$

where  $S_{exp}$  and  $S_{est}$  are the experimental and estimated surfaces, respectively,  $n$  is the number of data points considered in interval length (0.7-1 ppm) and  $m$  the number of gradients used. In this example,  $n$  and  $m$  had the same value for each sample. The average NRMSE obtained was of less than 1.5%.

To obtain particle-weighted lipoprotein sizes, we first divided each NMR area by their associated volume:

$$PN_i \propto \frac{A_i}{R_i^3}$$

where  $A_i$ ,  $R_i^3$  and  $PN_i$  are the area (au), volume ( $\text{\AA}^3$ ) and particle number (au/ $\text{\AA}^3$ ) of a given lipoprotein particle  $i$ .

Then, the mean particle size for each lipoprotein particle fraction was obtained multiplying the lipoprotein particle sizes by their fractional particle concentration relative to the total particle concentration of a given particle fraction:

$$VLDL \text{ Size } (\text{\AA}) = \frac{\sum_{i=1}^n R_i \cdot PN_i}{\sum_{i=1}^n PN_i}, i = 1, \dots, 3$$

$$LDL \text{ Size } (\text{\AA}) = \frac{\sum_{i=1}^n R_i \cdot PN_i}{\sum_{i=1}^n PN_i}, i = 4, \dots, 6$$

$$HDL \text{ Size } (\text{\AA}) = \frac{\sum_{i=1}^n R_i \cdot PN_i}{\sum_{i=1}^n PN_i}, i = 7, \dots, 9$$

Particle concentrations of each lipoprotein particle subclass were calculated by dividing the lipid volumes by the particle volumes. Lipid volumes were determined by using common conversion factors to

convert concentration units into volume units. Total particle concentrations of each main particle fraction were obtained by summing the concentrations of the corresponding particle subclasses.

Lipid concentration was determined using PLS models calibrated in the regions shown in Figure 4, namely: from 5.4 to 5.15 ppm, from 3.28 to 3.14 ppm, from 2.15 to 1.85 ppm, from 1.45 to 1 ppm and from 1 to 0.7 ppm. The reference lipids were obtained by sequential ultracentrifugation and correspond to cholesterol and triglycerides for three lipoprotein particle fractions (VLDL, LDL and HDL).

The method of the invention allows to obtain an advanced lipoprotein profile, as shown in Table 1. The ALT reports for three representative subjects from the whole group are summarized in Table 1 for illustration purposes. Subject 1 was normolipidemic, subject 2 presented high LDL cholesterol levels (hypercholesterolemic) and subject 3 presented high triglycerides and low HDL cholesterol levels (atherogenic dyslipidemia). The method of the invention provides total cholesterol (C), triglycerides (TG) and particle concentration (P) for the main lipoprotein fractions and their subclasses. Additionally, the method of the invention provides the size of the main lipoprotein fractions. Subject 1 showed normal lipid levels (defined as VLDL-TG<150 mg/dL, LDL-C<160 mg/dL, and HDL-C>40 mg/dL), subject 2 showed elevated LDL-C and normal VLDL-TG and HDL-C levels, and subject 3 showed elevated VLDL-TG, decreased HDL-C and normal LDL-C levels. It should also be pointed out that subject 3 had increased LDL-P despite normal LDL-C levels and that its small LDL-P concentration was higher than in subject 2. Thus, subjects with elevated triglycerides levels are

## Chapter 2

associated with increased LDL-P values because an increase in triglyceride concentration leads to the formation of greater concentrations of smaller LDL particles.

Advanced lipoprotein tests have shown statistical associations between these lipoprotein parameters and the risk for cardiovascular disease<sup>67</sup>. For example, in a study, the number of HDL particles (HDL-P), but not the high-density lipoprotein cholesterol (HDL-C) concentrations, were independently associated with carotid intima-media thickness, after adjusting for covariates<sup>68</sup>. Finally, the use of lipoprotein particle subclasses improved NMR-derived risk stratification for subclinical atherosclerosis compared with conventional lipid measures in the prediction models with risk factors of the Framingham risk score<sup>69</sup>.

### **CLAIMS**

1. An *in vitro* method for the characterization of lipoproteins in a sample, comprising the following steps:

- obtaining a 2D diffusion-ordered <sup>1</sup>H-NMR spectrum of the sample;
- performing a surface fitting of a portion of the spectrum corresponding to the methyl signal using a plurality of model functions, each model function corresponding to a given particle size associated to a lipoprotein fraction and subclass and including at least one model parameter to be estimated during the fitting, the estimated model parameters being the set of model parameters for which the difference between the NMR signal and the model signal built as a linear combination of the model functions is minimized, and

- identifying the lipoproteins present in the sample as those associated to the model functions contributing to the theoretical model signal resulting from the fitting,

wherein each model function is a triplet of lorentzian functions having the form:

$$\begin{aligned} \text{Triplet} = & \text{Lorentzian}(h_1, f - f_0, w, D) + \text{Lorentzian}(h_2, f, w, D) \\ & + \text{Lorentzian}(h_3, f + f_0, w, D), \end{aligned}$$

where  $h(\text{au})$ ,  $f(\text{ppm})$ ,  $w(\text{ppm})$ , and  $D(\text{cm}^2\text{s}^{-1})$  are, respectively, the intensity, chemical shift, width, and diffusion coefficient associated to a lipoprotein particle size, wherein the model parameters to be determined for each lipoprotein particle size are one or several from:  $f$ ,  $f_0$ ,  $h_1$ ,  $h_2$ ,  $h_3$ ,  $w$  and  $D$ ,

wherein for each model function:

$$h_1 = \alpha \cdot h_2, \text{ with } \frac{1}{4} \leq \alpha \leq \frac{3}{4}, \text{ and}$$

$$h_3 = \beta \cdot h_2, \text{ with } \frac{1}{4} \leq \beta \leq \frac{3}{4},$$

wherein the surface fitting is performed fixing at least one model parameter and using at least one other model parameter as a free parameter to be determined in the surface fitting, and

wherein the fixed model parameters are determined based on the lipoprotein particle size and on regression models, the regression models relating pairs of fixed model parameters and/or a model parameter and the lipoprotein particle size.

2. The *in vitro* method according to claim 1, wherein the triplets of lorentzian functions have the form:

$$\begin{aligned} \text{Triplet} = & \text{Lorentzian}(h_1, f - f_0, w, D) + \text{Lorentzian}(h_2, f, w, D) \\ & + \text{Lorentzian}(h_1, f + f_0, w, D) \end{aligned}$$

## Chapter 2

3. The *in vitro* method according to any of the previous claims, wherein

$$h_1 = \frac{h_2}{2}, \text{ and/or}$$

$$f_0 = 0.01 \text{ ppm.}$$

4. The *in vitro* method according to any of the previous claims, wherein the lipoprotein particle sizes are defined based on NMR, HPLC, Gradient Gel Electrophoresis or Atomic Force Microscope experiments.

5. The *in vitro* method according to any of the previous claims, wherein at least one of the chemical shifts, width, and diffusion coefficient is fixed and at least the signal intensity of the central lorentzian ( $h_2$ ) is used as a free parameter.

6. The *in vitro* method according to any of the previous claims, wherein the regression models used are obtained from the deconvolution of the methyl signal of a plurality of NMR spectra using a plurality of model lorentzian functions with the intensity, chemical shift, width, and diffusion coefficient being free model parameters estimated to minimize the difference between the NMR methyl signal and the model signal built as a linear combination of the model functions, the regression models respectively relating at least (i) the chemical shift and the lipoprotein particle size, and/or (ii) the width and the lipoprotein particle size.

7. The *in vitro* method according to any of claims 1 to 5, wherein the regression models relating pairs of model parameters and/or a model parameter and the lipoprotein particle size are built according to the following steps:

- obtaining a 2D diffusion-ordered  $^1\text{H}$ -NMR spectrum for a plurality of



samples;

- for each sample, performing a surface fitting of a portion of the spectrum corresponding to the methyl signal using a plurality of model functions, each model function being dependent on the model parameters to be fixed, wherein all the model parameters to be fixed are estimated during the surface fitting as the set of model parameters for which the difference between the NMR signal and the model signal built as a linear combination of the model functions is minimized, and
- using the model parameters estimated in the previous step to build regression models relating pairs of model parameters and/or a model parameter and the lipoprotein particle size,

wherein the model functions used are preferably lorentzian function triplets of the form:

$$\begin{aligned} \text{Triplet}_j = & \text{Lorentzian}(h_{1j}, f_j - f_{0j}, w_j, D_j) \\ & + \text{Lorentzian}(h_{2j}, f_j, w_j, D_j) \\ & + \text{Lorentzian}(h_{3j}, f_j + f_{0j}, w_j, D_j). \end{aligned}$$

8. The *in vitro* method according to any of the previous claims, wherein the plurality of samples used to build the regression models comprise at least 100 samples and a percentage of at least 9% of the samples corresponds to individuals having a profile of diabetes mellitus and at least 25% of these patients having a profile of atherogenic dyslipidaemia.

9. The *in vitro* method according to any of the previous claims, wherein the diffusion coefficient of the model functions is estimated from the lipoprotein particle size by means of the Einstein Stokes equation

$$D = \frac{kT}{6\pi\eta R_H}$$

## Chapter 2

with  $k$  ( $J K^{-1}$ ) being Boltzmann constant,  $T$  (K) temperature,  $\eta$  (Pa s) viscosity and  $R_H$  ( $\text{\AA}$ ) the lipoprotein particle size.

10. The *in vitro* method according to any of the previous claims, the method further including correcting the estimated diffusion coefficients to take into account dilution effects, based on a relation between the NMR area and the diffusion coefficient obtained for several dilutions of a sample wherein the sum of the concentration of total cholesterol and triglycerides of said sample is higher than 300 mg/dL.

11. The *in vitro* method according to any of the previous claims, further comprising determining one or more of: average size of lipoprotein particle fractions, average size of lipoprotein particle subclasses, fraction and/or subclass lipoprotein particle concentration, lipid concentration of at least one lipoprotein particle fraction and/or lipid concentration of at least one lipoprotein particle subclass.

12. The *in vitro* method according to claim 11, wherein the average particle size of a lipoprotein particle fraction is determined as:

$$Size (\text{\AA}) = \frac{\sum_{j=1}^n R_j * PN_j}{\sum_{j=1}^n PN_j},$$

$n$  being the number of lipoprotein particle subclasses included in the lipoprotein particle fraction,  $R$  ( $\text{\AA}$ ) being the lipoprotein particle size and  $PN_j$  being the particle number for said lipoprotein particle size, wherein the particle number ( $PN$ ) for a lipoprotein  $j$  is determined as:

$$PN_j \propto \frac{A_j}{R_j^3}$$

with  $A$ (au) being the area associated to each model function.

13. The *in vitro* method according to any of the previous claims, wherein the area associated to a lipoprotein model function is corrected

to consider only the contribution of the lipids included in the lipoprotein particle core.

14. The *in vitro* method according claim 13 wherein the corrected area ( $A'$ ) is determined using the following expression:

$$A' = A \cdot \frac{(9 \cdot (R - s)^3)}{[(9 \cdot (R - s)^3) + 6 \cdot p \cdot (R^3 - (R - s)^3)]}$$

with  $A$  (au) and  $R$ (Å) being respectively the area and lipoprotein particle size associated to each model function,  $s$ (Å) being the lipoprotein particle shell thickness and  $p$  being the ratio of protein mass in the shell of the particle relative to the total mass in the particle shell.

**Table 1.** Summary of lipoprotein parameters using the method of the invention.

		Subject 1	Subject 2	Subject 3
Lipids (mg/dL)	VLDL-TG	13.7	22.6	150.3
	LDL-C	105.4	161.8	127.0
	LDL-TG	14.9	20.9	18.4
	HDL-C	66.5	49.5	34.4
	HDL-TG	7.1	6.6	11.0
Particle Concentration*	VLDL-P	12.4	22.0	106.3
	Large VLDL-P	0.2	0.3	5.9
	Medium VLDL-P	1.0	1.9	21.6
	Small VLDL-P	11.1	19.7	78.8
	LDL-P	980.6	1399.1	1230.4
	Large LDL-P	80.0	184.3	23.7
	Medium LDL-P	212.4	406.8	310.5
	Small LDL-P	688.2	808.0	896.1
	HDL-P	32.2	27.1	25.9
	Large HDL-P	2.4	1.3	0.3
Medium HDL-P	10.0	6.8	3.6	
Small HDL-P	19.8	19.0	22.0	
Size (nm)	VLDL	39.0	38.9	42.2
	LDL	19.7	20.1	19.5
	HDL	8.2	8.0	7.8

\*VLDL/LDL: nmol/L; HDL:  $\mu$ mol/L

## Chapter 2

### **2.3.2 Industrial Development**

As it was mentioned before in the introduction of this section, the research group in which the technology was developed was part of the Metabolomic Platform (MP), a joint research facility created by URV, CIBERDEM and also partners with the IISPV, whose main goal is to offer metabolomic services to the biomedical and clinical research groups from CIBERDEM and URV. However, the specific industrial development of the Liposcale test which includes an optimization of the production process and the creation of the proper regulatory environment for clinical applications necessary to introduce a competitive test in the market was outside of the scope of the MP.

As a consequence, Biosfer Teslab was created as an independent institution to carry out these tasks. Since its creation, Biosfer has worked to provide analytical services to study, diagnose and treat alterations in lipid metabolism and its associated cardiovascular risk. The aim of the company is to become the European benchmark for biofluid analysis, by using high performance technologies that allow clinicians to provide better tools for diagnosis and treatment of metabolic diseases.

The company's strategy in the medium to long term is based on a constant commitment to biomedical research through collaboration with different groups and scientific societies at international level and participation in different clinical studies, to favor the company's position over potential competitors by distinguishing it with the technological know-how in the field of advanced nuclear magnetic resonance tests.

To consolidate the strategy, the company initially wagers on a mixed business model in which alliances are generated with research centres equipped with NMR spectrometers, allowing Biosfer to act as a clinical analysis laboratory in both a research and a clinical environment. This first stage of market development precedes the association, via the licensing of the technology, with specialized laboratories with the necessary analytical capacity to deal with large volumes of samples once the market has matured.

In this regard, Biosfer Teslab is currently partner to different agreements of clinical and scientific collaboration: with the Spanish Nephrology Society and with the Spanish Arteriosclerosis Society to generate the scientific-based on evidences to facilitate the introduction of the ALT tests to the clinic; and with the Institute of Health Research (INCLIVA) and the Principe Felipe Research Institute (CIPF) of Valencia, the Andalusian Center for Nomedicine and biotechnology (BIONAND) and The Institute of Physical Chemistry "Rocasolano" (IQFR-CSIC); excellence centres for  $^1\text{H}$ -NMR spectroscopy, with the objective to ensure the production capability enabling alternatives NMR facilities.

Therefore, the cross-validation procedures between laboratories for the use of the spectrometers of these institutes for the application of the Liposcale test are being successfully developed (See figure below).

## Chapter 2

		Bruker				JEOL
		600 MHz cryo	600 MHz	500 MHz	400 MHz	400 MHz
URV	Intact serum	BT Protocol	BT Protocol	BT Protocol		
	275 uL dil	BT Protocol	BT Protocol	BT Protocol		
	200 uL dil		BT Protocol	BT Protocol		
	100 uL dil		BT Protocol			
INCLIVA	275 uL dil		BT Protocol			
CIPF	275 uL dil			BT Protocol		
BIONAND	275 uL dil		Bruker Protocol			
IFQR	275 uL dil		BT Protocol			
UK	275 uL dil					

Completed
Pending

**Figure 1. NMR Cross-validation for Liposcale application.** The Figure illustrates the status of the cross-validation processes with the different centres, spectrometers and dilution protocols.

As previously said, Biosfer Teslab obtained the advanced lipoprotein test based on two-dimensional NMR spectrum for the clinical study of lipoproteins created in a pure research framework. To adapt the Liposcale test to the needs of the market in terms of versatility and price, the company opts for a process of constant optimization that began with the migration of the software used in its creation (MATLAB) to the free software Phyton. This migration ensured the possibility to integrate all the programming routines in a closed and automatized software, reduced the computational time and, at the same time, diminished dramatically the production costs, since Python is a free open source platform.



## Chapter 2

Government of Catalonia, and it is expected to be forthcoming in the first quarter of 2018 as illustrated below:

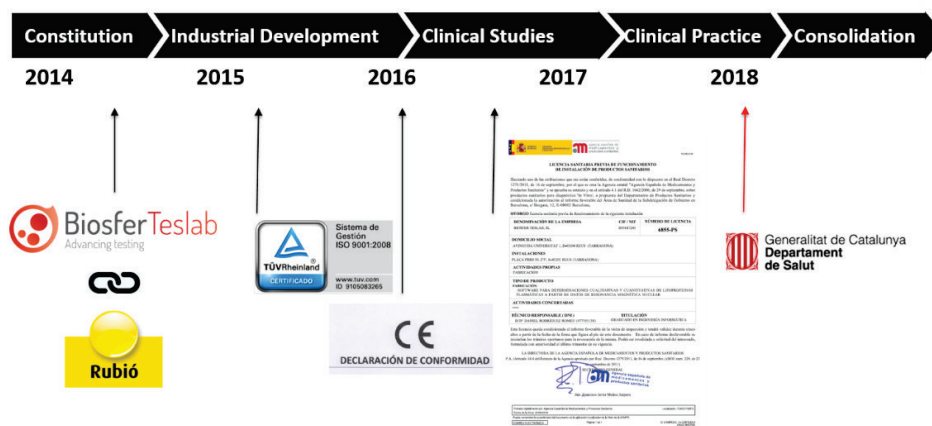


**Figure 3.** Main milestones reached since 2014.

To be able to execute the industrial development of the Liposcale test, as well as to open lines of research for the glycoproteins, low molecular weight metabolites (LMWM) and lipidomic characterization by using NMR technology that complement it, the company has received several public competitive aids detailed in the following figure:

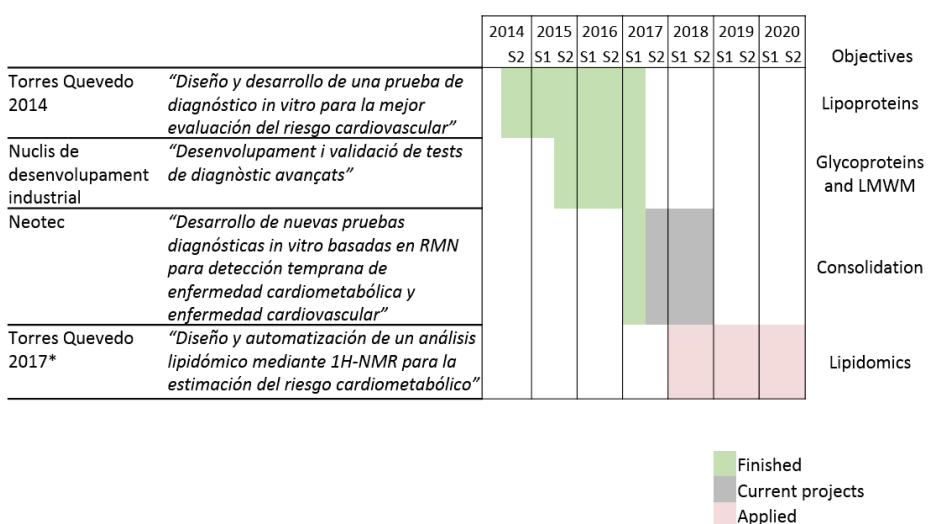


**Figure 4.** Research lines of Biosfer Teslab.



In short, the development of new advanced tests will involve the commercialization of new systems for the evaluation of cardiovascular problems using a technology (NMR) which is currently not used in this field and which represents significant improvements in the results, compared to the existing tests on the current market. The development of these tests therefore will suppose a qualitative leap for Biosfer that will position the company among the leaders in the fields of biofluid analysis by high performance technologies, since once the signals obtained by NMR are characterized, the tests will combine this information with classical values to predict major vascular complications such as subclinical atherosclerosis, arterial stiffness, insulin resistance and the clinical status of patients.

Health care system does not offer currently any similar services since advanced tests are not included in any clinical guide at national level and clinical analyses carried out to evaluate the cardiovascular risk include only a basic lipid profile of cholesterol and triglycerides. By contrast, American and Canadian endocrinology guidelines are opening the door to the incorporation of advanced resonance-based tests, such as advanced lipoprotein tests, to include the concentration of LDL particles below a limit as a therapeutic target, a parameter obtained from tests based on NMR.

Company's consolidation will be effective from the time it enters the clinical market by licensing of the technology to specialized laboratories. To this end, the company is wagering on participation in different clinical studies to generate scientific evidence, product

## Chapter 2

attributes for different clinical applications and dissemination to the national and international clinical community with the current characterization of lipoproteins, as well as complementing the current lipoprotein test with other metabolites to be distinguished from the competition.

### 2.3.3 Clinical applications developed by Biosfer Teslab

With the ultimate goal of basic research being moved to clinical practice, the Biosfer team has promoted scientific-based research studies in order to generate more clinical evidence in collaboration with other entities.

The advanced lipoprotein test, together with the complete molecular profiling in which Biosfer is currently working on (i.e. the glycoprotein, the low molecular weight metabolite and the lipidic extract characterization by NMR), has been applied in different fields of application in a collaborative framework, being the PhD candidate an active part of the research groups. The following table summarizes these specific collaborations:

**Table 1.** Research collaboration studies in which the Liposcale test has been applied.

	Institution	Field	Liposcale	GLYC	LMWM	Extracts	Congresses	Articles	
2014	HUJXXIII	Head and neck cancer							
	CLINIC	DM2						70,71	
2015	HSCSP	Nutritional intervention							
	Carlos Haya	Obesity							72
	HUSJ	Preservation studies							
	Carlos Haya	LALD							
	VHIR	Postprandial response							
	NC University	Nutritional intervention							73,74
	HUJXXIII	VIH							
	HUJXXIII	DM1							
	HUSJ	PCSK9							75,76
	INCLIVA	CVD							
	HUSJ	DM2 – arteriosclerosis							



## Chapter 2

In this way, the Lipidic Contour was developed to summarize complete set of the lipoprotein variables obtained by using DOSY-NMR in relation to developing cardiovascular disease in the future.

The following figure exemplifies the previous concept (considering only lipoprotein profile parameters that are clearly associated with atherosclerotic processes): the arterial contour represents the patient's profile (orange contour) with respect to mean values from a general population, represented by a black circle. The area defined by the patient's arterial contour decreases when its profile is associated with higher cardiovascular risk (i.e. values higher than the reference population's mean for VLDL-C, VLDL-TG, VLDL-P, LDL-C, LDL-TG, S-LDL-P, HDL-TG variables; or lower than reference population's mean for LDL-Z, HDL-Z and M-HDL-P variables). Variables contributing to a decrease in the arterial contour area are marked in red, while variables that contribute to an increase in the arterial contour area are marked in green. Variables whose values are close to the reference population's mean appear in yellow.

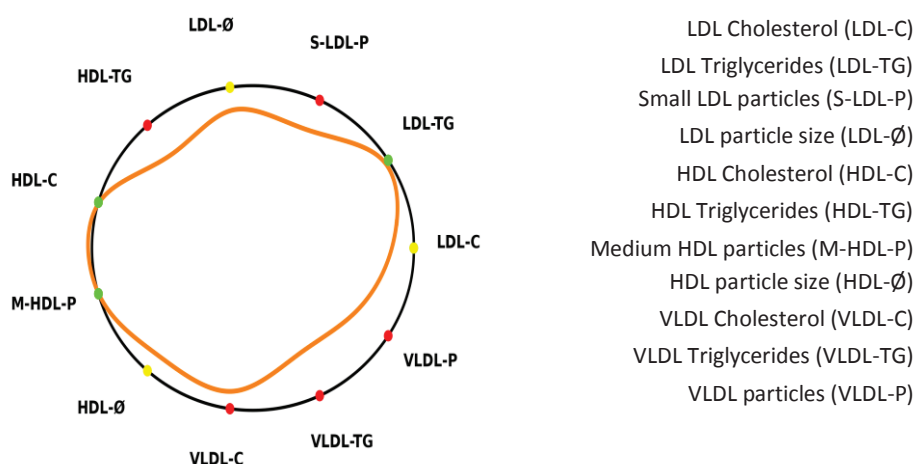


**Figure 5.** Example of a Lipidic Contour.

## **2.4 References**



1. Vance, D. E. & Vance, J. E. *Biochemistry of lipids, lipoproteins and membranes*. (Elsevier, 2008).
2. Crook, M. A. *et al.* CLINICAL BIOCHEMISTRY & METABOLIC MEDICINE. *Clin. Biochem. Metab. Med.* (2012).
3. Rosenson, R. S. *et al.* HDL measures, particle heterogeneity, proposed nomenclature, and relation to atherosclerotic cardiovascular events. *Clin. Chem.* **57**, 392–410 (2011).
4. Carmena, R., Duriez, P. & Fruchart, J.-C. Atherogenic Lipoprotein Particles in Atherosclerosis. *Circulation* **109**, III-2-III-7 (2004).
5. Sachdeva, A. *et al.* Lipid levels in patients hospitalized with coronary artery disease: An analysis of 136,905 hospitalizations in Get With The Guidelines. *Am. Heart J.* **157**, 111--117.e2 (2009).
6. Millán, J. *et al.* Lipoprotein ratios: Physiological significance and clinical usefulness in cardiovascular prevention. *Vasc. Health Risk Manag.* **5**, 757–65 (2009).
7. Lewis, G. F. & Rader, D. J. New Insights Into the Regulation of HDL Metabolism and Reverse Cholesterol Transport. *Circ. Res.* **96**, 1221–1232 (2005).
8. Cromwell, W. C. & Otvos, J. D. Low-density lipoprotein particle number and risk for cardiovascular disease. *Curr. Atheroscler. Rep.* **6**, 381–387 (2004).
9. Redgrave, T. G., Roberts, D. C. & West, C. E. Separation of plasma lipoproteins by density-gradient ultracentrifugation. *Anal. Biochem.* **65**, 42–9 (1975).
10. Kunitake, S. T. & Kane, J. P. Factors affecting the integrity of high density lipoproteins in the ultracentrifuge. *J. Lipid Res.* **23**, 936–40 (1982).
11. Kulkarni, K. R., Garber, D. W., Marcovina, S. M. & Segrest, J. P. Quantification of cholesterol in all lipoprotein classes by the VAP-II method. *J. Lipid Res.* **35**, 159–68 (1994).
12. Toshima, Gen and Iwama, Yuka and Kimura, Fumiko and Matsumoto, Yukie and Miura, Mizuho and Takahashi, Junichiro and Yasuda, Hidemi and Arai, Nobuaki and Mizutani, Hisashi and Hata, K. and others. LipoSERCH; Analytical GP-HPLC method for lipoprotein profiling and its applications. *J Biol Macromol* **13**, 21-- 32 (2013).

## Chapter 2

13. Rainwater, D. L. *et al.* Production of polyacrylamide gradient gels for the electrophoretic resolution of lipoproteins. *J. Lipid Res.* **33**, 1876–81 (1992).
14. Savorani, F., Rasmussen, M. A., Mikkelsen, M. S. & Engelsen, S. B. A primer to nutritional metabolomics by NMR spectroscopy and chemometrics. *Food Res. Int.* **54**, 1131–1145 (2013).
15. Lindon, J. C., Nicholson, J. K., Holmes, E. & Everett, J. R. Metabonomics: Metabolic processes studied by NMR spectroscopy of biofluids. *Concepts Magn. Reson.* **12**, 289–320 (2000).
16. Kroon, P. The order-disorder transition of the core cholesteryl esters of human plasma low density lipoprotein. A proton nuclear magnetic resonance study. *J. Biol. Chem.* (1981).
17. Ala-Korpela, M. Serum nuclear magnetic resonance spectroscopy: one more step toward clinical utility. (2015).
18. Mallol, R., Rodriguez, M. A., Brezmes, J., Masana, L. & Correig, X. Human serum / plasma lipoprotein analysis by NMR : Application to the study of diabetic dyslipidemia. (2012). doi:10.1016/j.pnmrs.2012.09.001
19. Aru, V. *et al.* Quantification of lipoprotein profiles by nuclear magnetic resonance spectroscopy and multivariate data analysis. *TrAC Trends Anal. Chem.* **94**, 210–219 (2017).
20. Jeyarajah, E. J., Cromwell, W. C., Otvos, J. D. & al., et. Lipoprotein particle analysis by nuclear magnetic resonance spectroscopy. *Clin. Lab. Med.* **26**, 847–70 (2006).
21. Otvos, J. D., Jeyarajah, E. J. & Bennett, D. W. Quantification of plasma lipoproteins by proton nuclear magnetic resonance spectroscopy. *Clin. Chem.* **37**, (1991).
22. Otvos, J. D. Measurement of lipoprotein subclass profiles by nuclear magnetic resonance spectroscopy. *Clin. Lab.* **48**, 171–80 (2002).
23. Baumstark, D., Pagel, P., Eiglsperger, J., Pfahlert, V. & Huber, F. NMR-Spektroskopie – ein modernes Werkzeug zur Serum-Analytik von Lipoproteinen und Metaboliten. *LaboratoriumsMedizin* **38**, 137–149 (2014).
24. Soininen, P., Kangas, A. J., Würtz, P., Suna, T. & Ala-Korpela, M. Quantitative Serum Nuclear Magnetic Resonance Metabolomics in



- Cardiovascular Epidemiology and Genetics. *Circ. Cardiovasc. Genet.* **8**, (2015).
25. Mallol, R. *et al.* Liposcale: a novel advanced lipoprotein test based on 2D diffusion-ordered 1H NMR spectroscopy. *J. Lipid Res.* **56**, 737–746 (2015).
  26. Aulchenko, Y. S. *et al.* Loci influencing lipid levels and coronary heart disease risk in 16 European population cohorts. *Nat. Genet.* **41**, 47–55 (2009).
  27. Stokes, Y. M., Salmond, C. E., Carpenter, L. M. & Welby, T. J. Stability of total cholesterol, high-density-lipoprotein cholesterol, and triglycerides in frozen sera. *Clin. Chem.* **32**, (1986).
  28. Beckonert, O. *et al.* Metabolic profiling, metabolomic and metabonomic procedures for NMR spectroscopy of urine, plasma, serum and tissue extracts. (2007). doi:10.1038/nprot.2007.376
  29. Orla Teahan, †,‡ *et al.* Impact of Analytical Bias in Metabonomic Studies of Human Blood Serum and Plasma. (2006). doi:10.1021/AC051972Y
  30. Wold, S., Sjöström, M. & Eriksson, L. PLS-regression: a basic tool of chemometrics. *Chemom. Intell. Lab. Syst.* **58**, 109–130 (2001).
  31. Saudland, A. *et al.* Interval Partial Least-Squares Regression (iPLS): A Comparative Chemometric Study with an Example from Near-Infrared Spectroscopy. *Appl. Spectrosc. Vol. 54, Issue 3, pp. 413-419* **54**, 413–419 (2000).
  32. Paoletti, R. & Kritchevsky, D. *Advances in lipid research. Volume 6.* (Academic Press, 1968).
  33. Kaess, B. *et al.* The lipoprotein subfraction profile: heritability and identification of quantitative trait loci. *J. Lipid Res.* **49**, 715–23 (2008).
  34. Rudel, L. L., Marzetta, C. A. & Johnson, F. L. Separation and analysis of lipoproteins by gel filtration. in 45–57 (1986). doi:10.1016/0076-6879(86)29061-8
  35. Nichols, A. V, Krauss, R. M. & Musliner, T. A. Nondenaturing polyacrylamide gradient gel electrophoresis. *Methods Enzymol.* **128**, 417–31 (1986).

## Chapter 2

36. Rainwater, D. L., Moore, P. H., Shelledy, W. R., Dyer, T. D. & Slifer, S. H. Characterization of a composite gradient gel for the electrophoretic separation of lipoproteins. *J. Lipid Res.* **38**, 1261–6 (1997).
37. Rainwater, D. L., Moore, P. H. & Gamboa, I. O. Improved method for making nondenaturing composite gradient gels for the electrophoretic separation of lipoproteins. *J. Lipid Res.* **45**, 773–5 (2004).
38. Rainwater, D. L. Lipoprotein correlates of LDL particle size. *Atherosclerosis* **148**, 151–158 (2000).
39. Lounila, J. *et al.* Effects of orientational order and particle size on the NMR line positions of lipoproteins. *Phys. Rev. Lett.* **72**, 4049–4052 (1994).
40. Jeyarajah, E. J. Development and Validation of a <sup>1</sup>H-NMR Method for Lipoprotein Quantification and Coronary Heart Disease Risk Assessment. (2005).
41. Grundy, S. M., Pasternak, R., Greenland, P., Smith, S. & Fuster, V. Assessment of Cardiovascular Risk by Use of Multiple-Risk-Factor Assessment Equations. *Circulation* **100**, (1999).
42. Otvos, J. D., Jeyarajah, E. J. & Cromwell, W. C. Measurement issues related to lipoprotein heterogeneity. *Am. J. Cardiol.* **90**, 22–29 (2002).
43. Forte, T. M. & Nordhausen, R. W. [26] Electron microscopy of negatively stained lipoproteins. in 442–457 (1986). doi:10.1016/0076-6879(86)28086-6
44. Campos, H. *et al.* Low density lipoprotein particle size and coronary artery disease. *Arterioscler. Thromb. Vasc. Biol.* **12**, (1992).
45. Ala-Korpela, M. <sup>1</sup>H NMR spectroscopy of human blood plasma. *Prog. Nucl. Magn. Reson. Spectrosc.* **27**, 475–554 (1995).
46. Ala-Korpela, M. *et al.* <sup>1</sup>H NMR-based absolute quantitation of human lipoproteins and their lipid contents directly from plasma. *J. Lipid Res.* **35**, 2292–2304 (1994).
47. Ala-Korpela, M. *et al.* A comparative study of <sup>1</sup>H NMR lineshape fitting analyses and biochemical lipid analyses of the lipoprotein fractions VLDL, LDL and HDL, and total human blood plasm. *NMR Biomed.* **6**, 225–233 (1993).

48. Surakka, I. *et al.* A Genome-Wide Screen for Interactions Reveals a New Locus on 4p15 Modifying the Effect of Waist-to-Hip Ratio on Total Cholesterol. *PLoS Genet.* **7**, e1002333 (2011).
49. Vehtari, A. & Mäkinen, V. A novel Bayesian approach to quantify clinical variables and to determine their spectroscopic counterparts in 1 H NMR metabonomic data. *Bmc* (2007).
50. Kvalheim, O. M. Interpretation of partial least squares regression models by means of target projection and selectivity ratio plots. *J. Chemom.* **24**, 496–504 (2010).
51. Bathen, T. F., Krane, J., Engan, T., Bjerve, K. S. & Axelson, D. Quantification of plasma lipids and apolipoproteins by use of proton NMR spectroscopy, multivariate and neural network analysis. *NMR Biomed.* **13**, 271–288 (2000).
52. Berhe, D. T. *et al.* Prediction of total fatty acid parameters and individual fatty acids in pork backfat using Raman spectroscopy and chemometrics: Understanding the cage of covariance between highly correlated fat parameters. *Meat Sci.* **111**, 18–26 (2016).
53. Savorani, F., Kristensen, M., Larsen, F. H., Astrup, A. & Engelsen, S. B. High throughput prediction of chylomicron triglycerides in human plasma by nuclear magnetic resonance and chemometrics. *Nutr. Metab. (Lond).* **7**, 43 (2010).
54. Kristensen, M. *et al.* NMR and interval PLS as reliable methods for determination of cholesterol in rodent lipoprotein fractions. *Metabolomics* **6**, 129–136 (2010).
55. Liu, M., Tang, H., Nicholson, J. K. & Lindon, J. C. Use of 1H NMR-determined diffusion coefficients to characterize lipoprotein fractions in human blood plasma. *Magn. Reson. Chem.* **40**, S83–S88 (2002).
56. Dyrby, M. *et al.* Analysis of lipoproteins using 2D diffusion-edited NMR spectroscopy and multi-way chemometrics. *Anal. Chim. Acta* **531**, 209–216 (2005).
57. Davidson, M. H. *et al.* Clinical utility of inflammatory markers and advanced lipoprotein testing: Advice from an expert panel of lipid specialists. *J. Clin. Lipidol.* **5**, 338–367 (2011).

## Chapter 2

58. Mallol, R. *et al.* Surface fitting of 2D diffusion-edited <sup>1</sup>H NMR spectroscopy data for the characterisation of human plasma lipoproteins. *Metabolomics* **7**, 572–582 (2011).
59. Johnson Jr, C. Diffusion ordered nuclear magnetic resonance spectroscopy: principles and applications. *Prog. Nucl. Magn. Reson. Spectrosc.* **34**, 203–256 (1999).
60. Gerszten, R. E. & Wang, T. J. The search for new cardiovascular biomarkers. *Nature* **451**, 949–952 (2008).
61. Brunzell, J. D. *et al.* Lipoprotein Management in Patients With Cardiometabolic Risk. *J. Am. Coll. Cardiol.* **51**, (2008).
62. Warnick, G. R. *et al.* Polyacrylamide gradient gel electrophoresis of lipoprotein subclasses. *Clin. Lab. Med.* **26**, 803–46 (2006).
63. Okazaki, M., Usui, S., Fukui, A., Kubota, I. & Tomoike, H. Component Analysis of HPLC Profiles of Unique Lipoprotein Subclass Cholesterols for Detection of Coronary Artery Disease. *Clin. Chem.* **52**, (2006).
64. Caulfield, M. P. *et al.* Direct Determination of Lipoprotein Particle Sizes and Concentrations by Ion Mobility Analysis. *Clin. Chem.* **54**, (2008).
65. Mallol, R. *et al.* Particle size measurement of lipoprotein fractions using diffusion-ordered NMR spectroscopy. *Anal. Bioanal. Chem.* **402**, 2407–2415 (2012).
66. Nelson, G. *Blood lipids and lipoproteins: quantitation, composition, and metabolism.* (1972).
67. Sniderman, A. & Kwiterovich, P. O. Update on the detection and treatment of atherogenic low-density lipoproteins. *Curr. Opin. Endocrinol. Diabetes Obes.* **20**, 140–147 (2013).
68. Mackey, R. H. *et al.* High-density lipoprotein cholesterol and particle concentrations, carotid atherosclerosis, and coronary events: MESA (multi-ethnic study of atherosclerosis). *J. Am. Coll. Cardiol.* **60**, 508–16 (2012).
69. Wurtz, P. *et al.* High-throughput quantification of circulating metabolites improves prediction of subclinical atherosclerosis. *Eur. Heart J.* **33**, 2307–2316 (2012).

70. Amor, A. J. *et al.* Nuclear magnetic resonance lipoprotein abnormalities in newly-diagnosed type 2 diabetes and their association with preclinical carotid atherosclerosis. *Atherosclerosis* **247**, 161–169 (2016).
71. Amor, A. J. *et al.* Relationship between noninvasive scores of nonalcoholic fatty liver disease and nuclear magnetic resonance lipoprotein abnormalities: A focus on atherogenic dyslipidemia. *J. Clin. Lipidol.* **11**, (2017).
72. Rodriguez-Garcia, E. *et al.* Characterization of lipid profile by nuclear magnetic resonance spectroscopy (<sup>1</sup>H NMR) of metabolically healthy obese women after weight loss with Mediterranean diet and physical exercise. *Medicine (Baltimore)*. **96**, e7040 (2017).
73. Dias, C. B. *et al.* Improvement of the omega 3 index of healthy subjects does not alter the effects of dietary saturated fats or n-6PUFA on LDL profiles. *Metabolism*. **68**, (2017).
74. Dias, C. B., Amigo, N., Wood, L. G., Correig, X. & Garg, M. L. Effect of diets rich in either saturated fat or n-6 polyunsaturated fatty acids and supplemented with long-chain n-3 polyunsaturated fatty acids on plasma lipoprotein profiles. *Eur. J. Clin. Nutr.* (2017). doi:10.1038/ejcn.2017.56
75. Girona, J. *et al.* Circulating PCSK9 levels and CETP plasma activity are independently associated in patients with metabolic diseases. *Cardiovasc. Diabetol.* **15**, (2016).
76. Ibarretxe, D. *et al.* Circulating PCSK9 in patients with type 2 diabetes and related metabolic disorders. *Clínica e Investig. en Arterioscler.* **28**, 71–78 (2016).
77. Ibarretxe, D. *et al.* Impact of epidermal fatty acid binding protein on 2D-NMR-assessed atherogenic dyslipidemia and related disorders. *J. Clin. Lipidol.* **10**, (2016).
78. Barrilero, R. *et al.* Unravelling and Quantifying the ‘nMR-Invisible’ Metabolites Interacting with Human Serum Albumin by Binding Competition and T2 Relaxation-Based Decomposition Analysis. *J. Proteome Res.* **16**, (2017).



**Chapter 3. Study of the HDL fraction of  
diabetic patients by diffusion edited  
<sup>1</sup>H-NMR spectroscopy**





## **3.1 Introduction**



In this section, we present the results of an intervention trial designed to evaluate quantitative and qualitative effects of niacin and fenofibrate on the HDL fraction in patients with type 2 diabetes. These results include the following two original research articles:

- Amigó, N., Mallol, R., Heras, M., Martínez-Hervás, S., Blanco Vaca, F., Escolà-Gil, J. C., Plana, N., Yanes, O., Masana, L. & Correig, X. (2016). **Lipoprotein hydrophobic core lipids are partially extruded to surface in smaller HDL: “Herniated” HDL, a common feature in diabetes.** *Scientific Reports*, 6, 19249.  
<https://doi.org/10.1038/srep19249>
- Masana, L., Cabré, A., Heras, M., Amigó, N., Correig, X., Martínez-Hervás, S., Real, J. T., Ascaso, J. F., Quesada, H., Julve, J., Palomer, X., Vázquez-Carrera, M., Girona, J., Plana, N. & Blanco-Vaca, F. (2015). **Remarkable quantitative and qualitative differences in HDL after niacin or fenofibrate therapy in type 2 diabetic patients.** *Atherosclerosis*, 238(2).  
<https://doi.org/10.1016/j.atherosclerosis.2014.12.006>

Both works include the HDL fraction analysis by NMR spectroscopy in the framework of a prospective, randomized controlled intervention trial entitled LOWHDL: Characterization of High Density Lipoprotein (HDL) in Type 2 Diabetes (T2D) After Fenofibrate or Niacin Treatment (NCT02153879), sponsored by the IISPV and lead by Professor Lluís Masana.



**3.2 Lipoprotein hydrophobic core lipids are partially extruded to surface in smaller HDL: “Herniated” HDL, a common feature in diabetes**



### 3.2.1 Abstract

Recent studies have shown that pharmacological increases in HDL cholesterol concentrations do not necessarily translate into clinical benefits for patients, raising concerns about its predictive value for cardiovascular events. Here we hypothesize that the size-modulated lipid distribution within HDL particles is compromised in metabolic disorders that have abnormal HDL particle sizes, such as type 2 diabetes mellitus (DM2). By using NMR spectroscopy combined with a biochemical volumetric model we determined the size and spatial lipid distribution of HDL subclasses in a cohort of 26 controls and 29 DM2 patients before and after two drug treatments, one with niacin plus laropiprant and another with fenofibrate as an add-on to simvastatin. We further characterized the HDL surface properties using atomic force microscopy and fluorescent probes to show an abnormal lipid distribution within smaller HDL particles, a subclass particularly enriched in the DM2 patients. The reduction in the size, force cholesterol esters and triglycerides to emerge from the HDL core to the surface, making the outer surface of HDL more hydrophobic. Interestingly, pharmacological interventions had no effect on this undesired configuration, which may explain the lack of clinical benefits in DM2 subjects.

### 3.2.2 Introduction

The International Diabetes Federation recently announced that, prior to 2014, over 387 million people had been diagnosed with diabetes<sup>1</sup>. Type 2 diabetes mellitus (DM2) accounts for at least 90% of the cases of diabetes and it is increasing every year due to genetic

## Chapter 3

factors and changes in lifestyle. A typical feature of DM2 – as well as obesity, insulin resistance and the metabolic syndrome – is atherogenic dyslipidemia, which has emerged as an important risk factor for cardiovascular disease (CVD)<sup>2</sup>. Atherogenic dyslipidemia consists of a triad of increased blood concentrations of small and cholesterol-depleted low-density lipoprotein (LDL) particles, decreased high-density lipoprotein cholesterol (HDL-C) and increased total triglycerides. It should be noted that it has become established therapeutic practice to increase HDL-C concentrations to decrease cardiovascular risk. However, despite the strong inverse association of HDL-C plasma levels with coronary heart disease found in epidemiological studies<sup>3,4</sup>, recent evidence has raised serious concerns about the ability of HDL-C concentration to assess cardiovascular risk and, hence, whether it should be a good target for therapeutic interventions<sup>5,6</sup>. Indeed, several recent clinical trials involving therapeutic elevation of HDL-C were prematurely terminated on the basis of futility<sup>7-9</sup>.

Recent structure-function studies have suggested that HDL-C is not such a good marker of cardiovascular risk because HDL concentration does not always reflect HDL function<sup>9-11</sup>. In some circumstances the potentially protective functions of HDL may be compromised despite high concentrations of HDL-C<sup>12</sup>. This highlights the need to characterize lipoprotein particles using a range of additional parameters such as size, particle number and chemical composition<sup>13</sup>, which is expected to improve the assessment of CVD risk and guide lipid-lowering therapies<sup>14</sup>.



In this context, the structure of lipoproteins has been inferred to date from compositional analyses using the classical theoretical description of Shen and colleagues<sup>15</sup>, by which the structure of circulating lipoproteins is consistent with a spherical model of radius  $r$  in which a spherical liquid core of cholesterol esters and triglycerides is surrounded by a monolayer of free cholesterol and phospholipids, with proteins closely packed with the hydrophilic head groups of phospholipids on the outer surface of the particle. On the basis of an updated version of the spherical model proposed by Shen et al. and experimental data on HDL by <sup>1</sup>H-NMR spectroscopy, the theoretical size of HDL particles has been estimated and a positive correlation found with the HDL-C/ApoA-I ratio<sup>16</sup>. In this regard, the emergence of experimental techniques mainly based on NMR spectroscopy makes it possible to characterize the size and particle number of lipoprotein particles<sup>16,17</sup>. This opens up a new scenario for studying lipoprotein structure and function. Specific HDL sizes (i.e., subclasses) and, in particular, the balance between large and small HDL particles seems to be important for evaluating cardiovascular risk<sup>13</sup>. Recent studies suggest that HDL particle number (HDL-P) may be a more suitable and independent risk factor than HDL-C<sup>18,19</sup> or a combination of both parameters, HDL-C/HDL-P, can determine the antiatherogenic function of HDLs, rather than either parameter alone<sup>20</sup>.

Yet despite these advances, if HDL particle size and number are to be used in clinical practice for cardiovascular risk management, the ability of existing techniques to estimate consistent HDL size, concentration and lipid content needs to be evaluated. Interestingly, the

## Chapter 3

development of these novel techniques has revealed that there is a discrepancy between the absolute values of HDL-P obtained by NMR and the values generated using the classical model of spherical lipoprotein structures proposed by Shen<sup>15</sup>. In particular, determination of HDL-P by NMR gives higher particle numbers than simulations based on the Shen model<sup>16</sup>. This discrepancy between experimental and theoretical data has led to modifications being made to the classical Shen model<sup>21,22</sup>. However, none of these studies have investigated the clinical implications of changes in the HDL structure.

Our study aims to gain greater insight into how some of the aforementioned HDL parameters are related (for example, the mean HDL size and the HDL subclass distribution), and how these parameters are affected by the lipid and protein concentrations in the healthy and the DM2 pathological state with atherogenic dyslipidemia. For this purpose, we used classical biochemical enzymatic techniques and advanced <sup>1</sup>H-NMR spectroscopy, atomic force microscopy (AFM) and fluorescence experiments to model the HDL structure and to characterize the size, and the molecular composition and distribution of the HDL fraction. We also determined the balance between the three main HDL subclasses – namely, large, medium and small HDL – and characterized the differences in surface hydrophobicity between them. Finally, we performed the same analysis on the DM2 group after two pharmacological interventions with fenofibrate and niacin, respectively.

### **3.2.3 Results**

***HDL fraction analysis: from the biochemical composition and size of HDL fractions to the modification of the Shen model***

The biochemical information of the HDL fractions determined by enzymatic assays is described in Table 1. As expected for DM2 patients, with the characteristic feature of low HDL cholesterol, all the HDL constituent molecules were significantly lower for the DM2 group than for the CT group, except triglycerides that were significantly higher. Figure 1 illustrates the differences between the mean radius of the HDL fractions obtained from DOSY  $^1\text{H-NMR}$  data ( $R_N$ ) and the mean radius derived from the Shen model ( $R_S$ ) for the CT group and the DM2 patients (see Section 1, SI). We observed that in both groups,  $R_S$  were higher than expected for the mean size of the HDL fractions.

**Table 1.** HDL biochemical composition (mg / dl) of CT population and DM2 patients.

	CT (26)	DM2 (29)	p
T	11.1 [10.2 12.9]	13.1 [11.1 16.9]	0.0
G			12
E	28.5 [21.3 32.3]	17.8 [14.6 22.1]	<0.
C			001
F	10.0 [8.5 12.2]	8.2 [6.2 9.5]	0.0
C			03
P	59.7 [49.1 68.9]	45.0 [41.6 50.1]	0.0
L			02
P	113.0 [97.8 127.8]	98.5 [87.0 105.0]	0.0
rot			07

Data are expressed as median  $\pm$  25-75. TG: triglycerides, EC: esterified cholesterol, FC: free cholesterol, PL: phospholipids, Prot: protein.

## Chapter 3

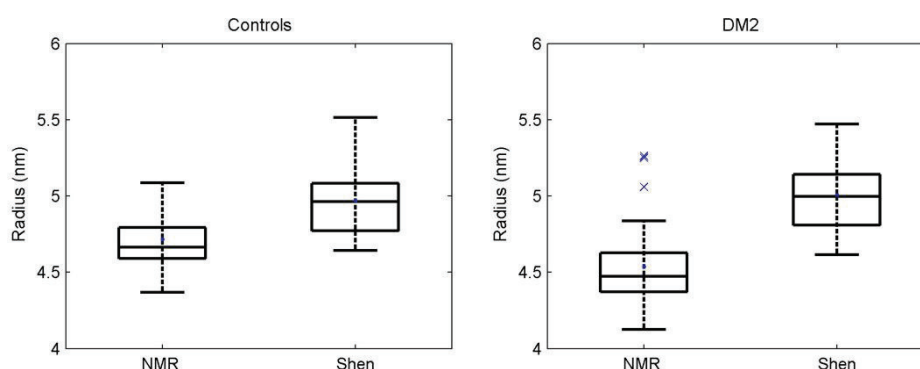


**Figure 1. Differences between the mean HDL radius measured by NMR and estimated by the Shen model.** The figure illustrates the differences between the mean radius obtained from NMR data and the radius derived from the Shen model for the CT group (n=26) and the DM2 patients (n=29).

Considering all the samples together, the mean radius measured by NMR was 4.6 [4.4-4.7] nm –expressed as median  $\pm$  [25-75] – which is consistent with previously reported HDL mean sizes considering the relative abundances of large, medium and small HDL particles<sup>19,23,24</sup>. On the other hand, the derived mean radius from the Shen model (see Materials and Methods Eq. 2) was 5.0 [4.8-5.1] nm in concordance to a distribution of HDL particles centred on large HDL particles. The p value between the  $R_N$  and  $R_S$  distributions was  $p < 0.001$ .

To solve the discrepancies between the biochemical composition and the experimental sizes, we newly modified the Shen model, increasing the geometrical ratio between surface volume ( $V_{\text{Shell}}$ ) and core volume ( $V_{\text{Core}}$ ) to obtain a better agreement between the biochemical composition and the experimental size, on the basis that smaller particles have a higher  $V_{\text{Shell}} / V_{\text{Core}}$  than larger particles. This modification led to some of the traditionally core lipids were located in the lipoprotein shell (see Materials and Methods). Table 2 reports the

main parameters obtained when our modified Shen model was used to analyse the HDL fractions. In agreement with current knowledge about lipoprotein disorders in DM2 patients, we found that the mean radius for the CT group determined by NMR was higher than for the DM2 group (4.7 nm and 4.5 nm, respectively) ( $p=0.002$ ). Interestingly, our modified model detected the presence of hydrophobic core lipids in the lipoprotein shell. The percentage of hydrophobic core lipids, basically esterified cholesterol (EC) and triglycerides (TG), occupying the external shell was 12% for the CT group, significantly less than the 20% found for the DM2 group ( $p=0.016$ ). This redistribution of the core lipids meant that 3% and 6% of the volume of the external shell was occupied by hydrophobic lipids in the CT and the DM2 groups, respectively ( $p=0.011$ ). In addition, the lipidic core composition was quite different: the percentage of the inner core occupied by TG was 30% for the CT group, much less than the 43% for the DM2 group ( $p<0.001$ ).

**Table 2.** HDL size and HDL lipid distribution between CT population and DM2 patients.

	CT (n=26)	DM2 (n=29)	P
Radius (nm)	4.7 [4.6 4.8]	4.5 [4.4 4.6]	0.002
% Core lipids in the surface	12 [0 20]	20 [13 27]	0.016
Relative Volume (%)			
Surface volume			
Core lipids	3 [0 6]	6 [4 7]	0.011
Prot	53 [51 56]	54 [51 56]	0.679
PL	37 [34 39]	34 [31 37]	0.022
FC	7 [6 8]	6 [5 7]	0.010
Internal core			

### Chapter 3

TG	30 [26 37]	43 [36 48]	<0.0001
EC	70 [63 74]	57 [52 64]	<0.0001

The table shows the mean HDL radius for the CT and the DM2 groups, the percentage (%) of the traditional core lipids (CL) located in the surface shell, and the percentage (%) of the surface volume occupied by the CL, the protein, the phospholipids and the free cholesterol; and the percentage (%) of the inner core volume occupied by the triglycerides and cholesterol. All the results are expressed as medians  $\pm$  25-75. Prot: protein, PL: phospholipids, FC: free cholesterol, TG: triglycerides, EC: esterified cholesterol.

The study design determined the plasma triglycerides levels of the DM2 subjects, and hence the HDL triglyceride levels, were significantly higher than those of the CT group. Independently, the mean size of the DM2 subjects was significantly reduced. Both conditions, high triglycerides and reduced size, were associated with a higher percentage of the core lipids in the surface, as these variables are correlated (see Section 2, SI, Figure S1 and Figure S2). In order to explore whether the redistribution of the core lipids in the surface was due to high TG or more specific reason for DM2, we analysed separately the association of the TG, the size and the percentage of core lipids in the surface for each group (see Section 2, SI, Fig S3). This analysis revealed a different behavior between the CT and the DM2 groups: while the levels of TG were highly associated with the percentage of the core lipids in the surface for the CT group (Pearson correlation coefficient  $r = 0.81$ ) this association was lost for the DM2 group ( $r = 0.35$ ). In the same direction, only the CT group presented a clear and inverse association between the size and the TG levels (see Section 2, SI, Fig S3). Therefore, the CT subjects with high TG levels presented a smaller size and, therefore, an increased percentage of core lipids in the surface. Alternatively, the levels of TG in the DM2 group were not associated with the size; being

possible to find subjects with low TG levels, and a reduced size, presenting a high percentage of hydrophobic core lipids in the surface. DM2, thus, was a clinical factor that emphasized the percentage of the core lipids in the surface independently of the TG levels.

The above results indicate differences in the composition and location of the hydrophobic lipids in the surface shell. The leakage of the hydrophobic lipids TG and EC to the surface may contribute to the change in polarity of the HDL surface and, in particular, the DM2 group should have a more hydrophobic HDL surface than the CT group. In order to verify the hypothesis that some of the core lipids are located in the surface shell, we carried out some fluorescence experiments to evaluate the surface polarity of lipoproteins. The fluorescent membrane probes are highly sensitive to the polarity of lipid membranes and lipid monolayers. We investigated the surface polarity of a subgroup of 8 CT subjects and 4 DM2 patients with three different membrane probes: Patman, Prodan and Laurdan. It has been widely reported that the fluorescence spectrum of these three probes in lipid membranes and in native lipoproteins and lipoprotein models is highly affected by the polarity of the microenvironment: a more hydrophobic microenvironment produces a blue shift of the emission maximum position<sup>25-27</sup>.

The fluorescence spectra of all three probes showed the same tendency: the wavelengths of the emission maxima ( $\lambda_{em}$ ) of the DM2 group were blue shifted, indicating that the surface microenvironment was more hydrophobic than in the CT group (see Section 3, SI Figure S4). The Prodan probe exhibited the clearest and best defined spectra,

## Chapter 3

which made it possible to quantify the different behaviour between groups. The emission wavelength was  $\lambda_{em} = 436.1$  nm for the CT group and  $\lambda_{em} = 434.1$  nm for the DM2 group, ( $p = 0.02$ ). To evaluate the dispersion of the measurements and facilitate the visualization of the differences between the CT and the DM2 group, we performed a principal component analysis (PCA) of the fluorescence raw data of two repetitions per sample (see Section 3, SI Figure S5).

### ***Application of the modified Shen model to the study of the HDL subclasses***

To further study the HDL fraction, we extended our modified Shen model to the three major HDL subclasses. We used the methylene signal of 1D diffusion-edited NMR spectra (LED) to obtain a qualitative picture of the distribution of particles in the three HDL subclasses (large, medium and small) which contain methylene groups in the constituting HDL molecules. The frequency at which the methylene groups of the lipids in lipoprotein particles resonate depends on the size of the particles that carry them. Larger particles resonate at higher frequencies<sup>28</sup>. We deconvoluted the methylene signal with a lorentzian curve for each of the three major HDL subclasses (see Materials and Methods) to mathematically reproduce the raw NMR data and compute the peak area of the methylene signal. Because the NMR peak areas are proportional to the concentration of molecules in solution, the area below each lorentzian curve of the methylene peak is proportional to the concentration of the methylene groups present in the cholesterol and triglyceride molecules carried by each HDL subclass and, hence,



proportional to the HDL particles of each subclass. Figure 2 shows that the CT group presented a higher percentage of the medium HDL particle subclass, than the DM2 group (41% and 34%, respectively) ( $p=0.014$ ). In contrast, the CT group presented a lower percentage of the small HDL subclass (42%) than the DM2 group (51%) ( $p=0.041$ ). The previous analysis of the mean sizes of the HDL fraction supported this distribution.

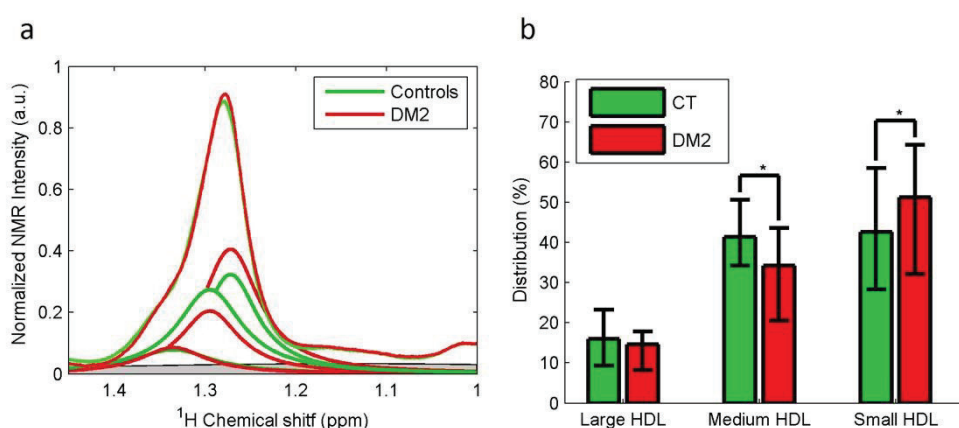


**Figure 2. Balance between large, medium and small HDL subclasses of CT population and DM2 patients.** a) The figure illustrates the average of the normalised NMR spectra and the means of the three lorentzian functions for the CT group ( $n=26$ ) and the DM2 patients ( $n=29$ ). The area under each curve represents the relative concentration of a particular subclass. b) % of integrated area. Data are expressed as medians  $\pm$  25-75.

Since no data were available on the biochemical composition and size for each subclass, we used the sizes and the concentrations of the molecules constituting each HDL subclasses described in the literature for healthy subjects<sup>23,29-32</sup>. We associated the large HDL subclass to HDL 2b, the medium HDL subclass to HDL 2a and the small HDL subclass to HDL 3<sup>33,34</sup>. The reported particle sizes were 6 nm, 5 nm and 4 nm for

## Chapter 3

large, medium and small HDL respectively, and the molecular composition of each subclass is detailed in Table S1 (see Section 4, SI).

Once the biochemical composition and size had been assigned, our modified model was applied to each subclass. As shown in Figure 3, our findings revealed that the small HDL subclass is much more affected by the space restrictions than the large or medium HDL subclasses. This has an effect on the proportion of core lipids in their surface shell. The resulting percentage of hydrophobic lipids increases as the size decreases: from 3% in the case of large HDL particles and 15% for the medium-sized particles, up to 56% for the smallest particles.

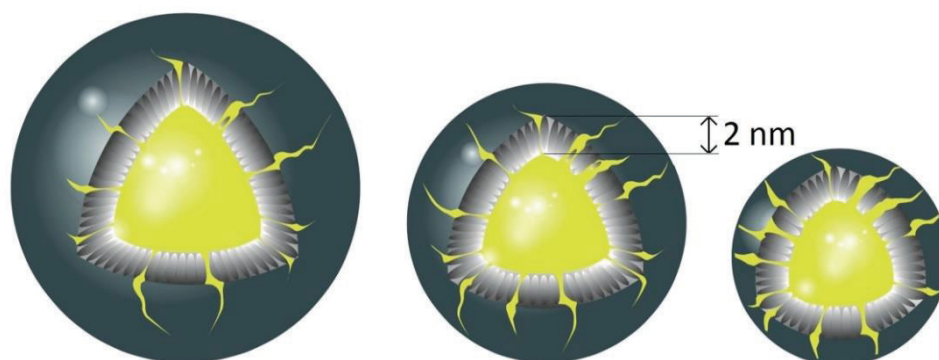


**Figure 3. Structural model for different subclasses of HDL particles.** The figure shows the differences in the amounts of core lipids located in the 2 nm shell depending on the lipoprotein size.

The mathematical models indicated that there were different amounts of hydrophobic lipids in the different HDL subclasses. We used Atomic Force Microscopy (AFM) to prove whether the surface polarity of lipoproteins depended on size. The size and the hydrophobicity of the HDL surface was qualitatively characterized as the adhesion force between the tip of the AFM probe (basically hydrophilic) and the

lipoprotein surface depends on the hydrophobic or hydrophilic nature of the sensed surface<sup>35,36</sup>.

Just as the model did, the AFM experiments showed that smaller particles had a more hydrophobic surface. We analyzed three different samples, and they all presented the same tendency: the adhesion force between the hydrophilic tip and the HDL surface was higher for large particles, indicating a more hydrophilic environment. The relation between the size and the adhesion force is represented in Figure S6 (see Section 5, SI). For the three samples, the correlation coefficients were 0.34, 0.52 and 0.36 respectively (p values 0.23, 0.01 and 0.19), revealing that as larger the particles were, they presented more hydrophilic surface (see Section 5, SI, Figure S7). These qualitative results reinforce the hypothesis that hydrophobic lipids in small particles rise to the surface.

***Characterization of the HDL fraction of DM2 subjects after fenofibrate and niacin treatments***

Finally, we characterized the HDL fraction of the DM2 group using two different, commonly used treatments with fenofibrate and niacin. As in the case above, we first used our modified Shen model to measure the lipid and protein concentrations (see Table 3) and the mean HDL size and obtain the fraction of the core lipids located in the external shell. Independently, we determined the HDL distribution in the large, medium and small subclasses by NMR.

**Table 3.** Treatment effects on the HDL biochemical composition (mg/dl) of DM2 patients.

	DM2	FF	p <sub>1</sub>	Ni	p <sub>2</sub>	p <sub>3</sub>
TG	13.3 [11.4 17.4]	12.9 [10.0 16.7]	0.149	13.3 [11.4 16.2]	0.192	0.702

### Chapter 3

EC	17.5 [14.6 22.1]	15.5 [13.7 22.0]	0.903	18.7 [14.5 25.3]	0.159	0.050
FC	8.5 [7.2 9.5]	6.9 [5.6 8.7]	0.027	7.9 [6.0 10.5]	0.931	0.023
PL	48.1 [42.8 51.9]	41.2 [37.6 53.6]	0.079	40.4 [31.6 56.0]	0.375	0.513
Prot	99.0 [86.8 112.0]	103.0 [81.8 114.5]	0.867	101.0 [87.8 126.0]	0.651	0.366

Data are expressed as medians  $\pm$  25-75 of the 24 DM2 subjects who finished both interventions. Comparative between the basal state and the post fenofibrate state ( $p_1$ ) and the post niacin state ( $p_2$ ); comparative between treatments ( $p_3$ ). FF: fenofibrate, Ni: niacin, TG: triglycerides, EC: esterified cholesterol, FC: free cholesterol, PL: phospholipids, Prot: protein.

Table 4 shows that neither of the treatments had any significant effect on the mean size and percentage (and the composition) of core lipids in the external shell, or the subclass distribution of the DM2 group. However, the effects of the treatments were quite different: the fenofibrate treatment tended to decrease the mean HDL size and the niacin treatment tended to increase it, leading to a statistically significant change in size when both treatments were compared ( $p=0.042$ ).

**Table 4.** Treatment effects on the HDL size and HDL lipid distribution of DM2 patients.

	DM2	FF	$p_1$	Ni	$p_2$	$p_3$
Radius (nm)	4.5 [4.4 4.6]	4.4 [4.4 4.7]	0.305	4.6 [4.3 4.7]	0.259	0.042
% Core lipids in the surface	20 [11 28]	22 [16 28]	0.578	15 [9 25]	0.532	0.484
Relative (%) volume						
Surface volume						
Core lipids	5 [4 7]	5 [4 7]	0.958	4 [2 8]	0.689	0.881
Prot	53 [50 56]	55 [53 59]	0.205	56 [53 58]	0.170	0.958
PL	35 [33 37]	33 [29 37]	0.305	31 [29 38]	0.170	0.434
FC	6 [5 7]	5 [4 6]	0.140	6 [6 7]	0.434	0.159
Internal core						

TG	43 [37 49]	40 [32 48]	0.434	40 [31 48]	0.205	0.217
EC	57 [51 63]	60 [52 68]	0.434	60 [52 69]	0.205	0.217

The table shows the treatment effects on the mean HDL radius, the percentage (%) of the traditional core lipids (CL) located in the surface shell, and the percentage (%) of the surface volume occupied by the CL, the protein, the phospholipids and the free cholesterol; and the percentage (%) of the inner core volume occupied by the triglycerides and cholesterol. All the results are expressed as medians  $\pm$  25-75 of the 24 DM2 subjects who finished both interventions. Comparative between the basal state and the post fenofibrate state ( $p_1$ ) and the post niacin state ( $p_2$ ); comparative between treatments ( $p_3$ ). FF: fenofibrate, Ni: niacin, Prot: protein, PL: phospholipids, FC: free cholesterol, TG: triglycerides, EC: esterified cholesterol.

As far as mean size is concerned, Figure 4 shows that the fenofibrate treatment tended to increase the relative concentration of the small HDL subclass, and that the niacin treatment tended to increase the relative concentration of the medium HDL subclass. These different effects were statistically significant when both treatments were compared ( $p=0.015$ ).

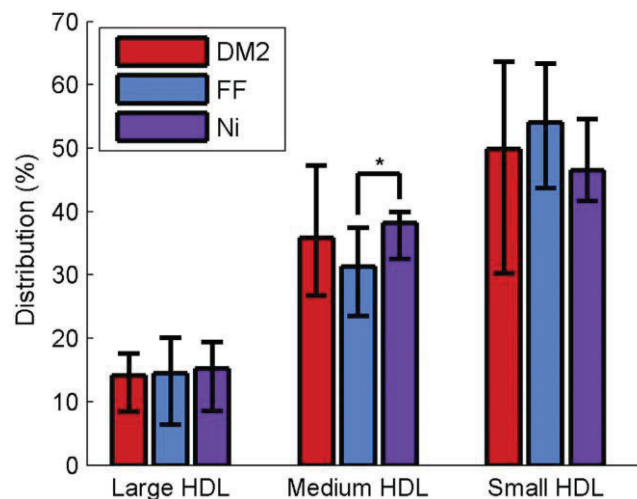


**Figure 4. Treatment effects on the balance between large, medium and small HDL subclasses of DM2 patients (% integrated area).** Data are expressed as medians  $\pm$  25-75 of the 24 DM2 subjects who finished both interventions. FF: fenofibrate, Ni: niacin.

### 3.2.4 Discussion

The current need to characterize HDL particles using a range of additional parameters such as size, particle number, subclass distribution and chemical composition increases since HDL-C does not always reflect HDL antiatherogenic function. Lipidomic and structural-function approaches suggest that the alterations of the lipidome<sup>37</sup> and the negatively charged enrichment of phospholipids<sup>38</sup> in the smaller HDL subfraction play a crucial role for HDL dysfunctionality.

Alternatively, the preceding analysis strongly supports the hypothesis that HDL functionality may be compromised in a pathological state such as DM2. Our results indicate that the HDL of a CT group is clearly different from that of a DM2 group, essentially due to the differences in HDL particle size and biochemical composition, and the implications for lipid relocation.

A reduction in size has consequences for the lipid distribution of HDL particles: Lipoproteins are spheres with a shell thickness of 2 nm that define an inner core cavity with a fixed volume. Therefore molecules are subject to spatial restrictions. The smaller the particle is, the tighter those spatial restrictions are. Thus, providing a lesser volume for hydrophobic lipids to rely on. Since volume of a sphere is proportional to the third power of its radius, the core volume is extremely sensitive to small changes in the radii. Consequently, as the pathological group has a smaller size, this phenomenon is emphasized.

To solve these spatial inconsistencies, we assumed that some of the lipids that are traditionally found inside the core (esterified cholesterol and triglycerides) have to rise to the lipoprotein surface for volumetric

reasons. Other modifications in the spherical model of lipoprotein structure have been reported previously: the spherical shape becomes more discoidal or cylindrical<sup>39</sup>, free cholesterol can be found in the inner core<sup>21,22</sup>, and proteins are closely packed on the outer surface of the particle<sup>15</sup>. All these three modifications increase the external shell volume and diminish the internal core volume. Consequently, the fraction of hydrophobic core lipids outside the lipoprotein shell also increases.

One of the limitations of our model is to consider that the entire volume of the apolipoproteins fills the surface shell, independently of the curvature radius. Energy derived computational models studying the stability of lipoprotein structure identify that the penetration of the alpha helices into the lipoprotein shell is modulated by the curvature radius, since they fill the space between the phospholipids head-groups<sup>40,41</sup>. The penetration of the amphiphilic helix alpha into the lipoprotein shell get higher as the size of the particles get smaller and more apolipoproteins are required to fill the gaps between phospholipids head-groups. The size-modulated integration of the apolipoprotein into the shell in the model would underestimate the surface volume of the HDL particles even more, increasing the fraction of the hydrophobic core lipids in the surface.

Another limitation of this study is to not consider the particular concentration and composition of the fatty acids (FA) chains constituting the TG and CE molecules. Also, hydrophobicity of TG is less than that of CE thus TG tends to be more readily exposed to the lipid-water interface. Furthermore, the TG exposure to the surface is likely to

## Chapter 3

be dependent on its miscibility in the phospholipid monolayer<sup>42</sup>. For that reason, the concentration and, particularly, the composition of the FA chains, might have an effect on the whole surface polarity of the HDL particles. Therefore, the change on the hydrophobicity of the small HDL particles induced by the presence of the core lipids in the surface in the DM2 group may be slightly reduced due to the increased concentration of TG molecules in the HDL particles. However, the modifications of the polarity due to the composition of the core lipids can be considered as a second order effect because CE is the major component for both, the CT and the DM2 group.

Fluorescence studies supported our hypothesis by providing experimental evidence that confirms that DM2 HDL particles have a different surface polarity. In our opinion, fluorescence is the only technique able to distinguish the polarity of the immediate surroundings of phospholipids because fluorescence dyes can be found among phospholipid molecules. The changes in the probe microenvironment are caused by the presence of hydrophobic lipid molecules instead of possible protein posttranslational modifications associated with the pathological state.

Both the high concentration of triglycerides in the HDL of the DM2 group and the higher number of small particles – which present the most abnormal lipids distribution – may explain the dysfunctional behaviour of HDL communicated by several researchers<sup>43,44-45</sup>. Moreover, the lipid composition of the hydrophobic lipids that leaks to the surface is significantly different<sup>44</sup>. The high concentration of triglycerides found in the DM2 group could accentuate the changes in



the surface polarity even more. The mechanisms behind these HDL changes are not well established. We communicated<sup>44</sup> that this group of diabetic patients have higher cholesterol-ester transfer protein activity, what could contribute to HDL smaller size and triglyceride enrichment.

The hydrophobic and hydrophilic forces regulating the molecular interaction between lipoproteins, enzymes and cell membranes, and the conformation of apolipoproteins may be compromised<sup>45-47</sup>.

Surprisingly, despite the benefits of the two treatments on the lipid content – lower triglyceride count and higher cholesterol – the pathological state is not totally reversed after 12 weeks treatment with either fenofibrate or niacin, although we cannot exclude a more extensive HDL reparation after longer intervention periods. One possible reason for this is that the changes in the HDL triglyceride concentration and the mean radius that modulates the lipoprotein particle distribution are not enough. Instead, they hamper the correct distribution of HDL lipids and force them to leak to the external lipoprotein shell like a *lipidic hernia*.

### 3.2.5 Methods

**Study subjects.** A complete description of the population has recently been published<sup>44</sup>. Briefly, 29 type 2 diabetic patients (DM2) were recruited: 18 male and 11 female, aged between 30 and 70 years old, and with HDL not exceeding 50 mg/dl in men or 60 mg/dl in women. The exclusion criteria were as follows: smoker, diagnosed with diabetes less than three months before, triglyceride levels above 400 mg/dl, glycated hemoglobin higher than 9%, albuminuria above 300

### Chapter 3

mg/mg creatinine, chronic kidney disease (estimated glomerular filtration rate  $<30$  ml/min/1.73 m<sup>2</sup>), advanced retinopathy, neuropathy, cardiovascular disease in the last three months, chronic liver insufficiency, neoplastic disease or any chronic or incapacitating disease. The CT group consisted of 26 age- and gender-matched subjects without diabetes and with HDL cholesterol higher than 40 mg/dl for men or 50 mg/dl for women. After a 6-week lipid-lowering drug wash-out, the patients with type 2 diabetes were randomly distributed into two groups. One group received 20 mg simvastatin plus 145 mg fenofibrate, and the other group received 20 mg simvastatin plus 2 g niacin plus laropiprant for a 12-week period. After a washout period of 6 weeks, they interchanged the treatments for 12 weeks more. At the end of the study, 24 DM2 patients finished both treatments after 5 discontinued interventions.

Fasting blood samples were collected in EDTA tubes and centrifuged immediately for 15 min at 4°C at 1500 x g at the basal point, after each intervention period in the DM2 group, and at the basal point in the CT group. Plasma samples were then kept at -80°C until further analysis. The entire study and all related experimental protocols were approved by the Ethical Committee of the Sant Joan University Hospital (Reus, Spain) and the Ethical Committee of the Clinical University Hospital (Valencia, Spain). All subjects provided their written informed consent before participating in the study. The study was carried out in accordance with the standards set by the Declaration of Helsinki and Good Clinical Practice guidelines.

**Lipoprotein fractionation and HDL analysis.** Prior to the NMR analysis, total HDL was isolated from plasma using sequential preparative ultracentrifugation at 1.21 g/ml density using previously described techniques<sup>48</sup>. Ultracentrifuged HDL (ucHDL) fractions were stored at -80°C until the biochemical studies were carried out. In the ucHDL fraction, cholesterol, triglycerides, total protein, phospholipids and apolipoproteins were quantified using enzymatic and nephelometric assays adapted to a COBAS 6000 autoanalyzer (Roche Diagnostics, Rotkreuz, Switzerland).

**NMR experiments.** <sup>1</sup>H-NMR spectra were recorded on a Bruker Avance III 600 spectrometer operating at 310 K using two different pulses: a 2-D double stimulated echo (DSTE) pulse program with 16 bipolar gradients to obtain the diffusion coefficients of HDL fraction as previously reported<sup>49</sup>; and a 1D diffusion-edited pulse sequence with bipolar gradients and longitudinal eddy-current delay (LED) scheme with two spoil gradients to determine the particle distribution between HDL subclasses. In both cases, the relaxation delay was 2 seconds and the Free Induction Decays (FIDs) were collected into 64 K complex data points and 64 scans per sample.

**Radius extraction.** DSTE methyl signal was fitted with one lorentzian curve to obtain the averaged diffusion coefficient ( $D_{coef}$ ) of the lipoprotein particles as previously reported<sup>50</sup>. Then, the hydrodynamic radii of the lipoprotein fractions ( $R_H$ ) were extracted from the Stokes-Einstein equation:

$$R_H = \frac{K_B T}{6\pi\eta D_{coef}} \quad (1)$$

## Chapter 3

where  $K_B$  is the Boltzmann constant,  $T$  is the temperature (310 K), and  $\eta$  is the mean viscosity of the solution ( $0.75 \pm 0.02$  mPa·s) measured at 310 K with a Cannon-Manning semi-micro capillary viscometer, in agreement with previous work<sup>49</sup>.

**Particle size distribution.** To obtain a qualitative picture of the size distribution of the HDL lipoproteins, we used the methylene signal from the LED NMR experiments. The methylene signal had enough resolution to be fitted with three lorentzians, one for each of the three different HDL subclasses (large, medium and small HDL). The area below each lorentzian curve is proportional to the concentration of particles of this particular subclass. Relative concentration of each subclass provides an estimation of the size distribution of HDL particles.

**Shen model.** We used the classical Shen model of a spherical lipoprotein particle as a starting point to estimate the mean HDL sizes for each sample. The Shen model describes lipoproteins as spheres with a surface shell 2 nm thick consisting of phospholipids (PL), proteins (Prot) and free cholesterol (FC) covering a hydrophobic core of esterified cholesterol (EC) and triglycerides (TG). Once the concentrations of these molecules had been measured (see Table 1), their associated volumes could be determined. The ratio between the volume of the surface shell and the volume of the internal core is related to the mean lipoprotein size as follows:

$$\frac{V_{Shell}}{V_{Core}} = \frac{\frac{4}{3}\pi R^3 - \frac{4}{3}\pi(R-2)^3}{\frac{4}{3}\pi(R-2)^3} = \frac{R^3}{(R-2)^3} - 1 \quad (2)$$

where the volume of the shell and the core was obtained from the concentration and the molecular volumes of each molecule:

$$V_{Shell} = [PL] \cdot v_{PL} + [Prot] \cdot v_{Prot} + [FC] \cdot v_{FC} \quad (3)$$

$$V_{Core} = [EC] \cdot v_{EC} + [TG] \cdot v_{TG} \quad (4)$$

**Modified Shen model.** The hypothesized discrepancies between the estimated mean sizes using the Shen model and the experimental ones, which were in agreement with the literature<sup>19,23,24</sup>, suggested that the lipid distribution within lipoprotein particles is not always well described by the Shen model. To solve these discrepancies, and on the basis that smaller particles have a higher  $V_{shell} / V_{Core}$  ratio than larger particles, we modified the classical spherical model to obtain a ratio for smaller sizes in order to some of the traditionally core lipids were located in the lipoprotein shell (increasing the  $V_{shell}$  and decreasing the  $V_{Core}$ ). The modified model is described in Equations 5, 6 and 7:

$$\frac{V_{Shell}^*}{V_{Core}^*} = \frac{R^3}{(R-2)^3} - 1 \quad (5)$$

$$V_{Shell}^* = V_{Shell} - V_{Core} \cdot \alpha \quad (6)$$

$$V_{Core}^* = V_{Core} \cdot (1 - \alpha) \quad (7)$$

## Chapter 3

where  $\alpha$  is the fraction of core lipids traditionally located in the surface shell.

Once the mean radii had been measured,  $\alpha$  was determined for each sample as follows: first, we computed the geometric ratio between the volume of the external part (the 2 nm shell) and the internal part (the core) using the measured radius in nm; and then, we determined  $\alpha$  by minimizing the difference between the biochemical ratio (right side of the Equation 8) and the geometrical ratio (left side) hence some of the core lipids could be located in the surface shell.

$$\frac{R^3}{(R-2)^3} - 1 = \frac{V_{Shell} + V_{Core} \cdot \alpha}{V_{Core} \cdot (1-\alpha)} \quad (8)$$

**Fluorescence study.** Three different fluorescent probes – Prodan, Patman and Laurdan – were purchased from SIGMA-ALDRICH and used to evaluate the surface properties of lipoproteins. The fluorescent probes were introduced into the samples as previously reported<sup>27</sup>. The fluorescence spectra of the probes in native HDL lipoproteins were recorded on a luminescence spectrofluorometer AMINCO Bowman Series 2 with a Quarzglas cuvette (Hellma), and the excitation wavelength was 350 nm. The fluorescence spectra were normalized with the maxima intensity equal to one.

**AFM experiments.** We used atomic force microscopy to measure the adhesion force between the tip of the AFM probe and the surface of the HDL particles on the basis of previously reported literature<sup>35,36</sup>. We obtained the topographic images as well as the adhesion force images by using the tapping force mode of AFM. The spring constant of the

cantilever was 0.31 N/m, the peak force amplitude was 100 nm and the peak force frequency was 2 KHz. We observed three samples and about 15 HDL particles per sample were measured. In order to quantitate the particle size and relate it to the adhesion force, the images were initially processed with the NanoScope software, Ver. 1.20r1sr3 (Veeco), and then exported to MATLAB, Ver. 7.9.0.529 (The MathWorks).

**Statistical analysis.** We performed two different statistical tests to detect differences between the variables studied: the mean size of the HDL fraction; the distribution between large, medium and small particles; and the distribution of the lipids traditionally found in the core (EC and TG) present in the lipoprotein shell. A statistical Mann-Whitney U test (two-tailed) was performed to identify significant differences between the CT and DM2 groups. This was followed by a Wilcoxon signed-rank test (two-tailed) to evaluate the treatment effects for paired samples (n=24). In the fluorescence experiments, a statistical Mann-Whitney U test (two-tailed) was performed to identify significant differences between the maximum position of the CT and DM2 spectra and a principal component analysis (PCA) was carried out using the emission spectra of the fluorescent probes as input variables.

### 3.2.6 References

1. Aguirre, F. *et al.* *IDF Diabetes Atlas: 6th edn*, <http://www.idf.org/diabetesatlas> (2013). (Date of access: 11/11/2015).
2. Chapman, M. J. *et al.* Triglyceride-rich lipoproteins and high-density lipoprotein cholesterol in patients at high risk of cardiovascular disease: evidence and guidance for management. *Eur. Heart J.* **32**, 1345–61 (2011).

### Chapter 3

3. Gordon, D. J. *et al.* High-density lipoprotein cholesterol and cardiovascular disease. Four prospective American studies. *Circulation* **79**, 8–15 (1989).
4. Barter, P. *et al.* HDL cholesterol, very low levels of LDL cholesterol, and cardiovascular events. *N. Engl. J. Med.* **357**, 1301–1310 (2007).
5. Vergeer, M., Holleboom, A. G., Kastelein, J. J. P. & Kuivenhoven, J. A. The HDL hypothesis: does high-density lipoprotein protect from atherosclerosis? *J. Lipid Res.* **51**, 2058–2073 (2010).
6. Rohatgi, A. *et al.* HDL Cholesterol Efflux Capacity and Incident Cardiovascular Events. *N. Engl. J. Med.* **371**, 2383–2393 (2014).
7. Rader, D. J. & Tall, A. R. The not-so-simple HDL story: Is it time to revise the HDL cholesterol hypothesis? *Nat. Med.* **18**, 1344–6 (2012).
8. Heinecke, J. The not-so-simple HDL story: A new era for quantifying HDL and cardiovascular risk? *Nat. Med.* **18**, 1346–1347 (2012).
9. Kingwell, B. A., Chapman, M. J., Kontush, A. & Miller, N. E. HDL-targeted therapies: progress, failures and future. *Nat. Rev. Drug Discov.* **13**, 445–64 (2014).
10. Escolà-Gil, J. C., Cedó, L. & Blanco-Vaca, F. High-density lipoprotein cholesterol targeting for novel drug discovery: where have we gone wrong? *Expert Opin. Drug Discov.* **9**, 119–24 (2014).
11. Escolà-Gil, J. C., Rotllan, N., Julve, J. & Blanco-Vaca, F. In vivo macrophage-specific RCT and antioxidant and antiinflammatory HDL activity measurements: New tools for predicting HDL atheroprotection. *Atherosclerosis* **206**, 321–327 (2009).
12. deGoma, E. M., deGoma, R. L. & Rader, D. J. Beyond high-density lipoprotein cholesterol levels evaluating high-density lipoprotein function as influenced by novel therapeutic approaches. *J. Am. Coll. Cardiol.* **51**, 2199–211 (2008).
13. Pirillo, A., Norata, G. D. & Catapano, A. L. High-density lipoprotein subfractions--what the clinicians need to know. *Cardiology* **124**, 116–25 (2013).
14. Stein, J. H. & McBride, P. E. Should advanced lipoprotein testing be used in clinical practice? *Nat. Clin. Pract. Cardiovasc. Med.* **3**, 640–1 (2006).



15. Shen, B., Scanu, A. & Kezdy, F. Structure of human serum lipoproteins inferred from compositional analysis. *Proc. Natl. Acad. Sci. USA* **74**, 837–841 (1977).
16. Mazer, N. A., Giulianini, F., Paynter, N. P., Jordan, P. & Mora, S. A comparison of the theoretical relationship between HDL size and the ratio of HDL cholesterol to apolipoprotein A-I with experimental results from the Women's Health Study. *Clin. Chem.* **59**, 949–58 (2013).
17. Mallol, R. *et al.* Liposcale: a novel advanced lipoprotein test based on 2D diffusion-ordered 1H NMR spectroscopy. *J. Lipid Res.* **56**, 737–746 (2015).
18. MacKey, R. H. *et al.* High-density lipoprotein cholesterol and particle concentrations, carotid atherosclerosis, and coronary events: MESA (Multi-Ethnic Study of Atherosclerosis). *J. Am. Coll. Cardiol.* **60**, 508–516 (2012).
19. Mora, S. *et al.* Lipoprotein particle profiles by nuclear magnetic resonance compared with standard lipids and apolipoproteins in predicting incident cardiovascular disease in women. *Circulation* **119**, 931–939 (2009).
20. Qi, Y., Fan, J., Liu, J. & Wang, W. Cholesterol-Overloaded HDL Particles Are Independently Associated With Progression of Carotid Atherosclerosis in a Cardiovascular Disease-Free Population: A Community-Based Cohort Study. *J. Am. Coll. Cardiol.* **65**, 355–363 (2015).
21. Kumpula, L. S. *et al.* Reconsideration of hydrophobic lipid distributions in lipoprotein particles. *Chem. Phys. Lipids* **155**, 57–62 (2008).
22. Yetukuri, L. *et al.* Composition and lipid spatial distribution of HDL particles in subjects with low and high HDL-cholesterol. *J. Lipid Res.* **51**, 2341–2351 (2010).
23. Rosenson, R. S. *et al.* HDL measures, particle heterogeneity, proposed nomenclature, and relation to atherosclerotic cardiovascular events. *Clin. Chem.* **57**, 392–410 (2011).
24. Hutchins, P. & Ronsein, G. Quantification of HDL particle concentration by calibrated ion mobility analysis. *Clin. Chem.* **60**, 1393–1401 (2014).
25. Krasnowska, E.K., Gratton, E. & Parasassi, T. Prodan as a membrane surface fluorescence probe: partitioning between water and phospholipid phases. *Biophys. J.* **74**, 1984–1993 (1998).
26. Krasnowska, E. K., Bagatolli, L. A., Gratton, E. & Parasassi, T. Surface properties of cholesterol-containing membranes detected by Prodan fluorescence. *Biochim. Biophys. Acta - Biomembr.* **1511**, 330–340 (2001).

### Chapter 3

27. Massey, J. & Pownall, H. Surface properties of native human plasma lipoproteins and lipoprotein models. *Biophys. J.* **74**, 869–878 (1998).
28. Ala-Korpela, M. *et al.* <sup>1</sup>H NMR-based absolute quantitation of human lipoproteins and their lipid contents directly from plasma. *J. Lipid Res.* **35**, 2292–2304 (1994).
29. Kontush, A. & Chapman, M.J. Composition. in *High-Density Lipoproteins* 3-38 (John Wiley & Sons, Inc., 2011).
30. Kontush, A. & Chapman, M.J. Heterogeneity. in *High-Density Lipoproteins* 39-58 (John Wiley & Sons, Inc., 2011).
31. Nobécourt, E. *et al.* Defective antioxidative activity of small dense HDL3 particles in type 2 diabetes: relationship to elevated oxidative stress and hyperglycaemia. *Diabetologia* **48**, 529–38 (2005).
32. Anderson, D., Nichols, A., Pan, S. & Lindgren, F. High density lipoprotein distribution: resolution and determination of three major components in a normal population sample. *Atherosclerosis* **29**, 161–179 (1978).
33. Blanche, P., Gong, E., Forte, T. & Nichols, A. Characterization of human high-density lipoproteins by gradient gel electrophoresis. *Biochim. Biophys. Acta* **665**, 408–419 (1981).
34. Chapman, M. J., Goldstein, S., Lagrange, D. & Laplaud, P. M. A density gradient ultracentrifugal procedure for the isolation of the major lipoprotein classes from human serum. *J. Lipid Res.* **22**, 339–358 (1981).
35. Carlson, J. W., Jonas, A. & Sligar, S. G. Imaging and manipulation of high-density lipoproteins. *Biophys. J.* **73**, 1184–1189 (1997).
36. Feng, M. *et al.* Adsorption of High Density Lipoproteins (HDL) on Solid Surfaces. *J. Colloid Interface Sci.* **177**, 364–371 (1996).
37. Ståhlman, M. *et al.* Dyslipidemia, but not hyperglycemia and insulin resistance, is associated with marked alterations in the HDL lipidome in type 2 diabetic subjects in the DIWA cohort: impact on small HDL particles. *Biochim. Biophys. Acta* **1831**, 1609–17 (2013).
38. Camont, L. *et al.* Small, dense high-density lipoprotein-3 particles are enriched in negatively charged phospholipids: relevance to cellular cholesterol efflux, antioxidative, antithrombotic, anti-inflammatory, and antiapoptotic functionalities. *Arterioscler. Thromb. Vasc. Biol.* **33**, 2715–23 (2013).

39. Gu, F. *et al.* Structures of discoidal high density lipoproteins: a combined computational-experimental approach. *J. Biol. Chem.* **285**, 4652–65 (2010).
40. Edelstein, C., Kezdy, F., Scanu, A. & Shen, B. Apolipoproteins and the structural organization of plasma lipoproteins: human plasma high density lipoprotein-3. *J. Lipid Res.* **20**, 143–153 (1979).
41. Phillips, J. C., Wriggers, W., Li, Z., Jonas, A. & Schulten, K. Predicting the structure of apolipoprotein A-I in reconstituted high-density lipoprotein disks. *Biophys. J.* **73**, 2337–46 (1997).
42. Tajima, S., Yokoyama, S. & Yamamoto, A. Mechanism of action of lipoprotein lipase on triolein particles: effect of apolipoprotein C-II. *J. Biochem.* **96**, 1753-1767 (1984).
43. Farbstein, D. & Levy, A.P. HDL dysfunction in diabetes: causes and possible treatments. *Expert Rev Cardiovasc Ther* **10**, 353-361 (2012).
44. Masana, L., *et al.* Remarkable quantitative and qualitative differences in HDL after niacin or fenofibrate therapy in type 2 diabetic patients. *Atherosclerosis* **238**, 213-219 (2015).
45. Kontush, A. & Chapman, M.J. Why is HDL functionally deficient in type 2 diabetes? *Curr. Diab. Rep.* **8**, 51-59 (2008).
46. Kontush, A. & Chapman, M.J. Functionally defective high-density lipoprotein: a new therapeutic target at the crossroads of dyslipidemia, inflammation, and atherosclerosis. *Pharmacol. Rev.* **58**, 342-374 (2006).
47. Zerrad-Saadi, A. *et al.* HDL3-mediated inactivation of LDL-associated phospholipid hydroperoxides is determined by the redox status of apolipoprotein A-I and HDL particle surface lipid rigidity: relevance to inflammation and atherogenesis. *Arterioscler. Thromb. Vasc. Biol.* **29**, 2169–75 (2009).
48. Schumaker, V.N. & Puppione, D.L. Sequential flotation ultracentrifugation. *Methods Enzymol* **128**, 155-170 (1986).
49. Mallol, R. *et al.* Particle size measurement of lipoprotein fractions using diffusion-ordered NMR spectroscopy. *Anal. Bioanal. Chem.* **402**, 2407–2415 (2012).
50. Johnson Jr, C. Diffusion ordered nuclear magnetic resonance spectroscopy: principles and applications. *Prog. Nucl. Magn. Reson. Spectrosc.* **34**, 203–256 (1999).

### 3.2.7 Supporting information

#### S.1 From biochemical data to the analytical expression of the lipoprotein radius

The Shen model describes lipoproteins as spheres with a surface shell 2 nm thick consisting of phospholipids (PL), proteins (Prot) and free cholesterol (FC) covering a core of esterified cholesterol (EC) and triglycerides (TG). We used the Shen model and biochemical information to directly determine the theoretical radius of the lipoprotein particles as follows:

First, we computed the geometric ratio between the volume of the outside (the 2 nm shell) and the inside (the core). The geometric expression for a sphere of known radius is:

$$Ratio_{geometry} = \frac{\frac{4}{3}\pi \cdot R^3 - \frac{4}{3}\pi \cdot (R - 2)^3}{\frac{4}{3}\pi \cdot (R - 2)^3} = \frac{R^3}{(R - 2)^3} - 1 \quad (1)$$

Second, we found that this ratio was equal to the one obtained using the biochemical information and the Shen model:

$$Ratio_{bioq.} = \frac{V_{Exterior}}{V_{Interior}} = \frac{R^3}{(R - 2)^3} - 1 \quad (2)$$

where:

$$V_{Exterior} = V_{FreeCholesterol} + V_{Protein} + V_{Phospholipids} \quad (3)$$

$$V_{Interior} = V_{EsterifiedCholesterol} + V_{Triglycerides} \quad (4)$$

$$V_{molecule} = [molecule] \cdot v_{molecule} \quad (5)$$

Finally, rearranging Eq. 2 we found the analytical expression for the radius:

$$R_s = \frac{20}{1 - \left(\frac{V_{Exterior}}{V_{Interior}} + 1\right)^{-\frac{1}{3}}} \quad (6)$$

Molecular volumes were 1.058, 1.021, 1.102, 0.984 and 0.738 ml/mg for the EC, FC, TG, PL and Prot, respectively.

### S.2 Correlation between triglycerides levels, size and percentage of core lipids in the surface

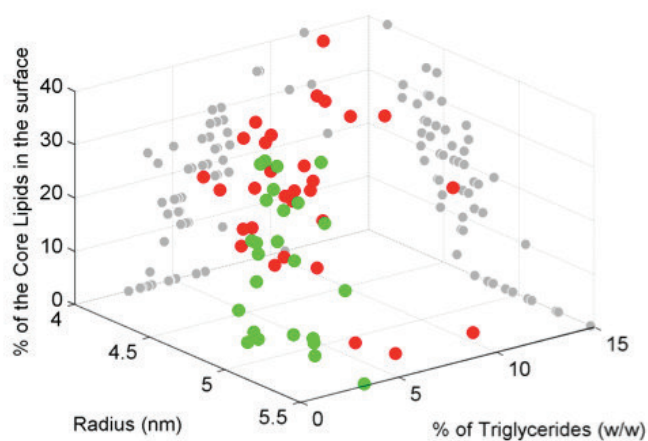


**Figure S1 Percentage of the core lipids in the surface in relation to the size (nm) and the percentage of the triglycerides levels (w/w) of the HDL particles.** Green circles represent the CT group and red circles the DM2 group.

### Chapter 3

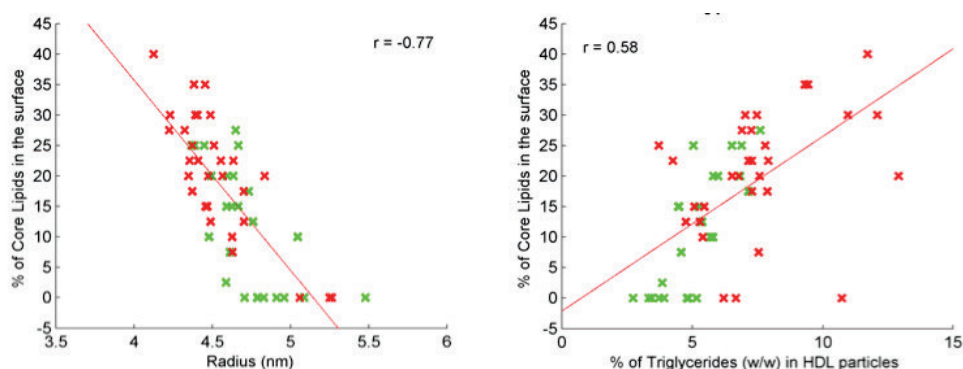


**Figure S2. a) Percentage of the core lipids vs. Size. b) Percentage of the core lipids vs. TG.** Green color represents the CT group and red color, the DM2 group. R is the Pearson correlation coefficient.

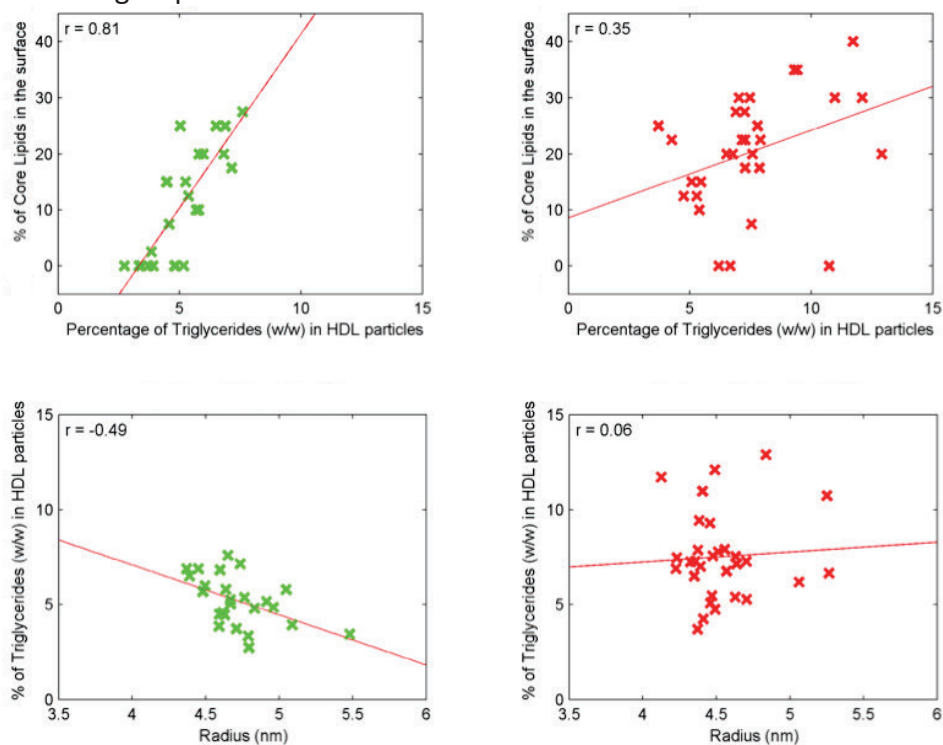


**Figure S3. Scatter plots of the TG levels (w/w) and Percentage of the core lipids in the surface for a) CT group and b) for DM2 group; scatter plots of the Size (nm) and the TG levels (w/w) for c) CT group and d) for DM2 group.** Green color represents the CT group and red, the DM2 group. R is the Pearson correlation coefficient.

### S.3 Fluorescence analysis

Fluorescence experiments were performed in a subgroup of the samples (CT n=8 and DM2 n=4) in order to observe differences in the surface polarity of the two groups. Three different fluorescent probes (Prodan, Patman and Laurdan) were used to evaluate the surface properties of lipoproteins.

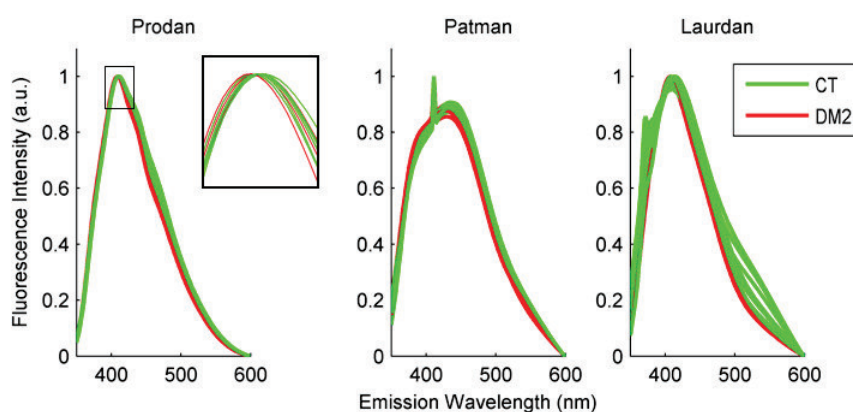


**Figure S4. Fluorescence spectra of Prodan, Patman and Laurdan.**

The fluorescence spectra of all three probes showed the same tendency: the wavelengths of the emission maxima ( $\lambda_{em}$ ) of the DM2 group were blue shifted (towards shorter wavelengths), indicating a more hydrophobic surface microenvironment than the CT group.

To evaluate the dispersion of the measurements and display the differences between the CT and the DM2 group, we performed a principal component analysis (PCA) of the fluorescence intensity between 350 and 600 nm of two repetitions per sample.

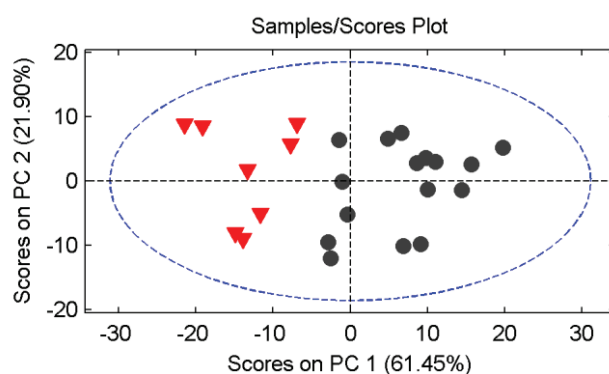


**Figure S5. Principal component analysis of the fluorescence raw data of two repetitions per sample.** Red triangles represent the DM2 group and black circles, the CT group.

#### S.4 HDL subclass analysis

The biochemical composition of each subclass was calculated considering the molecular weight of FC, CE, PL and TG was 387, 650, 787 and 885, respectively.

**Table S1:** Chemical composition of lipids and protein of each HDL subclass.

	Large HDL	Medium HDL	Small HDL
<b>FC</b>	7	4	3
<b>CE</b>	22	19	20
<b>PL</b>	30	30	20
<b>TG</b>	4	3	3
<b>Prot</b>	37	44	54

Data are expressed as w/w. TG: triglycerides, CE: cholesteryl esters, FC: free cholesterol, PL: phospholipids, Prot: protein.

#### S.5 Atomic force microscopy experiments

We used atomic force microscopy to measure the adhesion force between the tip of the AFM probe and the surface of the HDL. We obtained topographic images and their adhesion force map. The



adhesion force between the tip of the AFM probe and the sensed surface is inversely associated with the surface hydrophobicity.

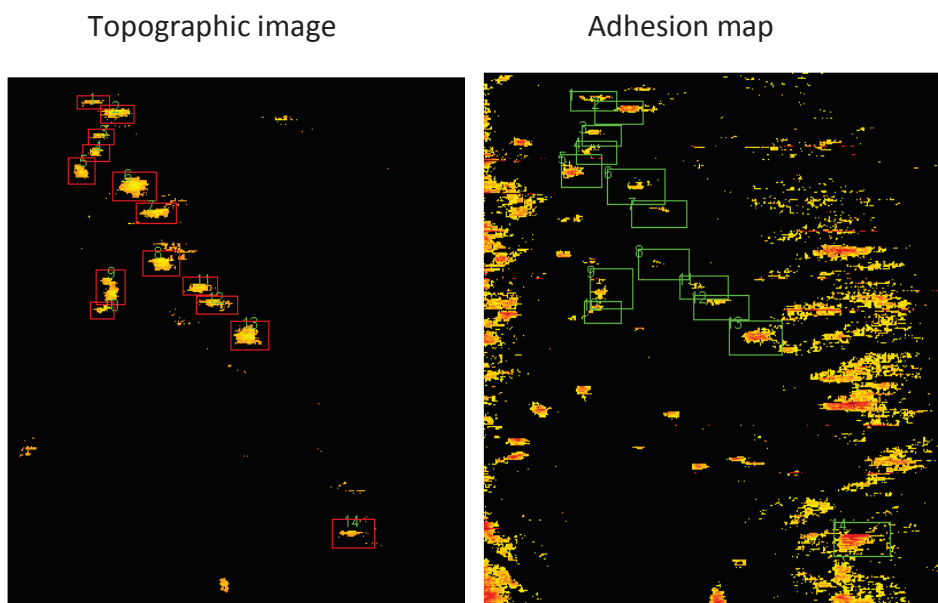


**Figure S6. AFM topographic image and adhesion map of HDL particles.** Lipoproteins of different size (red squares on the topographic image) interacted with the AFM tip. The adhesion map shows the adhesion force between the tip and the lipoprotein surface for each lipoprotein particle (green squares on the adhesion map).

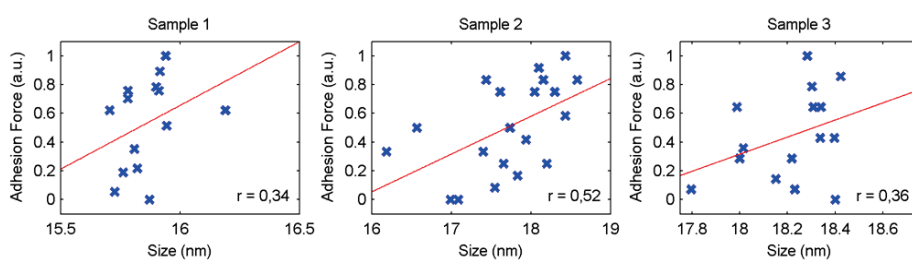


**Figure S7. Scatter plots of HDL size by the tip adhesion force.**



### **3.3 Remarkable quantitative and qualitative differences in HDL after niacin or fenofibrate therapy in type 2 diabetic patients**



### 3.3.1 Abstract

HDL-increasing drugs such as fenofibrate and niacin have failed to decrease the cardiovascular risk in patients with type 2 diabetes. Drug-mediated quantitative and qualitative HDL modifications could be involved in these negative results. To evaluate the quantitative and qualitative effects of niacin and fenofibrate on HDL in patients with type 2 diabetes, a prospective, randomised controlled intervention trial was conducted. Thirty type 2 diabetic patients with low HDL were randomised to receive either fenofibrate (FFB) or niacin plus laropiprant (ERN/LPR) as an add-on to simvastatin treatment for 12 weeks according to a crossover design. At the basal point and after each intervention period, physical examinations and comprehensive standard biochemical determinations and HDL metabolomics were performed. Thirty nondiabetic patients with normal HDL were used as a basal control group. ERN/LRP, but not FFB, significantly increased HDL cholesterol. Neither ERN/LRP nor FFB reversed the HDL particle size or particle number to normal. ERN/LRP increased apoA-I but not apoA-II, whereas FFB produced the opposite effect. FFB significantly increased pre $\beta$ 1-HDL, whereas ERN/LRP tended to lower pre $\beta$ 1-HDL. CETP and LCAT activities were significantly decreased only by ERN/LRP. PAF-AH activity in HDL and plasma decreased with the use of both agents. Despite their different actions on antioxidant parameters, none of the treatments induced detectable antioxidant improvements.

ERN/LRP and FFB had strikingly different effects on HDL quantity and quality, as well as on HDL cholesterol concentrations. When prescribing

## Chapter 3

HDL cholesterol increasing drugs, this differential action should be considered.

### **3.3.2 Introduction**

Cardiovascular (CV) diseases are responsible for approximately 50% of deaths in patients with type 2 diabetes<sup>1</sup>. In the presence of additional CV risk factors, achieving a low density lipoprotein (LDL) concentration below 70 mg/dl is recommended<sup>2</sup>. Even if the LDL target is achieved, an important residual risk remains. A portion of this residual risk has been attributed to lipid profile alterations, as well as plasma LDL concentrations<sup>3</sup>. Patients with type 2 diabetes usually have profound lipid metabolism derangement, which is characterized by low high density lipoprotein (HDL) and high triglyceride concentrations. This lipid pattern is referred to as atherogenic dyslipidemia because of its high vascular damaging capacity. The inverse association between circulating HDL cholesterol concentrations and CV disease risk is unquestionable<sup>4</sup>. In many epidemiological studies, HDL cholesterol below 40 mg/dl in men and 45 mg/dl in women has been associated with an increased CV disease risk<sup>2</sup>. Recent data from the “Emerging Risk Factors Collaboration” confirmed that HDL cholesterol is inversely associated to coronary heart disease after adjusting for lipid and non-lipid risk factors<sup>5</sup>.

Despite this strong epidemiological association, increasing HDL cholesterol by medications has not produced a beneficial impact on CV disease risk. In recent years, clinical outcome intervention trials using fibrates, niacin and cholesteryl ester transfer protein (CETP) inhibitors have had negative results<sup>6</sup>. Among the fibrate intervention trials, only

the VA-HIT study using gemfibrozil showed a 22% relative CV disease risk reduction associated with a 6% increase in HDL cholesterol<sup>7</sup>. More recent studies using fenofibrate (FIELD and ACCORD)<sup>6,8</sup> did not show a beneficial effect, albeit post hoc analyses suggested a marginal benefit in the atherogenic dyslipidemia subgroup. Similarly, two studies that used niacin as an add-on to statin treatment, AIM-HIGH and HPS2-THRIVE, were prematurely stopped due to a lack of efficacy<sup>9,10</sup>. In all of these trials, the effect on HDL cholesterol concentrations was relatively poor, with mean increases ranging from 0% to 6%. The failure of the fibrate and niacin trials has been attributed to a lack of effect on lipid parameters or a poor study design, among other reasons. Beyond these circumstances, the complex composition and metabolism of HDL particles must be considered. Data from proteomic and lipidomic studies have shown the heterogeneity of this lipoprotein family, which is involved in many biological functions<sup>11–15</sup>. Moreover, HDL has considerable plasticity and is capable of changing its composition according to the environmental needs. Although reverse cholesterol transport is considered to be the key HDL antiatherogenic function, other biological effects of HDL are equally important, including its anti-inflammatory, endothelial protective, and antioxidant capacities<sup>16</sup>. The cholesterol content in HDL is only a subrogated marker of the HDL particle concentration and has a weak correlation with HDL functions<sup>17</sup>. The anti-inflammatory, antioxidant, and endothelial protective or antiapoptotic effects of HDL seem to be more related to the HDL particle shape, size, number and composition. All of these characteristics are altered by pathological conditions such as type 2

## Chapter 3

diabetes mellitus (T2DM)<sup>18</sup>. Many efforts have been made to evaluate the clinical impact of HDL function rather than HDL cholesterol concentrations. Recently, the HDL cholesterol efflux capacity was observed to be a better indicator of HDL CV protection than HDL cholesterol<sup>19</sup>. Despite this evidence, HDL cholesterol concentrations remain the primary treatment determinant, and the efficacy of medication is assessed by its capacity to increase HDL cholesterol.

In this study, we hypothesized that global HDL particle alterations of T2DM patients are reversed by neither ERN/LRP nor FFB despite their HDL cholesterol increasing effect and that both drugs impact differently in HDL particle size distribution, composition and HDL metabolic determinants in these patients.

### **3.3.3 Patients and methods**

***Subjects and design of the study.*** Thirty type 2 diabetic patients, 19 male and 11 female, ranging in age from 30 to 70 years old and with HDL not exceeding 50 mg/dl in men or 60 mg/dl in women were recruited. This HDL cut off points were selected to avoid the impact of genetic factors associated to high HDL values. The exclusion criteria were as follows: smoker, diagnosed with diabetes less than three months before, triglyceride levels above 400 mg/dl, glycated haemoglobin higher than 9%, albuminuria above 300 mg/mg creatinine, chronic kidney disease (estimated glomerular filtration rate <30 ml/min/1.73 m<sup>2</sup>), advanced retinopathy, neuropathy, cardiovascular disease in the last three months, chronic liver insufficiency, neoplastic disease or any chronic or incapacitating disease. The control group consisted of 30 age and gender-matched subjects without diabetes and



with HDL cholesterol higher than 40 mg/dl for men or 50 mg/dl for women. After a 6-week lipid-lowering drug wash-out, the patients with type 2 diabetes were randomly distributed into two groups. One group received 20 mg simvastatin plus 145 mg fenofibrate, and the other group received 20 mg simvastatin plus 2 g niacin plus laropiprant for a 12-week period. After this intervention period, the patients followed a new 6-week lipid-lowering drug wash-out; subsequently, they were shifted to the other lipid-lowering drug, in a crossover design, for a 12-week period (Figure 1). Physical examinations, anthropometry and blood extraction for standard biochemical and metabolic tests were obtained at the basal point and after each intervention period in the type 2 diabetes group and at the basal point in the control group. All of the study investigations were conducted according to the principles expressed in the Declaration of Helsinki. The study was approved by the Ethic Committees of the recruiting hospitals. All of the subjects provided their written informed consent before participating in the study.

***Sample collection and storage.*** At the time points indicated in the flow chart (Figure 1), fasting blood samples were collected in serum tubes with EDTA and were centrifuged immediately at 1500 *g* for 15 min at 4 °C. Aliquots of plasma and serum were stored at -80 °C until the analyses were performed (except for pre $\beta$ 1-HDL).

## Chapter 3

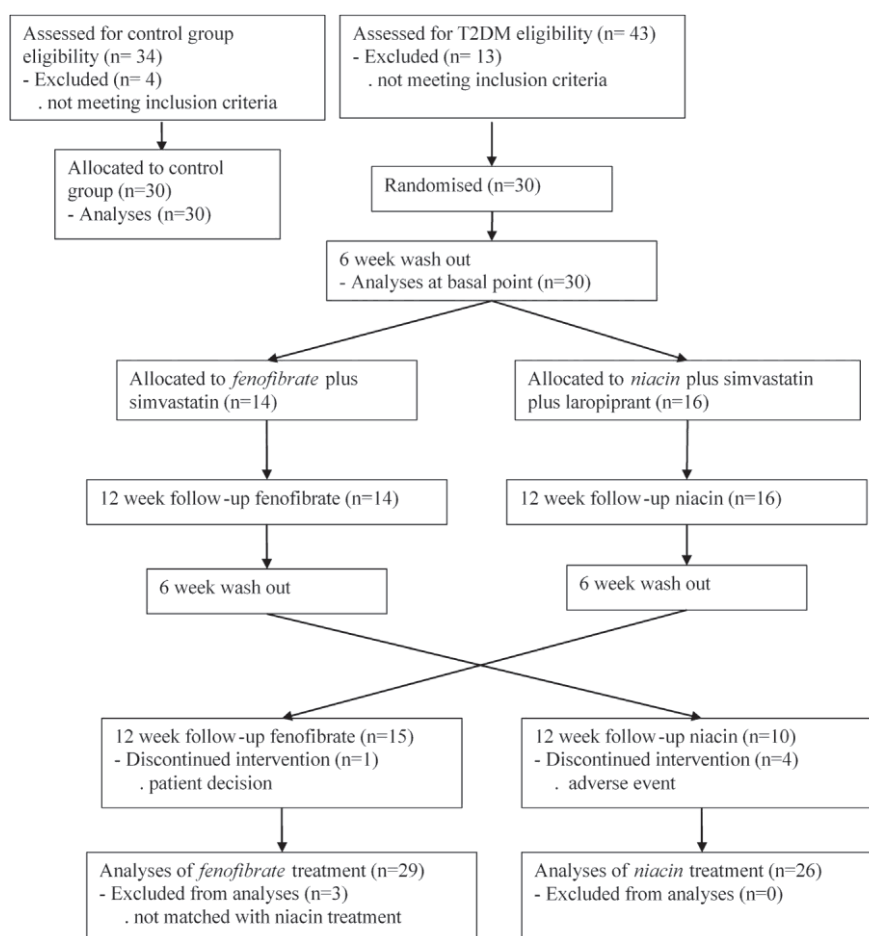


**Figure 1.** Flow chart of participant enrolment, randomisation and analysis.

**Standard lipid analyses.** Biochemical parameters, lipids, apolipoproteins, fructosamine and homocysteine were measured using colourimetric, enzymatic and immunoturbidimetric assays (Spinreact, SA, Spain; Wako Chemicals GmbH, Germany; Polymedco, NY) adapted to a Cobas Mira Plus autoanalyser (Roche Diagnostics, Spain)<sup>20–22</sup>. Enzymes and protein concentrations are outlined in the supplemental materials.

**Pre $\beta$ 1-HDL measurements.** To determine pre $\beta$ 1-HDL measurements, plasma samples were immediately placed on ice in a 50% sucrose solution. Pre $\beta$ 1-HDL was analysed using a quantitative ELISA (Daichii, Japan).

**HDL isolation using ultracentrifugation.** Total HDL was isolated from plasma using sequential preparative ultracentrifugation (uc) at 1.21 mg/dl density according to previously described techniques<sup>23</sup>. Ultracentrifuged HDL (ucHDL) fractions were stored at 80 °C until biochemical studies were performed.

**Plasma and HDL oxidation status.** The OxyStat (Biomedica, Wien) colorimetric assay was used for the quantitative determination of lipid peroxides in apoB-depleted plasma after the precipitation of b-lipoproteins using phosphotungstic acid and magnesium ions (Roche Diagnostics). The results are expressed as  $\mu\text{mol/L}$  lipoperoxides/mg apoA-I. Serum paraoxonase 1 (PON1) and paraoxonase 3 (PON3) concentrations were determined using an in-house ELISA and rabbit polyclonal antibodies generated against synthetic peptides with sequences specific for mature PONs. The employed peptides were CRNHQSSYQTRLNALREVQ (specific for PON1) and CRVNASQEVEPVEPEN (specific for PON3). The details of these methods have been previously reported<sup>24</sup>. Serum PON1 lactonase activity was analysed by measuring 5-thiobutyl butyrolactone (TBBL) hydrolysis, as previously described<sup>25,26</sup>.

HDL antioxidant activity was determined by conjugated diene formation by incubating the patient's HDL (0.1 mg/ml apoA-I) with human LDL (0.1 mg/ml apoB, obtained from a pool of normolipidemic individuals) in the presence of 2.5  $\mu\text{mol/L}$   $\text{CuSO}_4$ . Continuous monitoring

## Chapter 3

at an absorbance of 234 nm was performed in a microplate reader (BioTek Synergy, Winooski, VT, USA) at 37 °C for 4 h. The kinetics of LDL in the LDL+ HDL incubations were calculated by subtracting the kinetics of HDL incubated without LDL; the lag phase was calculated as previously described<sup>27</sup>.

**HDL composition analyses.** In the ucHDL fraction, cholesterol, triglyceride, total protein, phospholipid, apolipoprotein AI (apoA-I) (Roche Diagnostics), apolipoprotein A-II (apoA-II), apolipoprotein E (apoE), apolipoprotein CII (apoC-II), and apolipoprotein CIII (apoC-III) (Kamiya Biomedical Company) contents were quantified using enzymatic and nephelometric assays adapted to a BM/HITACHI 911 autoanalyser (Spinreact S.A.U., Spain).

**HDL analyses by 2D diffusion-ordered <sup>1</sup>H-NMR spectroscopy (DOSY).** The ucHDL fraction samples were analysed using nuclear magnetic resonance (NMR) spectroscopy and a modified existing protocol<sup>28</sup>. The <sup>1</sup>H-NMR spectra were recorded using a BrukerAvance III spectrometer at 310 K. We used the double stimulated echo (DSTE) pulse program with bipolar gradient pulses and a longitudinal eddy current delay (LED). The DSTE methyl signal was fitted with one lorentzian function to obtain the averaged diffusion coefficient of the lipoprotein particles. The hydrodynamic radii of the lipoprotein fractions were extracted from the Stokes-Einstein equation. Further details about the ucHDL NMR feature extraction and HDL particle size distribution and number calculations are outlined in the supplemental material.

**Statistical analysis:** Normal distributed data are shown as the mean ± SD values, and non-normal distributed data are shown as the median

(interquartile range). We performed two different statistical tests to detect differences between the studied variables. A statistical Mann-Whitney U test was performed to identify significant differences between the control group and the group comprising patients with type 2 diabetes, followed by a Wilcoxon signed-rank test to evaluate the treatment effects for paired samples. We performed alpha corrections due to multiple testing by multiplying the  $p$  value by the number of related variables tested (lipids, enzymes, oxidation, HDL subclasses). We excluded any carryover effect by the Fleiss method. There were no significant differences (by  $t$  test) in the results obtained in any of the variables after the same treatment, regardless of the intervention order<sup>29</sup>. Subsequently, the data of the two sequences were combined and analysed as described in the design section. The analyses were performed using SPSS software (IBM SPSS Statistics, version 20).  $P < 0.05$  was considered to be statistically significant.

#### 3.3.4 Results

✓ **Baseline differences.** The anthropometric and clinical characteristics of these groups are presented in Supplemental Table 1S. In Table 1, we show the lipid metabolism and oxidation parameters and HDL subclass distribution in both T2DM patients and controls. As expected, the patients with T2DM had lower HDL cholesterol and apoA-I. The total number of HDL particles was lower in T2DM patients ( $P = 0.009$ ). The difference was primarily due to the medium-sized HDL particles ( $P = 0.004$ ) (Table 1). They had higher pre $\beta$ 1-HDL and CETP activity and lower PON1. HDL from T2DM patients had less cholesterol and apoE and more triglycerides and apoC-III (Supplemental Table 2S). Because of the side

## Chapter 3

effects of the medications, one patient withdrew from the study during the fenofibrate treatment, and four patients withdrew during the niacin treatment. The anthropometric and clinical characteristics of these groups are presented in Supplemental Table 3S.

**Table 1.** Biochemical characteristics of control population and T2DM patients.

	Control (n=30)	T2DM (n=30)	<i>P</i>
<i>Lipoproteins</i>			
Cholesterol (mmol/L)	5.42 ± 0.99	6.14 ± 1.24	<b>0.030</b>
Triglycerides (mmol/L)	0.95 (0.73-1.20)	2.39 (1.63-3.49)	<b>&lt;0.001</b>
HDL-C (mmol/L)	1.51 ± 0.36	1.05 ± 0.28	<b>&lt;0.001</b>
ApoA-I (g/L)	149 ± 15	132 ± 15	<b>&lt;0.001</b>
ApoA-II (g/L)	30.3 ± 3.9	28.6 ± 4.8	0.095
ApoB-100 (g/L)	96 ± 22	121 ± 26	<b>0.001</b>
Preβ1-HDL (µg/ml)	17.8 (11.6-22.6)	22.8 (15.5-27.7)	<b>0.027<sup>a</sup></b>
<i>Enzymes</i>			
CETP mass (µg/ml)	2.5 ± 0.7	2.5 ± 0.7	0.906
CETP activity (pmol/h*µl)	7.2 ± 2.0	9.2 ± 2.9	<b>0.006</b>
LCAT mass (µg/ml)	9.6 ± 1.4	10.7 ± 1.9	<b>0.006</b>
LCAT activity (FER)	6.28 ± 4.6	11.3 ± 10.6	0.152
PAF-AH (µmol/min*ml)	19.7 ± 5.1	22.7 ± 7.5	0.101
PAF-AH in HDL (µmol/min*ml)	11.9 ± 4.9	12.6 ± 5.8	0.644
<i>Oxidation</i>			
PON1 (mg/L)	78.6 ± 23.9	62.0 ± 23.4	<b>0.007</b>
PON3 (mg/L)	1.4 ± 0.5	1.6 ± 0.5	0.255
Lactonase activity (U/L)	6.4 ± 2.9	7.6 ± 2.1	<b>0.021<sup>a</sup></b>
Paraoxonase activity (U/L)	269.2 ± 101.9	320.2 ± 146.4	0.193
LOOH in HDL (µmol/mg)	0.15 ± 0.10	0.19 ± 0.10	<b>0.044<sup>a</sup></b>
Antioxidant capacity (% dienes)	100.1 ± 21.7	91.6 ± 25.9	0.208
<i>HDL subclass particle concentration (µmol/L)</i>			
Large HDL	0.6 (0.4-0.8)	0.5 (0.4-0.7)	0.196
Medium HDL	3.9 (2.9-5.3)	2.9 (1.8-4.2)	<b>0.004</b>
Small HDL	7.8 (6.1-9.7)	7.8 (6.2-10.2)	1

Total HDL	13.6 (11.0-15.2)	10.8 (10.0-12.6)	<b>0.009</b>
-----------	------------------	------------------	--------------

Normal distributed data are given as mean  $\pm$  SD and non-normal distributed data as the median (interquartile range). The control population and T2DM patients were analysed using the Mann–Whitney *U* test. Bold signifies P value. <sup>a</sup> Results lost statistical significance at  $P \leq$  after we adjusted for inflation caused by multiple testing.

**Changes induced by fenofibrate.** Despite a significant decrease in plasma TG, FFB did not increase HDL cholesterol or apoA-I (Table 2). Conversely, it increased apoA-II and pre $\beta$ 1-HDL (Table 2) and decreased HDL apoC-III whereas HDL apoE remained unchanged (Supplemental Table 4S). LCAT and CETP activities did not vary with treatment. FFB decreased the number of medium size HDL particles (Table 2 and Figure 2). Regarding oxidative parameters, FFB decreased both paraoxonase and PAF-AH activities without significant changes in LOOH and antioxidant capacity (Table 2).

**Changes induced by niacin.** ERN/LRP significantly increased HDL cholesterol and apoA-I, and showed a tendency to decrease pre $\beta$ 1-HDL (Table 2). CETP and LCAT mass and activity were decreased after treatment. ERN/LRP did not show any effect on HDL subclass distribution (Table 2 and Figure 2). Regarding oxidation, PAF-AH and paraoxonase activities were significantly decreased by ERN/LRP (Table 2).

**Comparison between treatments.** Although ERN/LRP significantly increased HDL cholesterol, the total HDL particle number was not significantly modified by any of the treatments (Table 2).

### Chapter 3

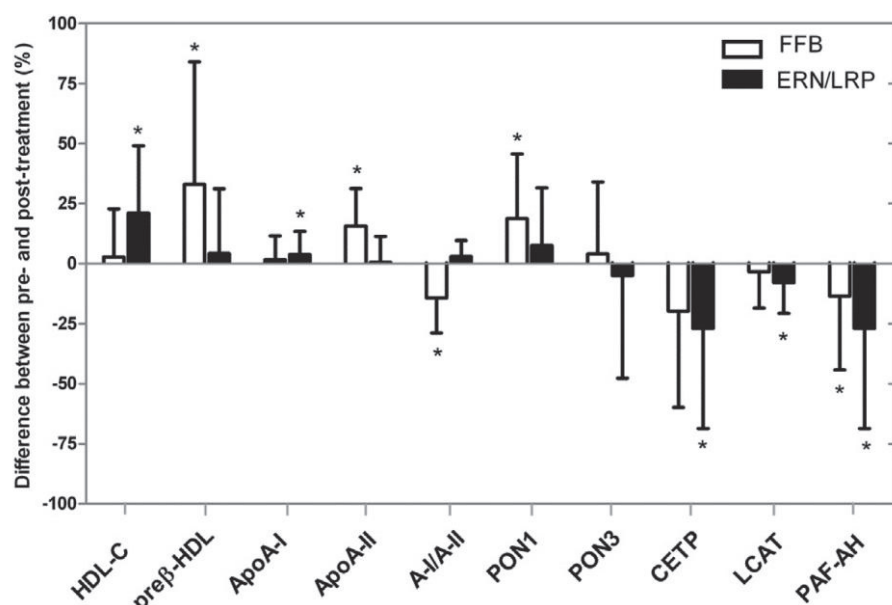


**Figure 2.** Percentage of change between baseline and post-FFB and post-ERN/LRP of HDL lipids, apolipoproteins and enzymes. The data represent the mean  $\pm$  SD values;  $n = 26$ . The effect of treatment was analysed using the paired sample Wilcoxon signed rank test, \* $P < 0.05$ .

The HDL spectra of medium and large HDL particles were different between controls and T2DM and were not reversed to normal after any treatment (Figure 3A). No differences in the NMR spectrum of small HDL were observed. Figure 3B shows the average HDL particle sizes, confirming that the HDL from T2DM patients is smaller than that of controls, and neither FFB nor ERN/LRP fully correct this alteration. The mean radius for the healthy group (4.7 nm) was higher than that of the T2DM group (4.5 nm) ( $P = 0.002$ ). FFB tended to shift the distribution towards smaller particles, whereas RN/LRP treatment increased the relative concentration of the medium HDL subclass, which consequently, although not significantly, approached the healthy state. The effects of different treatments on the mean HDL radius were significantly different ( $P = 0.042$ ).



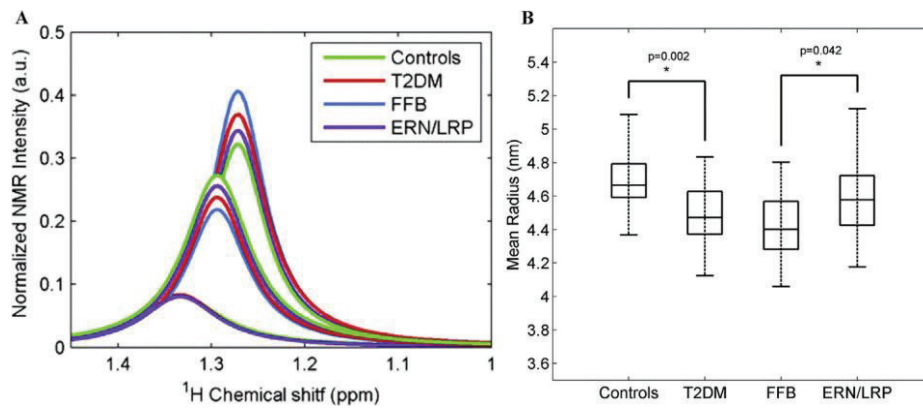


**Figure 3.** HDL particle size distribution in controls and T2DM patients before and after ERN/LRP and FFB treatments. A) The coloured curves are the means of the three normalised functions for each group. The area under each curve represents the relative lipid concentration of a particular subclass. B) The mean HDL radius in controls and T2DM patients before and after ERN/LRP and FFB treatments.

**Table 2. Biochemical characteristics at baseline and post ERN/LPR and FFB treatments in T2DM.**

	T2DM Baseline (n=26)	T2DM Post-FFB (n=26)	P FFB vs. baseline*	T2DM Post-ERN/LPR (n=26)	P ERN/LPR vs baseline*	P between treatments**
<b>Lipoproteins</b>						
Cholesterol (mmol/L)	6.17 ± 1.27	4.50 ± 0.96	<b>&lt;0.001</b>	4.41 ± 0.77	<b>&lt;0.001</b>	0.818
Triglycerides (mmol/L)	2.50 (1.98-4.20)	1.86 (1.38-2.62)	<b>0.006</b>	1.50 (1.07-2.35)	<b>0.003</b>	0.058
HDL-C (mmol/L)	1.03 ± 0.29	1.03 ± 0.28	0.620	1.22 ± 0.36	<b>0.003</b>	<b>0.022<sup>a</sup></b>
ApoA-I (g/L)	1.32 ± 0.16	1.33 ± 0.16	0.284	1.37 ± 0.19	<b>0.032</b>	<b>0.022<sup>a</sup></b>
ApoA-II (g/L)	0.285 ± 0.050	0.327 ± 0.054	<b>&lt;0.001</b>	0.285 ± 0.047	0.576	<b>&lt;0.001</b>
ApoB-100 (g/L)	1.20 ± 0.27	0.93 ± 0.24	<b>&lt;0.001</b>	0.85 ± 0.22	<b>&lt;0.001</b>	<b>0.011<sup>a</sup></b>
Preβ1-HDL (µg/ml)	25.5 (16.5-27.9)	28.8 (22.4-37.8)	<b>0.005</b>	21.3 (17.7-29.1)	0.603	<b>0.016<sup>a</sup></b>
<b>Enzymes</b>						
CETP mass (µg/ml)	2.6 ± 0.7	2.1 ± 0.5	<b>&lt;0.001</b>	2.1 ± 0.6	<b>&lt;0.001</b>	0.435
CETP activity (pmol/h*µl)	9.6 ± 2.9	8.3 ± 2.0	0.080	7.8 ± 2.0	<b>0.004</b>	0.065
LCAT mass (µg/ml)	10.6 ± 2.0	9.7 ± 1.8	<b>&lt;0.001</b>	9.9 ± 2.3	<b>0.025<sup>a</sup></b>	0.559
LCAT activity (470nm/390nm)	11.8 ± 10.8	7.7 ± 8.1	0.180	3.8 ± 5.6	<b>0.010<sup>a</sup></b>	<b>0.046<sup>a</sup></b>
PAF-AH (µmol/min*ml)	22.2 ± 7.6	18.1 ± 6.9	<b>0.006</b>	17.8 ± 6.7	<b>0.020<sup>a</sup></b>	0.663
PAF-AH in HDL (µmol/min*m)	12.2 ± 5.7	10.0 ± 3.5	<b>0.008</b>	9.6 ± 4.2	<b>0.007</b>	0.463
<b>Oxidation</b>						

PON1 (mg/L)	63.2 ± 24.7	73.7 ± 27.2	<b>0.015<sup>a</sup></b>	65.5 ± 23.6	0.248	0.060
PON3 (mg/L)	1.6 ± 0.5	1.5 ± 0.7	0.865	1.4 ± 0.5	0.135	0.196
Lactonase activity (U/L)	7.2 ± 1.6	6.2 ± 2.3	0.065	6.8 ± 2.4	0.469	0.339
Paraoxonase activity (U/L)	292.4 ± 114.1	265.1 ± 92.1	<b>0.023<sup>a</sup></b>	273.9 ± 105.9	<b>0.020<sup>a</sup></b>	0.716
LOOH in HDL (µmol/mg)	0.20 ± 0.11	0.19 ± 0.10	0.638	0.23 ± 0.12	0.086	<b>0.046<sup>a</sup></b>
Antioxidant capacity (% diene)	95.0 ± 22.9	87.4 ± 44.6	0.226	96.1 ± 38.4	0.778	0.128
HDL subclass particle concentration (µmol/L)						
Large HDL	0.5 (0.4-0.7)	0.5 (0.2-0.7)	0.909	0.6 (0.4-0.8)	0.114	<b>0.029<sup>a</sup></b>
Medium HDL	3.3 (2.1-4.3)	2.4 (1.9-3.2)	<b>0.044<sup>a</sup></b>	3.3 (2.4-3.9)	0.361	<b>0.032<sup>a</sup></b>
Small HDL	7.8 (6.0-10.0)	8.1 (6.4-9.1)	0.989	7.1 (5.7-8.4)	0.301	0.139
Total HDL	10.8 (9.8-12.5)	10.6 (9.6-13.2)	0.395	10.9 (8.9-13.0)	0.346	0.986

Normal distributed data are given as mean ± SD and non-normal distributed data as the median (interquartile range). Pre-treatment baseline data were compared with post-treatment data using the paired sample Wilcoxon signed rank test; \*P, the effect of treatment was analysed using the paired sample Wilcoxon signed rank test; \*\*P. Bold signifies P value. <sup>a</sup> Results lost statistical significance at P < 0.05 after we adjusted for α inflation caused by multiple test.

### 3.3.5 Discussion

Three essential messages are obtained from our study. The first message is that pharmacological intervention with ERN/LRP and FFB in T2DM patients leads to important HDL particle modifications, beyond HDL cholesterol concentrations. The second message is that these composition changes differ according to the HDL cholesterol-increasing medication used. The third message is that neither ERN/LRP nor FFB reverses diabetic HDL alterations *ad integrum*. These differences could, in part, be explained by the mechanisms of action of both medications. FFB is a PPAR $\alpha$  agonist that increases proteins associated with lipolysis activity, whereas niacin, among other mechanisms, reduces adipose tissue lipolysis<sup>30,31</sup>. The post-treatment HDL particles differ depending on the medication used, and they also differ from normal; therefore, the expected effect on cardiovascular risk should be unequal. HDL cholesterol, which is the primary variable that is expected to be modified by ERN/LRP and FFB, increases in different proportions. Although niacin produced a mean 18% increase, FFB did not significantly modify HDL cholesterol. These results are in concordance with previous publications that show similar effects of niacin and FFB<sup>6,8-10</sup>. Niacin was also the only medication that produced a significant increase in apoA-I. However, consistent with previous observations, only FFB induced a significant 15% increase in apoA-II<sup>32</sup>. Patients with T2DM had significantly higher pre $\beta$ 1- HDL particles, which were further increased by FFB, whereas niacin tended to decrease the levels of pre $\beta$ 1-HDL. The clinical repercussion of this fact is not clear. Both high and low levels of pre $\beta$ 1-HDL have been associated with cardiovascular risk and the

presence of cardiovascular risk factors<sup>33,34</sup>. These discrepancies can be explained by different mechanisms, including increased synthesis, decreased maturation, or both, that can be involved in the origin of pre $\beta$ 1-HDL plasma accumulation. Patients with T2DM had higher CETP activity, which tended to be reduced by both treatments, although only after ERN/LRP, this tendency was statistically significant, which suggests that partial inhibition of CETP could be a mechanism that explains the effects of both ERN/LRP and FFB on HDL cholesterol concentrations. T2DM patients had a high LCAT mass, but no significant differences in activity were observed. ERN/LRP significantly reduced LCAT activity in T2DM patients. Despite a different marginal effect on PAF-AH and PON 1 mass and activity, neither fenofibrate nor niacin treatment was associated with better oxidation profile markers according to the lipoperoxide concentration in apoB-lipoprotein-containing depleted plasma, which is an indirect index of HDL oxidation, and the capability of HDL to protect against LDL oxidation. Diabetic patients had an HDL fraction with increased proportions of apoA-II and C-III and half the concentration of apoE. Although FFB increased apoA-II, niacin reduced its concentration. FFB reduced apoC-III; however, neither FFB nor ERN/LRP modified the proportion of apoE. The biological impact of these differences is not known (Supplemental Tables 3S and 4S). We speculate that the increased apoA-II after FFB treatment may modify apolipoprotein exchange between HDL and triglyceride-rich particles, thus decreasing lipoprotein lipase activity and influencing both triglyceride and HDL cholesterol concentrations<sup>35</sup>.

## Chapter 3

The NMR results reinforced that HDL from T2DM patients is clearly different from the healthy group in terms of particle size and number. T2DM patients had fewer HDL particles, and the HDL particles from T2DM patients had smaller radii. These alterations were not reversed by ERN/LRP or FFB.

Some limitations of our study are that the intervention period of the study was only 12 weeks; therefore, our results cannot be extrapolated over a longer period of time. The sample size is small due to the comprehensive analyses performed, including metabolomics techniques. This rather small sample size allows only the detection of large effects; however, it does warrant enough power for the main results of the study. The ERN preparation was associated with LRP, so we cannot exclude the lipid effects associated with this product, although if they exist, they seem to be very light.

ERL/LRP has been withdrawn from the market, although other niacin-based pills are available in different countries, and FFB is widely available. The overall conclusions of our work are that neither ERN/LPP nor FFB reverse HDL particle abnormalities associated to T2DM. Moreover, these two drugs act differently on HDL. Our results should contribute to a better understanding of the negative results observed in randomized controlled trials using niacin or fenofibrate. In our hands these two drugs don't improve HDL particle composition, size and metabolism, despite a marginal impact on HDL cholesterol concentrations. Clinicians prescribing these drugs must be aware of their overall impact on HDL particles and lipoprotein metabolism.

Supplementary data related to this article can be found at <http://dx.doi.org/10.1016/j.atherosclerosis.2014.12.006>.

### 3.3.6 References

1. Rydén, L., Standl, E., Bartnik, M. & Berghe, G. Guidelines on diabetes, pre-diabetes, and cardiovascular diseases: full text‡: The Task Force on Diabetes and Cardiovascular Diseases of the European. *Eur. Hear.* (2007).
2. Perk, J. *et al.* European Guidelines on cardiovascular disease prevention in clinical practice (version 2012): The Fifth Joint Task Force of the European Society of Cardiology and Other Societies on Cardiovascular Disease Prevention in Clinical Practice (constituted by representatives of nine societies and by invited experts) \* Developed with the special contribution of the European Association for Cardiovascular Prevention & Rehabilitation (EACPR). *Eur. Heart J.* **33**, 1635–1701 (2012).
3. Mooradian, A. D. Dyslipidemia in type 2 diabetes mellitus. *Nat. Rev. Endocrinol.* (2009).
4. Chapman, M. J. *et al.* Triglyceride-rich lipoproteins and high-density lipoprotein cholesterol in patients at high risk of cardiovascular disease: evidence and guidance for management. *Eur. Heart J.* **32**, 1345–61 (2011).
5. The Emerging Risk Factors Collaboration\* *et al.* Major Lipids, Apolipoproteins, and Risk of Vascular Disease. *JAMA* **302**, 1993 (2009).
6. Keech, A. *et al.* Effects of long-term fenofibrate therapy on cardiovascular events in 9795 people with type 2 diabetes mellitus (the FIELD study): randomised controlled trial. *Lancet* **366**, 1849–1861 (2005).
7. Robins, S. J. *et al.* Relation of Gemfibrozil Treatment and Lipid Levels With Major Coronary Events. *JAMA* **285**, 1585 (2001).
8. Group, T. A. S. Effects of Combination Lipid Therapy in Type 2 Diabetes Mellitus. *N. Engl. J. Med.* **362**, 1563–1574 (2010).
9. Investigators, T. A.-H. Niacin in Patients with Low HDL Cholesterol Levels Receiving Intensive Statin Therapy. *N. Engl. J. Med.* **365**, 2255–2267 (2011).
10. Haynes, R. *et al.* HPS2-THRIVE randomized placebo-controlled trial in 25 673 high-risk patients of ER niacin/laropiprant: trial design,

## Chapter 3

pre-specified muscle and liver outcomes, and reasons for stopping study treatment. *Eur. Heart J.* **34**, 1279–1291 (2013).

11. Vaisar, T. *et al.* Shotgun proteomics implicates protease inhibition and complement activation in the antiinflammatory properties of HDL. *J. Clin. Invest.* **117**, 746–756 (2007).

12. Davidson, W. S. *et al.* Proteomic Analysis of Defined HDL Subpopulations Reveals Particle-Specific Protein Clusters: Relevance to Antioxidative Function. *Arterioscler. Thromb. Vasc. Biol.* **29**, 870–876 (2009).

13. Kontush, A., Lhomme, M. & Chapman, M. Unraveling the complexities of the HDL lipidome. *J. Lipid Res.* **54**, 2950–2963 (2013).

14. Camont, L. *et al.* Small, Dense High-Density Lipoprotein-3 Particles Are Enriched in Negatively Charged Phospholipids: Relevance to Cellular Cholesterol Efflux, Antioxidative, Antithrombotic, Anti-Inflammatory, and Antiapoptotic Functionalities. *Arterioscler. Thromb. Vasc. Biol.* **33**, 2715–2723 (2013).

15. Kontush, A. & Chapman, M. Why is HDL functionally deficient in type 2 diabetes? *Curr. Diab. Rep.* **8**, 51–59 (2008).

16. Soran, H., Hama, S., Yadav, R. & Durrington, P. N. HDL functionality. *Curr. Opin. Lipidol.* **23**, 353–366 (2012).

17. Escolà-Gil, J. C., Cedó, L. & Blanco-Vaca, F. High-density lipoprotein cholesterol targeting for novel drug discovery: where have we gone wrong? *Expert Opin. Drug Discov.* **9**, 119–124 (2014).

18. Morgantini, C. *et al.* Anti-inflammatory and Antioxidant Properties of HDLs Are Impaired in Type 2 Diabetes. *Diabetes* **60**, (2011).

19. Khera, A. V. *et al.* Cholesterol Efflux Capacity, High-Density Lipoprotein Function, and Atherosclerosis. *N. Engl. J. Med.* **364**, 127–135 (2011).

20. Girona, J. *et al.* Oxidized to non-oxidized lipoprotein ratios are associated with arteriosclerosis and the metabolic syndrome in diabetic patients. *Nutr. Metab. Cardiovasc. Dis.* **18**, 380–7 (2008).

21. Goldstein, D. E. *et al.* Tests of glycemia in diabetes. *Diabetes Care* **18**, 896–909 (1995).



22. Lussier-Cacan, S. *et al.* Plasma total homocysteine in healthy subjects: sex-specific relation with biological traits. *Am. J. Clin. Nutr.* **64**, 587–93 (1996).
23. Schumaker, V. N. & Puppione, D. L. Sequential flotation ultracentrifugation. *Methods Enzymol.* **128**, 155–170 (1986).
24. Aragonès, G. *et al.* Measurement of serum PON-3 concentration: method evaluation, reference values, and influence of genotypes in a population-based study. *J. Lipid Res.* **52**, 1055–61 (2011).
25. Marsillach, J. *et al.* The measurement of the lactonase activity of paraoxonase-1 in the clinical evaluation of patients with chronic liver impairment. *Clin. Biochem.* **42**, 91–98 (2008).
26. Gaidukov, L. & Tawfik, D. S. The development of human sera tests for HDL-bound serum PON1 and its lipolactonase activity. *J. Lipid Res.* **48**, 1637–46 (2007).
27. Ribas, V. *et al.* Human apolipoprotein A-II enrichment displaces paraoxonase from HDL and impairs its antioxidant properties: a new mechanism linking HDL protein composition and antiatherogenic potential. *Circ. Res.* **95**, 789–97 (2004).
28. Mallol, R. *et al.* Particle size measurement of lipoprotein fractions using diffusion-ordered NMR spectroscopy. *Anal. Bioanal. Chem.* **402**, 2407–2415 (2012).
29. Fleiss, J. L. *The crossover study, in: The Design and Analysis of Clinical Experiments.* (John Wiley & Sons, Inc., 1986).
30. Villines, T. C., Kim, A. S., Gore, R. S. & Taylor, A. J. Niacin: The Evidence, Clinical Use, and Future Directions. *Curr. Atheroscler. Rep.* **14**, 49–59 (2012).
31. Noonan, J. E. *et al.* An update on the molecular actions of fenofibrate and its clinical effects on diabetic retinopathy and other microvascular end points in patients with diabetes. *Diabetes* **62**, 3968–75 (2013).
32. Taskinen, M.-R. *et al.* Relationships of HDL cholesterol, ApoA-I, and ApoA-II with homocysteine and creatinine in patients with type 2 diabetes treated with fenofibrate. *Arterioscler. Thromb. Vasc. Biol.* **29**, 950–5 (2009).

### Chapter 3

33. Guey, L. T. *et al.* Relation of increased prebeta-1 high-density lipoprotein levels to risk of coronary heart disease. *Am. J. Cardiol.* **108**, 360–6 (2011).
34. Hirayama, S. *et al.* Pre beta1-HDL concentration is a predictor of carotid atherosclerosis in type 2 diabetic patients. *Diabetes Care* **30**, 1289–91 (2007).
35. Julve, J. *et al.* Human apolipoprotein A-II determines plasma triglycerides by regulating lipoprotein lipase activity and high-density lipoprotein proteome. *Arterioscler. Thromb. Vasc. Biol.* **30**, 232–8 (2010).

## **Chapter 4. Lipoprotein analysis for diet and nutritional interventions assessment**



## **4.1 Introduction**



Nutritional interventions and dietary habits assessment are the perfect study examples where the use of NMR derived lipoprotein characterization can provide information about pathophysiological mechanisms involving atherosclerosis and CVD and external agents such as long chain omega-3 fatty acids.

The present chapter describes how nutrition and, in particular the n-3 fatty acids modulate the lipoprotein profile in an epidemiological association study and two nutritional interventions. Firstly, we present an epidemiological study involving more than 26,000 apparently healthy women to evaluate the associations between the fish consumption and n-3, and the lipoprotein profile determined by NMR by using the technology commercialized by Liposcience. This original research resulted from the doctoral stay at the unit of preventive medicine (Brigham and Women's Hospital) under the supervision of Dr. Samia Mora. Currently, after the internal review which includes an external data check of all the developed software code for statistical analysis and the results, the document is being prepared for submission as an original article as follows:

- Amigó N., Akinkuolie, A.O., Chiuve, S.E., Correig, X., Cook, NR & Mora, S. Fish consumption omega-3 fatty acids and NMR lipoprotein subfractions in 26.034 apparently healthy women.

Complementary, we wanted to present in the same section two published works of an intervention trial designed to evaluate the effect of diets enriched with either SFA or n-6 PUFA, and supplemented with LCn-3PUFA on the lipoprotein profile by using the Liposcale test.

- Dias, C. B., Amigó, N., Wood, L. G., Mallol, R., Correig, X., & Garg, M. L. (2016). Improvement of the omega 3 index of healthy

## Chapter 4

subjects does not alter the effects of dietary saturated fats or n-6PUFA on LDL profiles. *Metabolism: Clinical and Experimental*, 68.

<https://doi.org/10.1016/j.metabol.2016.11.014>

- Dias, C. B., Amigo, N., Wood, L. G., Correig, X., & Garg, M. L. (2017). Effect of diets rich in either saturated fat or n-6 polyunsaturated fatty acids and supplemented with long-chain n-3 polyunsaturated fatty acids on plasma lipoprotein profiles. *European Journal of Clinical Nutrition*.  
<https://doi.org/10.1038/ejcn.2017.56>

These two works are the result of an international collaboration with the Dra. Cintia Botelho Dias during her visit to Biosfer Teslab during August 2015. The three works demonstrate how lipoprotein characterization by NMR can be an evaluation tool for diet and nutritional interventions.



## **4.2 Fish consumption, omega-3 fatty acids and NMR lipoprotein subfractions in 26,034 apparently healthy women**

**CHAPTER UNDER REVISION**

**4. 3 Improvement of the omega 3 index of healthy subjects does not alter the effects of dietary saturated fats or n-6PUFA on LDL profiles**



### 4.3.1 Abstract

Dietary fat composition is known to modulate circulating lipid and lipoprotein levels. Although supplementation with long chain omega-3 polyunsaturated fatty acids (LCn-3PUFA) has been shown to reduce plasma triglyceride levels, the effect of the interactions between LCn-3PUFA and the major dietary fats consumed has not been previously investigated.

In a randomized controlled parallel design clinical intervention, we examined the effect of diets rich in either saturated fatty acids (SFA) or omega-6 polyunsaturated fatty acids (n-6PUFA) on plasma lipid levels and lipoprotein profiles (lipoprotein size, concentration and distribution in subclasses) in subjects with an adequate omega 3 index. Twenty six healthy subjects went through a four-week pre-supplementation period with LCn-3PUFA and were then randomized to diets rich in either n-6PUFA or SFA both supplemented with LCn-3PUFA.

The diet rich in n-6PUFA decreased low density lipoprotein (LDL) particle concentration (-8%,  $p=0.013$ ) and LDL cholesterol (LDL-C) level (-8%,  $p=0.021$ ), while the saturated fat rich diet did not affect LDL particle number or LDL-C levels significantly. Nevertheless, dietary saturated fatty acids increased LCn-3PUFA in plasma and tissue lipids compared with n-6PUFA, potentially reducing other cardiovascular risk factors such as inflammation and clotting tendency.

Improvement on the omega 3 index of healthy subjects did not alter the known effects of dietary saturated fats and n-6PUFA on LDL profiles.

### 4.3.2 Introduction

Incorporation of long chain omega 3 polyunsaturated fatty acids (LCn-3PUFA) into cell membranes, in particular docosahexaenoic acid (DHA, 22:6n-3), modulate biophysical properties and functionality of the cell membranes<sup>1,2</sup>. Dietary supplementation with LCn-3PUFA have been shown to reduce the risk of cardiovascular disease (CVD) and other chronic diseases, by reducing blood triglycerides and inflammation and increasing high density lipoprotein cholesterol, among other mechanisms<sup>3,4</sup>, although some controversy is still observed in the literature<sup>5</sup>. Thus, an optimal omega-3 index [eicosapentaenoic acid (EPA, 20:5n-3) plus 22:6n-3 in erythrocytes] of 8% or greater has been suggested for the prevention of chronic diseases and for health promotion<sup>6</sup>.

Other dietary fatty acids, such as omega 6 polyunsaturated fatty acids (n-6PUFA) from vegetable oils and saturated fatty acids (SFA) from animal or plant sources, may influence LCn-3PUFA absorption and incorporation into plasma and tissue lipids<sup>7,8</sup>. Our group has previously demonstrated that a diet enriched with saturated fatty acids and supplemented with LCn-3PUFA was more efficient in improving the incorporation of LCn-3PUFA into plasma and tissue lipids than a diet enriched with n-6PUFA, although an increase in low density lipoprotein cholesterol (LDL-C) was also observed with the SFA enriched diet<sup>8</sup>.

Due to their capacity to modulate membrane composition and function, LCn-3PUFA may also influence the efficacy of other dietary fatty acids to alter blood lipid levels and lipoprotein profiles. In spite of the association between SFA and CVD and elevated blood lipid levels<sup>4</sup>,

## Chapter 4

studies in animal<sup>9</sup> and human<sup>10</sup> models have demonstrated that SFA increase plasma triglyceride level only when the diet is deficient in n-3PUFA. Therefore, we aimed to determine if an improvement in the omega-3 index of healthy subjects would modulate the effect of the dietary SFA and n-6PUFA on plasma lipid levels [total cholesterol, LDL-C, high density lipoprotein cholesterol (HDL-C) and triglycerides] and lipoprotein profiles (lipoprotein size, concentration and distribution in subclasses). Furthermore, we hypothesize that a saturated fat rich diet does not adversely affect lipid and lipoprotein profiles compared to a diet rich in n-6PUFA in the context of an adequate omega-3 index.

### 4.3.3 Material and Methods

**Study Population.** Twenty nine healthy adults (16 females and 13 males) aged between 21 and 65 years were recruited. Subject's exclusion criteria were: use of lipid-lowering drugs (e.g. statins); regular consumption of fish oil supplements within the past month; regular consumption of 2 or more fish meals a week over the past month; any history of congestive heart failure, stroke, myocardial infarction, coronary artery bypass graft, or atherosclerotic CVD; history of diabetes, renal disease, gastrointestinal disorder or liver disease. Smokers and pregnant or breast feeding women were also excluded.

**Study design.** In this randomized controlled, parallel, dietary intervention trial design, subjects consumed 4x1g fish oil capsules [100 mg 20:5n-3: 500 mg 22:6n-3 each (EPAX 1050TG, Norway)] for 4 weeks. Subjects were then randomized to a diet rich in either saturated fatty acids (SFA+LCn-3PUFA diet) or n-6PUFA (n-6PUFA+LCn-3PUFA diet)

for a further ten-day period, while continuing fish oil supplementation (Figure 1). Subjects on the SFA+LCn-3PUFA diet group consumed daily 24g of butter, 40g of white chocolate (providing 30g total fat, 20.9g saturated fat) and 4x1g fish oil capsules; they were also advised on how to use more foods containing SFA for cooking, while reducing n-6PUFA intake. Subjects on the n-6PUFA+LCn-3PUFA diet consumed daily 20g of margarine (Flora original), 42g of sunflower seeds (providing 30g total fat, 20g n-6PUFA) and 4x1g fish oil capsules; they were also advised on how to use more foods and oils containing n-6PUFA for cooking, while reducing SFA intake. Following an overnight fast, subjects visited the Nutraceuticals Research Clinic facility at the University of Newcastle on three occasions; before LCn-3PUFA supplementation, after 4 weeks of supplementation and after the dietary intervention with the SFA+LCn-3PUFA and the n-6PUFA+LCn-3PUFA diets. All subjects were advised not to change their physical activity status or any other aspect of their habitual diet. After pre-supplementation with LCn-3PUFA, subjects were allocated to one of the 2 diets using computer generated random tables ([www.randomization.com](http://www.randomization.com), seed 7027 for males and seed 4586 for females). Nutrient intake prior and during the intervention period was assessed using a three-day food record (2 week days and one weekend day) and the software FoodWorks 7 Professional (Xyris software). At each visit, blood samples and anthropometric measurements were collected following an overnight fast (10 hours) and 24 hours refrain from strenuous exercise and alcohol consumption. Blood samples were assessed for plasma lipid levels, lipoprotein profiles and fatty acid composition of plasma and erythrocyte lipids. Physical activity



## Chapter 4

(International Physical Activity Questionnaire long form), medical history and consumption of medications, supplements and alcohol were also assessed at each visit. This study was conducted according to the guidelines laid down in the Declaration of Helsinki, all procedures involving human subjects were approved by the University of Newcastle Human Research Ethics Committee (protocol H-2012-0117), and the study was registered with the Australia New Zealand Trial registry (registration identification number ACTRN12614001051639, <http://www.anzctr.org.au/>). All subjects gave their written informed consent before participation.

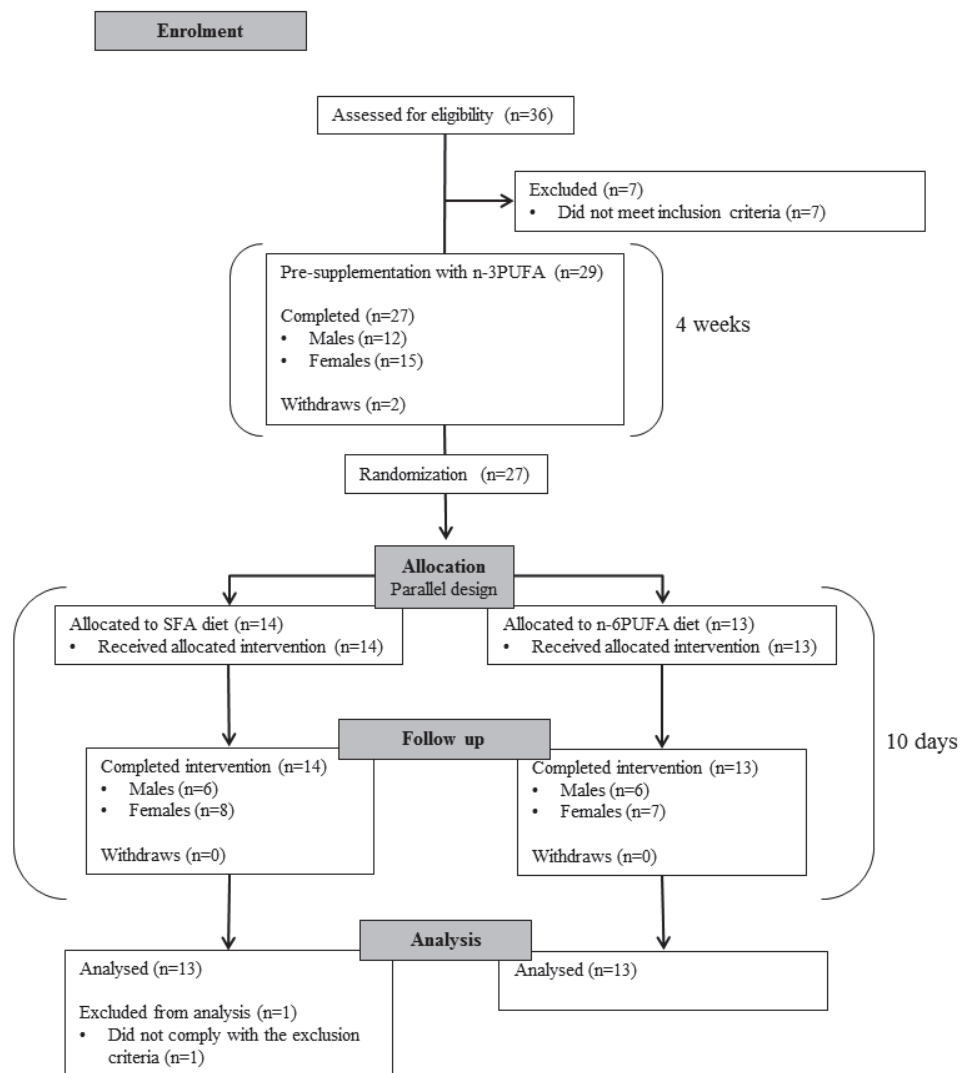


**Figure 1.** Schematic representation of the study schedule.

Compliance was monitored by count back of fish oil capsules and other food products provided, interview with volunteers about their food consumption at the end of the trial, evaluation of their dietary records, and analysis of plasma fatty acid composition. No subject showed any signs of intolerance to the supplements provided.

## Chapter 4

***Plasma and erythrocyte sample preparation.*** Fasting blood samples were collected in EDTA vacutainer. Plasma was immediately separated from erythrocytes by centrifugation (1000 g x 15 minutes at 4°C) and both fractions were stored at -80°C until analyzed.

***Plasma and erythrocyte fatty acid composition.*** Incorporation of fatty acids in plasma and erythrocytes was determined using gas chromatography following trans-esterification as described previously<sup>8</sup>.

***Plasma lipoprotein profiles.*** Frozen plasma samples (500µl) were shipped on dry ice to Biosfer Teslab (Reus, Spain) for the analysis of lipoprotein profiles by nuclear magnetic resonance (NMR). The determination of lipoprotein size, concentration and lipoprotein subclasses distribution have been previously reported by Mallol and colleagues<sup>11</sup>. Briefly, particle concentration and diffusion coefficients were obtained from the measured amplitudes and attenuation of the particles' spectroscopically distinct lipid methyl group NMR signals, using the 2D diffusion-ordered <sup>1</sup>H-NMR spectroscopy (DSTE) pulse. The methyl signal was surface fitted with 9 lorentzian functions associated with each lipoprotein subclass of the main lipoprotein groups (VLDL, LDL and HDL). The area of each lorentzian function was related to the lipid concentration of each lipoprotein subclass, and the size of each subclass was calculated from their diffusion coefficient. The concentration of each lipoprotein subclass was calculated by dividing the lipid volume by the particle volume of a given class. Lipid volumes were determined by using common conversion factors to convert concentration units into volume units<sup>12</sup>. The different lipoprotein subclasses correspond to the following diameter size ranges: large VLDL, 68.5 to 95.9 nm, medium

VLDL, 47 to 68.5 nm, small VLDL, 32.5 to 47 nm, very large LDL, 24 to 32.5 nm, medium-large LDL, 20.5 to 24 nm, small LDL, 17.5 to 20.5 nm, very large HDL, 10.5 to 13.5 nm, medium-large HDL, 8.5 to 10.5 nm and small HDL, 7.5 to 8.5 nm.

**Plasma lipid profile, glucose and high sensitivity C-reactive protein.** Blood samples were collected in lithium heparin vacutainers. Plasma was immediately separated from erythrocytes by centrifugation (3000 g x 10 min at 4°C) and analyzed for total cholesterol, triglycerides, glucose and C-reactive protein by the accredited Hunter New England Area Pathology Service.

**Statistical analysis.** Sample size calculation was based on an anticipated 30% (0.45 mmol/L) change in plasma triglycerides (primary outcome) with triglyceride standard deviation 0.387 mmol/L, level of significance 0.05 and 80% power<sup>13</sup>. Thirteen subjects were then recruited in each group.

All data are presented as median and interquartile range (IQR). Kruskal-Wallis test was used for comparing the randomized groups before dietary intervention. Pre-supplementation period data were compared using Wilcoxon signed-rank test. Data obtained before and after dietary intervention were compared within group using Wilcoxon signed-rank test and data on change were compared between groups using Kruskal-Wallis test. For all tests a p-value lower than 0.05 was considered statistically significant. Mat Lab R2010a (MathWorks) was used to perform the statistical analysis.

## Chapter 4

### 4.3.4 Results

From the 29 subjects recruited (15 on the SFA+LCn-3PUFA diet and 14 on the n-6PUFA+LCn-3PUFA diet), 2 dropped from the study, 1 did not comply with the study protocol and 1 had lipoprotein profiles data missing. Therefore, 3 subjects (2 on the SFA+LCn-3PUFA diet and 1 on the n-6PUFA+LCn-3PUFA diet) were excluded from all data analysis and one subject was excluded only from the lipoprotein profiles analysis. Twenty six subjects were then included in the statistical analysis, 13 on the SFA+LCn-3PUFA diet (5 males and 8 females) and 13 on the n-6PUFA+LCn-3PUFA diet (6 males and 7 females).

The pre-supplementation period efficiently increased the consumption of LCn-3PUFA and their incorporation into blood lipids. Percentage of 20:5n-3 and 22:6n-3 increased in plasma and erythrocyte lipids at the expense of monounsaturated fatty acids and n-6PUFA as expected, indicating compliance with the study protocol. The LCn-3PUFA supplements consumed have been previously characterized<sup>8</sup>. During pre-supplementation, there was an increase in body mass index (BMI) and percentage body fat. There was also a significant decrease in total triglycerides consistent with a decrease in the concentration of total, large, medium and small VLDL particles. Very large and medium-large LDL particle concentration increased, without significant change to LDL-C. Very large HDL particle concentration decreased, while medium-large HDL particle concentration, HDL average size and HDL-C increased (Tables A.1 to A.5 in the supplementary appendix).

**Table 1.** Subjects characteristics at randomization.

	SFA+LCn3PUFA	n-6PUFA+LCn3PUFA	P
Age (years)	32.0 (29.0)	28.0 (37.8)	0.777
BMI (Kg/m <sup>2</sup> )	24.4 (4.5)	23.5 (4.4)	0.758
Body fat (%)	27.0 (20.7)	22.6 (16.7)	0.758
Glucose (mmol/L)	5.10 (0.45)	5.00 (0.83)	1.000
Triglycerides (mmol/L)	0.76 (0.55)	0.86 (0.56)	0.489
Total cholesterol (mmol/L)	4.80 (1.53)	5.40 (1.25)	0.719
LDL-C (mmol/L)	2.31 (0.98)	2.65 (0.73)	0.807
HDL-C (mmol/L)	1.46 (0.38)	1.26 (0.32)	0.370
hsCRP (mmol/L)	1.00 (1.60)	0.90 (1.80)	0.699
Plasma LCn-3PUFA (%)	7.98 (2.63)	8.01 (1.51)	0.412
Omega 3 index (20:5n-3+22:6n-3)	10.45 (1.86)	10.77 (1.77)	0.356

Data presented as median (interquartile range - IQR). P, p-value for comparison between groups; BMI, body mass index; LDL-C, low density lipoprotein cholesterol; HDL-C, high density lipoprotein cholesterol; hsCRP, high sensitivity C-reactive protein; LCn-3PUFA, long chain omega-3 polyunsaturated fatty acids [eicosapentaenoic acid (20:5n-3) + docosapentaenoic acid (22:5n-3) + docosahexaenoic acid (22:6n-3)].

At randomization, both groups were of similar age, body mass index, percentage body fat, plasma lipid levels, lipoprotein profiles and plasma and erythrocyte fatty acid composition, except for docosapentaenoic acid (22:5n-3) percentage (Tables 1 and A.2 to A.5). Subjects in both groups also had similar energy and nutrient consumption, except for the percentage energy from total fat. During the dietary intervention, subjects on the n-6PUFA+LCn3PUFA diet reduced their carbohydrate consumption while increasing total fat consumption compared to subjects on the SFA+LCn3PUFA diet, despite subjects in both groups being advised not to change the consumption of nutrients other than the fat type. Subjects on the SFA+LCn3PUFA diet

## Chapter 4

increased their saturated fat consumption and reduced their linoleic acid consumption in contrast with subjects in the n-6PUFA+LCn3PUFA diet (Table A.1).

After the n-6PUFA+LCn3PUFA diet, the percentage of plasma linoleic acid increased and the LCn-3PUFA (20:5n-3, 22:5n-3 and 22:6n-3) decreased, compared to the SFA+LCn3PUFA diet (Figure 2). A similar pattern was observed in erythrocyte lipids with an increase in percent linoleic acid and a decrease in percent 20:5n-3 in the n-6PUFA+LCn3PUFA group compared to the SFA+LCn3PUFA group (Figure 3). After the n-6PUFA+LCn3PUFA diet there was a decrease in total cholesterol and LDL-C, as well as a decrease in LDL triglycerides and total, very large, medium-large and small LDL particle concentration compared to the SFA+LCn3PUFA diet (Figures 4 and 5). However, the concentration of small LDL was not increased significantly after consumption of the SFA+LCn3PUFA diet. There were no further changes in body composition or other lipoprotein profiles (Tables A.2 to A.5).

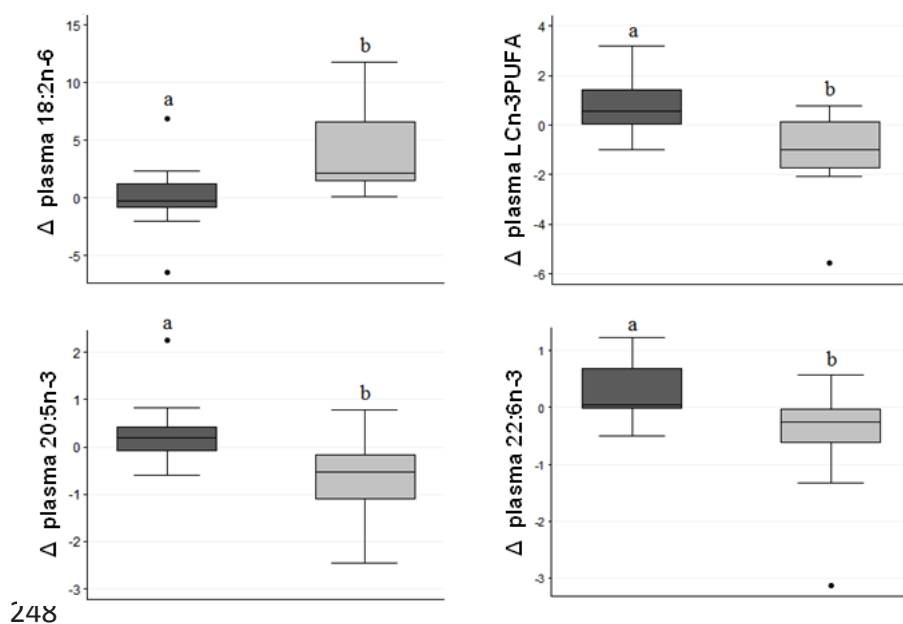


**Figure 2. Change in plasma linoleic acid (18:2n-6) and long chain omega-3 polyunsaturated fatty acids (20:5n-3, 22:5n-3, 22:6n-3) (% from total fatty acids detected).** Data presented as median (interquartile range - IQR). Different lower case letters represent significant difference ( $p < 0.05$ ) between changes caused by dietary intervention with either (■) SFA+LCn-3PUFA ( $n=12$ , 5 males and 7 females) or (▒) n-6PUFA+LCn-3PUFA ( $n=13$ , 6 males and 7 females). Dots represent outliers.

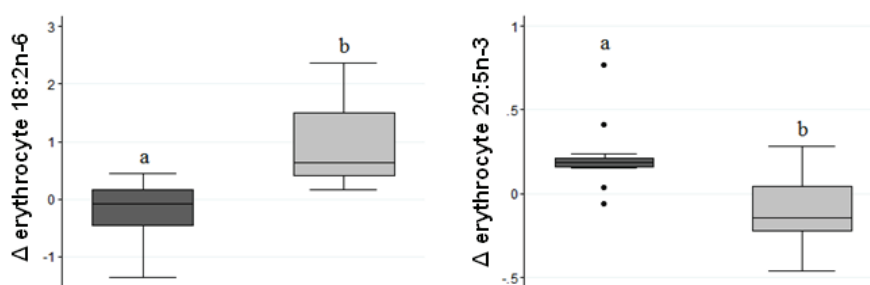


**Figure 3. Change in erythrocyte linoleic acid and eicosapentaenoic acid (20:5n-3) (% from total fatty acids detected).** Data presented as median (interquartile range - IQR). Different lower case letters represent significant difference ( $p < 0.05$ ) between changes caused by dietary intervention with either (■) SFA+LCn-3PUFA ( $n=12$ , 5 males and 7 females) or (▒) n-6PUFA+LCn-3PUFA ( $n=13$ , 6 males and 7 females). Dots represent outliers.

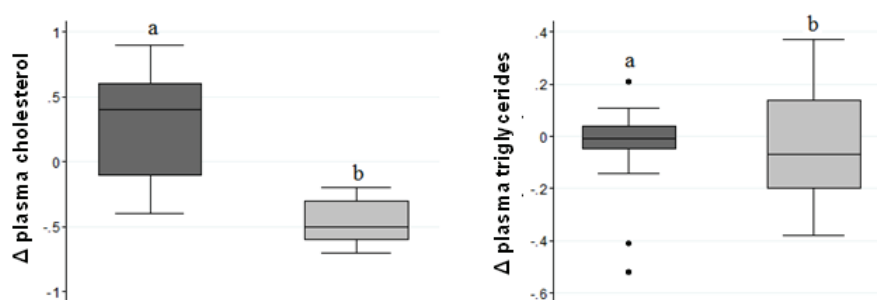


**Figure 4. Change in plasma total cholesterol (mmol/L) and triglycerides (mmol/L).** Data presented as median (interquartile range - IQR). Different lower case letters represent significant difference ( $p < 0.05$ )



## Chapter 4

between changes caused by dietary intervention with either (■) SFA+LCn-3PUFA (n=12, 5 males and 7 females) or (▒) n-6PUFA+LCn-3PUFA (n=13, 6 males and 7 females). Dots represent outliers.

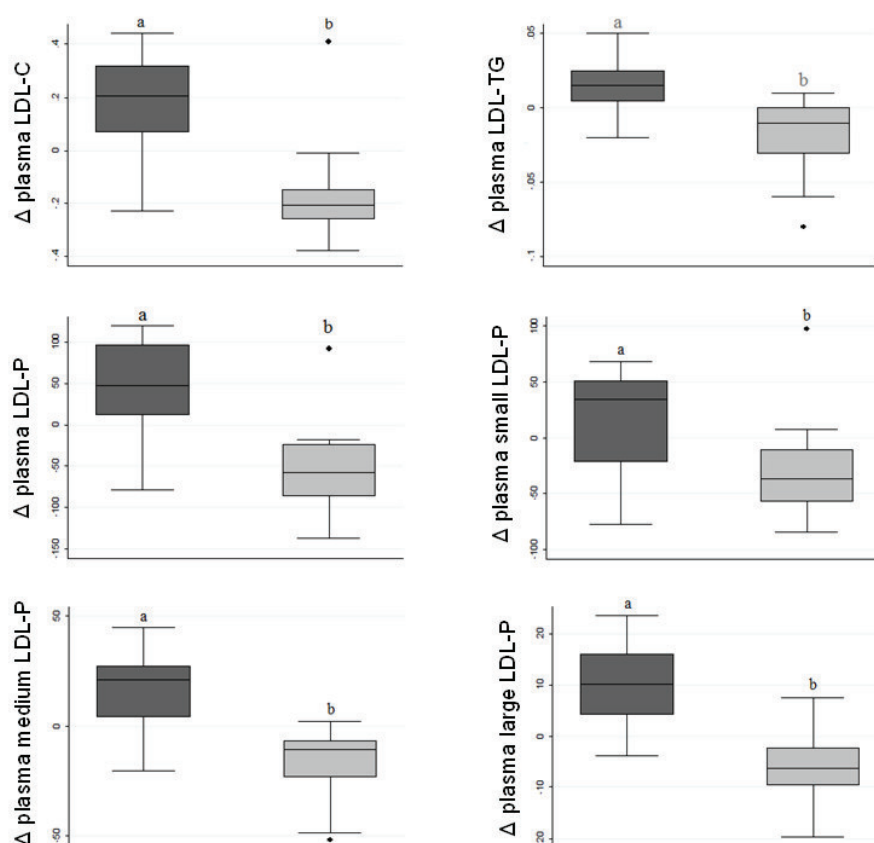


**Figure 5. Change in lipoprotein profiles. Data presented as median (interquartile range - IQR).** LDL, low density lipoprotein; C, cholesterol (mmol/L); TG, triglycerides (mmol/L); P, particle (nmol/L). Different lower case letters represent significant difference ( $p < 0.05$ ) between changes caused by dietary intervention with either (■) SFA+LCn-3PUFA (n=12, 5 males and 7 females) or (▒) n-6PUFA+LCn-3PUFA (n=13, 6 males and 7 females). Dots represent outliers.

### 4.3.5 Discussion

This clinical intervention was designed to determine if improving the LCn-3PUFA status by prior dietary supplementation with fish oil

would modulate the effect of the major dietary fats (SFA versus n-6PUFA) on lipoprotein profiles and plasma lipid levels. A diet rich in saturated fatty acids raised LDL-C compared to a diet rich in n-6PUFA despite LCn-3PUFA supplementation. However, the increase in LDL-C was primarily due to an increase in very large and medium-large LDL particles that are known to be less atherogenic than small LDL particles<sup>14-16</sup>, which were not significantly elevated by saturated fat consumption.

The n-6PUFA+LCn3PUFA diet caused a decrease in total, very large, medium-large and small LDL particles as well as a decrease in LDL-C and LDL-triglycerides (LDL-TG) compared to the SFA+LCn3PUFA diet. Similar effects have been observed previously in a study assessing the effects of a diet enriched with n-6PUFA<sup>17</sup>. Additionally, an epidemiological study has demonstrated an inverse association between serum n-6PUFA and the concentration of total and small LDL particles and a positive association with large LDL<sup>18</sup>. Indeed, n-6PUFA have been demonstrated to increase LDL-r transcription and synthesis<sup>19</sup>, improving the transfer of LDL particles from the bloodstream to the liver. N-6PUFA also increase the catabolism of Apolipoprotein B-100, impairing the formation of new LDL particles<sup>20</sup>. In contrast most dietary saturated fatty acids reduce the expression of hepatic LDL-r<sup>21</sup>, impairing the capitation of LDL particles, and consequently LDL-C, by the liver. Dietary saturated fatty acids have also been associated with an increase in the concentration of large LDL particles in healthy<sup>22</sup> and obese<sup>23</sup> men. In the present intervention an SFA rich diet supplemented with LCn-3PUFA increased the concentration of very large and medium-large LDL

## Chapter 4

particles, without a significant increase to the total concentration of LDL particles. In epidemiological studies, total LDL particle concentration and small LDL particle concentration were inversely associated with CVD risk independently of the LDL-C level, while large LDL particles were not associated with increased risk<sup>14,16</sup>. Therefore, the higher LDL-C levels observed after consumption of the SFA rich diet compared to the n-6PUFA rich diet may not necessarily heighten the CVD risk, particularly when LCn-3PUFA intake is adequate.

Interestingly, saturated fat consumption for 10 days resulted in further increase in erythrocyte 20:5n-3 and 22:6n-3 percentage whereas n-6PUFA diet induced a significant decline in the percentage of all LCn-3PUFA in plasma and a non-significant reduction in erythrocyte 20:5n-3 percentage despite an increase in 22:6n-3 percentage. These results are in agreement with our previous observations that saturated fat enhances incorporation of LCn-3PUFA into plasma and tissue lipids, while n-6PUFA and LCn-3PUFA compete for incorporation<sup>8,9</sup>. These results may have important implications when considering the health effects of LCn-3PUFA. Despite the negative effects of SFA on cholesterol levels, greater incorporation of LCn-3PUFA following supplementation with a background diet rich in saturated fats has the potential to result into greater anti-inflammatory and anti-aggregatory effects. The importance of background dietary fat on the health effects of LCn-3PUFA supplementation therefore merits further exploration.

Furthermore, animal studies have demonstrated that diets rich in n-6PUFA compared to diets rich in SFA, promote a shift of the cholesterol and triglyceride pools from the circulation into tissue lipids,

especially the liver, despite supplementation with plant or marine n-3PUFA<sup>24,25</sup>. Fat accumulation in the liver may promote increased systemic inflammation, atherosclerosis and metabolic syndromes<sup>26</sup>, being potentially more detrimental in the long term than elevated plasma cholesterol. Therefore, further studies are warranted to understand the effect of the background diet on inflammation, fat accumulation in the tissues and other risk factors in subjects consuming an adequate amount of LCn-3PUFA.

Among the study strengths are its unique design, the addition of a pre-supplementation period to eliminate bias due to difference in omega-3 index, the high compliance with the study diets and supplementation (over 80% compliance) and the monitoring of the participants' life-style (physical activity and general health) throughout the trial.

Some limitations of this study should be considered. The mixed population recruited for the intervention may have been a confounder, as sex and age dependent effects were not accounted for. The decrease in carbohydrate intake during the n-6PUFA-LCn-3PUFA diet, not observed during the SFA-LCn-3PUFA diet, may have been another confounder. Although previous studies demonstrate that high fat diets cause changes in plasma lipids in 8 days or less<sup>27,28</sup>, the short duration of the dietary intervention may also have been a limiting factor, as longer intervention periods are likely to show greater changes in lipoprotein profiles. In longer term dietary interventions, saturated fatty acids do not seem to be associated with cardiovascular disease risk factors<sup>29</sup>. Moreover, the sample size may have been small to assess differences in

## Chapter 4

the profile of some lipoproteins, as the changes in the short term may be small in magnitude, especially for HDL profiles.

In conclusion, improvement in the LCn-3PUFA status in the pre-supplementation period modulated the effect of SFA and n-6PUFA on most lipoprotein profiles. Nevertheless, a diet enriched with n-6PUFA still decreased LDL particle and cholesterol concentration. The cholesterol-raising effects of dietary saturated fats were accompanied by a greater increase in the proportion of plasma and tissue LCn-3PUFA, which may potentially reduce other cardiovascular risk factors such as inflammation and clotting tendency. This study sheds further light on the effect of the various classes of fatty acids. Furthermore, future intervention studies must consider LCn-3PUFA status as a confounding factor in the determination of the health effects of the main dietary fats.

Supplementary data to this article can be found online at: <http://dx.doi.org/10.1016/j.metabol.2016.11.014>.

### 4.3.6 References

1. Stillwell, W. & Wassall, S. R. Docosahexaenoic acid: membrane properties of a unique fatty acid. *Chem. Phys. Lipids* **126**, 1–27 (2003).
2. Chapkin, R. S., Wang, N., Fan, Y.-Y., Lupton, J. R. & Prior, I. A. Docosahexaenoic acid alters the size and distribution of cell surface microdomains. *Biochim. Biophys. Acta - Biomembr.* **1778**, 466–471 (2008).
3. Eslick, G. D., Howe, P. R. C., Smith, C., Priest, R. & Bensoussan, A. Benefits of fish oil supplementation in hyperlipidemia: a systematic review and meta-analysis. *Int. J. Cardiol.* **136**, 4–16 (2009).
4. Yamagishi K, Nettleton JA, F. A. Plasma fatty acid composition and incident heart failure in middle-aged adults: The Atherosclerosis Risk in Communities (ARIC) Study. *Am. Heart J.* **156**, 965–974 (2008).

5. Rizos, E. C., Ntzani, E. E., Bika, E., Kostapanos, M. S. & Elisaf, M. S. Association between omega-3 fatty acid supplementation and risk of major cardiovascular disease events: a systematic review and meta-analysis. *JAMA* **308**, 1024–33 (2012).
6. Harris, W. S. The omega-3 index as a risk factor for coronary heart disease. *Am. J. Clin. Nutr.* **87**, 1997S–2002S (2008).
7. Friesen, R. W. & Innis, S. M. Linoleic acid is associated with lower long-chain n-6 and n-3 fatty acids in red blood cell lipids of Canadian pregnant women. *Am. J. Clin. Nutr.* **91**, 23–31 (2010).
8. Dias, C., Wood, L. & Garg, M. Effects of dietary saturated and n - 6 polyunsaturated fatty acids on the incorporation of long - chain n - 3 polyunsaturated fatty acids into blood lipids. *Eur. J. Clin. Nutr. Adv. online Publ.* **13**, (2016).
9. MacDonald-Wicks, L. K. & Garg, M. L. Incorporation of n-3 fatty acids into plasma and liver lipids of rats: Importance of background dietary fat. *Lipids* **39**, 545–551 (2004).
10. Rivellese, A. A. *et al.* Effects of dietary saturated, monounsaturated and n-3 fatty acids on fasting lipoproteins, LDL size and post-prandial lipid metabolism in healthy subjects. *Atherosclerosis* **167**, 149–158 (2003).
11. Mallol, R. *et al.* Surface fitting of 2D diffusion-edited 1H NMR spectroscopy data for the characterisation of human plasma lipoproteins. *Metabolomics* **7**, 572–582 (2011).
12. Jeyarajah, E. J., Cromwell, W. C., Otvos, J. D. & al., *et.* Lipoprotein particle analysis by nuclear magnetic resonance spectroscopy. *Clin. Lab. Med.* **26**, 847–70 (2006).
13. Micallef, M. A. & Garg, M. L. The lipid-lowering effects of phytosterols and (n-3) polyunsaturated fatty acids are synergistic and complementary in hyperlipidemic men and women. *J. Nutr.* **138**, 1086–90 (2008).
14. Mackey RH, McTigue KM, Chang YF, Barinas-Mitchell E, Evans RW, Tinker LF, *et al.* Lipoprotein particles and size, total and high molecular weight adiponectin, and leptin in relation to incident coronary heart disease among severely obese postmenopausal women:

## Chapter 4

The Women's Health Initiative Observational Study. *BBA Clin.* **3**, 243–250 (2015).

15. Mackey RH, Kuller LH, Sutton-Tyrrell K, Evans RW, Holubkov R, M. K. Lipoprotein subclasses and coronary artery calcium in postmenopausal women from the healthy women study. *Am. J. Cardiol.* **90**, 71–76 (2002).

16. Blake, G. J., Otvos, J. D., Rifai, N. & Ridker, P. M. Low-Density Lipoprotein Particle Concentration and Size as Determined by Nuclear Magnetic Resonance Spectroscopy as Predictors of Cardiovascular Disease in Women. *Circulation* **106**, 1930–1937 (2002).

17. Mostad, I. L., Bjerve, K. S., Lydersen, S. & Grill, V. Effects of marine n-3 fatty acid supplementation on lipoprotein subclasses measured by nuclear magnetic resonance in subjects with type II diabetes. *Eur. J. Clin. Nutr.* **62**, 419–429 (2008).

18. Choo, J. *et al.* Serum n-6 fatty acids and lipoprotein subclasses in middle-aged men: the population-based cross-sectional ERA-JUMP study. *Am. J. Clin. Nutr.* **91**, 1195–203 (2010).

19. Mustad, V. A., Ellsworth, J. L., Cooper, A. D., Kris-Etherton, P. M. & Etherton, T. D. Dietary linoleic acid increases and palmitic acid decreases hepatic LDL receptor protein and mRNA abundance in young pigs. *J. Lipid Res.* **37**, 2310–23 (1996).

20. Ooi, E., Watts, G., Ng, T. & Barrett, P. Effect of Dietary Fatty Acids on Human Lipoprotein Metabolism: A Comprehensive Update. *Nutrients* **7**, 4416–4425 (2015).

21. Fernandez, M. L. & West, K. L. Mechanisms by which dietary fatty acids modulate plasma lipids. *J. Nutr.* **135**, 2075–8 (2005).

22. Dreon, D. M. *et al.* Change in dietary saturated fat intake is correlated with change in mass of large low-density-lipoprotein particles in men. *Am. J. Clin. Nutr.* **67**, 828–36 (1998).

23. Krauss, R. M., Blanche, P. J., Rawlings, R. S., Fernstrom, H. S. & Williams, P. T. Separate effects of reduced carbohydrate intake and weight loss on atherogenic dyslipidemia. *Am. J. Clin. Nutr.* **83**, 1025–31; quiz 1205 (2006).

24. Garg, M. L., Sebokova, E., Wierzbicki, A., Thomson, A. B. R. & Clandinin, M. T. Differential effects of dietary linoleic and  $\alpha$ -linolenic acid on lipid metabolism in rat tissues. *Lipids* **23**, 847–852 (1988).
25. Garg, M. L., Wierzbicki, A. A., Thomson, A. B. R. & Clandinin, M. T. Dietary saturated fat level alters the competition between  $\alpha$ -linolenic and linoleic acid. *Lipids* **24**, 334–339 (1989).
26. Stefan, N., Kantartzis, K. & Häring, H.-U. Causes and Metabolic Consequences of Fatty Liver. *Endocr. Rev.* **29**, 939–960 (2008).
27. Bergeron, N. & Havel, R. J. Influence of diets rich in saturated and omega-6 polyunsaturated fatty acids on the postprandial responses of apolipoproteins B-48, B-100, E, and lipids in triglyceride-rich lipoproteins. *Arterioscler. Thromb. Vasc. Biol.* **15**, 2111–21 (1995).
28. Guay V, Lamarche B, Charest A, Tremblay AJ, C. P. Effect of short-term low- and high-fat diets on low-density lipoprotein particle size in normolipidemic subjects. *Metabolism* **61**, 76–83 (2012).
29. Siri-Tarino, P. W., Sun, Q., Hu, F. B. & Krauss, R. M. Meta-analysis of prospective cohort studies evaluating the association of saturated fat with cardiovascular disease. *Am. J. Clin. Nutr.* **91**, 535–46 (2010).



**4.4 Effect of diets rich in either saturated fat or n-6 polyunsaturated fatty acids and supplemented with long-chain n-3 polyunsaturated fatty acids on plasma lipoprotein profiles**



#### **4.4.1 Abstract**

Abnormalities in lipoprotein profiles (size, distribution and concentration) play an important role in the pathobiology of atherosclerosis and coronary artery disease. Dietary fat, among other factors, has been demonstrated to modulate lipoprotein profiles. We aimed to investigate if background dietary fat (saturated, SFA versus omega-6 polyunsaturated fatty acids, n-6PUFA) was a determinant of the effects of LCn-3PUFA supplementation, on lipoprotein profiles.

A randomized controlled clinical intervention trial in a parallel design was conducted. Healthy subjects (n=26) were supplemented with 400 mg eicosapentaenoic acid plus 2,000 mg docosahexaenoic acid) daily and randomised to consume diets rich in either SFA or n-6PUFA for a period of 6 weeks. Blood samples, collected at baseline and after six weeks of intervention, were assessed for plasma lipoprotein profiles (lipoprotein size, concentration and distribution in subclasses) determined using nuclear magnetic resonance spectroscopy (NMR).

Study participants receiving the SFA or the n-6PUFA enriched diets consumed similar percentage energy from fat (41% and 42% respectively,  $p=0.681$ ). However, subjects on the SFA diet consumed 50% more energy as saturated fat and 77% less as linoleic acid than those consuming the n-6PUFA diet ( $p<0.001$ ). The diets rich in SFA and n-6PUFA reduced the concentration of total very low density lipoprotein (VLDL) particles ( $p<0.001$ , both) and their subclasses and increased VLDL ( $p=0.042$  and  $p=0.007$ , respectively) and LDL ( $p=0.030$  and  $0.027$ , respectively) particle size. In addition, plasma triglyceride concentration

was significantly reduced by LCn-3PUFA supplementation irrespective of the dietary fat.

LCn-3PUFA modulated lipoprotein profiles in a similar fashion when supplemented in diets rich in either SFA or n-6PUFA.

#### **4.4.2 Introduction**

Abnormalities in lipoprotein profiles have been associated with coronary heart disease (CHD) risk in men<sup>1</sup> and women<sup>2-5</sup>. Evidence suggests that CHD risk is increased by larger very low density lipoprotein (VLDL) particle sizes, smaller high density lipoprotein (HDL) and low density lipoprotein (LDL) particle sizes and increased concentration of small LDL and large VLDL particles; although the ideal lipoprotein profiles for the prevention of CHD may vary according to age, gender and health status<sup>1,6</sup>. A variety of factors can modulate lipoprotein profiles, including dietary habits<sup>7</sup> or physical activity<sup>8</sup>.

Long chain omega-3 polyunsaturated fatty acids (LCn-3PUFA), despite some controversy<sup>9</sup>, are well known for their health benefits, particularly in the prevention of CHD, due to their capacity to help manage hyperlipidaemia<sup>10</sup>, inflammation<sup>11</sup> and platelet aggregation<sup>11,12</sup> as well as their potential to modulate lipoprotein profiles. Dietary supplementation with LCn-3PUFA has been shown to decrease the concentration of small HDL particles<sup>13</sup> and increase the concentration of large HDL particles<sup>13-15</sup> and the average HDL particle size<sup>16</sup>, although change in HDL particle size has not been observed in all studies<sup>15,17</sup>. LCn-3PUFA supplementation has also been shown to decrease VLDL particle size<sup>15,18</sup> and large and medium VLDL particle concentration<sup>14</sup>. However,

## Chapter 4

the effect of LCn-3PUFA supplementation on the LDL profile is heterogeneous. Some authors suggest an increase in LDL particle size<sup>15,19,20</sup>, while others have not observed change in LDL size<sup>17,21-23</sup> or have even observed a decrease in particle size<sup>13</sup>. The literature also suggests an increase in the concentration of medium and large LDL particles and a decrease in small particles, despite no change in the average size of the particles<sup>14,15,22</sup>.

In all the above mentioned studies involving LCn-3PUFA supplementation and lipoprotein profiles, little attention has been given to the other components of the diet, especially the amount and type of the fats consumed. The human diet comprises a mixture of fats and even after supplementation and increase in seafood consumption, LCn-3PUFA remains a minor proportion of the total fat consumed. We have recently demonstrated that LCn-3PUFA are incorporated in plasma and erythrocytes to a greater extent when consumed with a diet rich in saturated fats compared to a diet rich in n-6PUFA<sup>24</sup>. The aim of this study was to examine whether the background dietary fat induced changes in lipoprotein concentration, size and subclass distribution are modulated by co-supplementation with LCn-3PUFA.

### **4.4.3 Material, Subjects and Methods**

**Subjects.** Healthy adults aged between 18 and 65 years were recruited. Subjects were excluded if they were using lipid-lowering drugs (e.g. statins) or fish oil supplements; regularly consuming 2 or more fish meals per week; had any history of stroke, congestive heart failure, coronary artery bypass graft (CABG), myocardial infarction, or

atherosclerotic CVD; had diabetes, liver or gastrointestinal disease; were smokers; were pregnant or breast-feeding.

**Study design.** This randomized, parallel design, dietary intervention trial has been previously described<sup>24</sup>. In summary, subjects were randomized using computer generated random tables to diets supplemented with LCn-3PUFA and either enriched with saturated fatty acids (SFA+LCn-3PUFA diet) or n-6PUFA (n-6PUFA+LCn-3PUFA diet). Subjects in the SFA+LCn-3PUFA diet group consumed daily 24g of butter, 40g of white chocolate (30g fat, 20.9g saturated fat) and 4x1g fish oil capsules [100mg eicosapentaenoic acid (EPA) and 500mg docosahexaenoic acid (DHA) each (EPAX 1050TG, Norway)]. Participants were also encouraged to consume foods containing SFA, while reducing n-6PUFA intake. Subjects on the n-6PUFA+LCn-3PUFA diet received 20g of margarine, 42g of sunflower seeds (30g fat, 20g n-6PUFA) daily and 4x1g fish oil capsules. They were also guided on how to increase consumption of foods containing n-6PUFA while reducing SFA intake. All subjects were advised to maintain other aspect of their habitual diet and their usual physical activity status. Before starting and on their last week on the intervention, subjects completed a three day food record (2 week days and 1 weekend day), a physical activity questionnaire and a medical questionnaire, which included current medications and supplements, illnesses and alcohol consumption. FoodWorks 7 Professional (Xyris software) was used to assess the food records. A fasting blood sample was collected in EDTA vacutainers at baseline and following 6 weeks of dietary supplementation and plasma lipoprotein profiles were determined. Blood samples were also analysed for fatty

## Chapter 4

acids as previously reported<sup>24</sup>. Subjects were asked to refrain from vigorous exercise and alcohol consumption for 24 hours prior to the study day and fasted for at least 10 hours prior to each blood collection. The study was carried out in accordance with the guidelines provided in the Declaration of Helsinki. The study protocol was approved by the University of Newcastle's Human Research Ethics Committee (protocol H-2012-0117) and registered with the Australia New Zealand Trial registry (identification number ACTRN12613000962730, <http://www.anzctr.org.au/>). All participants gave written consent prior to participation.

Adherence to the dietary supplementation was determined by counting the left-over LCn-3PUFA capsules and interventional food products provided (butter, white chocolate, margarine and sunflower seeds), querying subjects about their food intake, assessing subjects' dietary records, and analysis of plasma fatty acid composition. None of the participants reported any signs of intolerance to the supplements or the study foods.

**Plasma Lipoprotein profiles.** Blood samples were centrifuged (1000 g x 15 minutes at 4°C) immediately after collection to separate plasma from erythrocytes and the fractions were stored at -80°C until analysed.

Plasma samples were analysed for lipoprotein profiles using nuclear magnetic resonance spectroscopy (NMR) at Biosfer Teslab (Reus, Spain). The detailed methods for the determination of lipoprotein profiles (size, concentration and subclass distribution) has been reported previously<sup>25</sup>. Lipid volumes were calculated by using common

conversion factors to convert concentration units into volume units<sup>26</sup>. The size range for different lipoprotein subclasses corresponded to: large VLDL, 68.5-95.9 nm; medium VLDL, 47-68.5 nm; small VLDL, 32.5-47 nm; very large LDL, 24-32.5 nm; medium-large LDL, 20.5-24 nm; small LDL, 17.5-20.5 nm; very large HDL, 10.5-13.5 nm; medium-large HDL, 8.5-10.5 nm; and small HDL, 7.5-8.5 nm.

**Statistical analysis.** This study was primarily designed to assess blood lipid levels, discussed in Dias et al<sup>24</sup>. Thirteen subjects were necessary to cause a 30% (0.45mmol/L) decrease in fasting plasma triglycerides with 0.387 mmol/L of standard deviation, 0.05 of significance level and 80% power.

All data are presented as median and interquartile range (IQR) and non-parametric statistical tests were employed on the analysis. Kruskal-Wallis test was used for baseline comparisons. Data at baseline and 6 weeks were compared within groups using Wilcoxon signed-rank test and data on change was compared between groups using Kruskal-Wallis test. Statistical analysis were performed using Mat Lab R2010a (MathWorks) and p-values lower than 0.05 were considered statistically significant.

#### 4.4.4 Results

From the 33 subjects who completed the intervention period (18 on the SFA+LCn-3PUFA diet and 15 on the n-6PUFA+LCn-3PUFA diet), 7 failed to adhere to the intervention diets or the supplementation (compliance lower than 80%) and were, therefore, excluded from the data analysis (Figure 1). Twenty six healthy subjects were then included



## Chapter 4

in the statistical analysis, 14 subjects on the SFA+LCn-3PUFA diet (3 males and 11 females) and 12 on the n-6PUFA+LCn-3PUFA diet (3 males and 9 females).

The concentration of LC-n-3PUFA in the fish oil capsules supplemented, measured using gas chromatography<sup>27</sup>, was more than 70% total LCn-3PUFA [14.3% EPA and 58.8% DHA] as previously described<sup>24</sup>.

Subjects' general characteristics, dietary intake and plasma and erythrocyte fatty acid composition have been discussed previously, the full discussion and other supporting materials are available in Dias et al<sup>24</sup>. Summary tables are also available in the supplementary material (Tables SM.1 to SM.3). In summary, subjects on the SFA+LCn-3PUFA and the n-6PUFA+LCn-3PUFA did not differ significantly in age [40.0 (15.0) and 43.5 (27.5), respectively], body mass index [22.2 (4.9) and 22.7 (4.3), respectively], percentage body fat [26.2 (18.5) and 26.4 (10.6), respectively] and blood lipids at baseline. As expected participants randomized to the SFA+LCn-3PUFA diet increased saturated fat and decreased linoleic acid intake ( $p < 0.01$ , both), while participants randomized to the n-6PUFA+LCn-3PUFA diet increased linoleic acid (LA) and decreased saturated fat intake ( $p < 0.01$ , both) compared to baseline values.

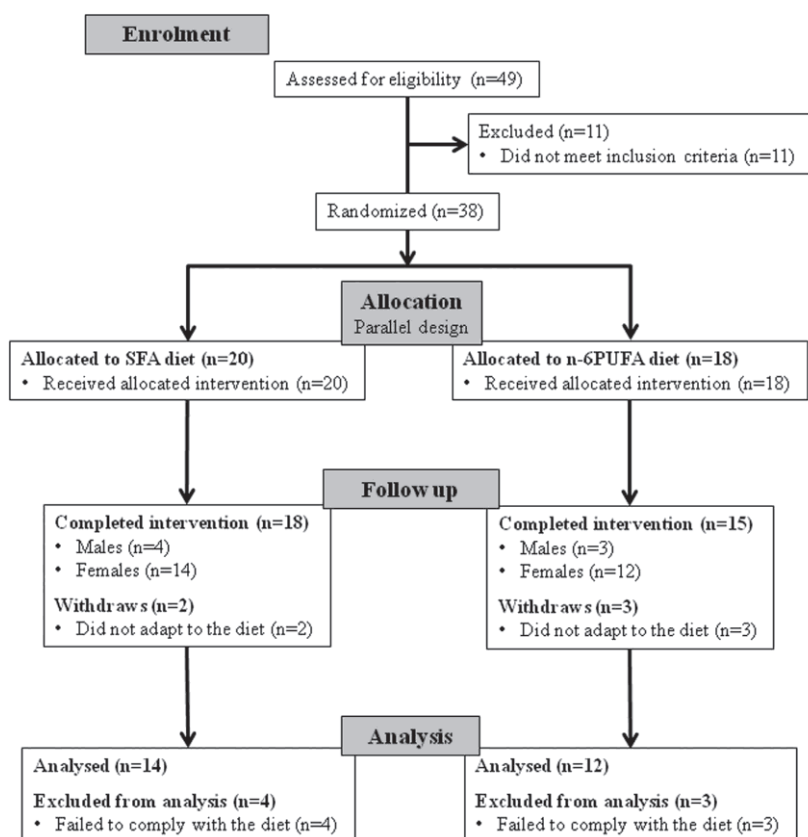


**Figure 1.** Enrolment schedule for the interventional trial.

Changes in dietary protein, total fat, carbohydrates and cholesterol did not differ significantly between dietary groups. There were no significant differences in plasma fatty acids between the two groups at baseline, except for percentage DHA which was significantly greater in the plasma of subjects randomized to the SFA+LCn-3PUFA diet. Changes in dietary patterns and plasma fatty acids suggest that participants complied with the study protocol. Change in plasma LCn-3PUFA [including EPA, docosapentaenoic acid and DHA] was significantly greater ( $p < 0.05$ ) after the consumption of the SFA+LCn-3PUFA diet compared to the n-6PUFA+LCn-3PUFA diet. There was also a significant

## Chapter 4

increase in percentage LA and a concomitant decrease in percentage arachidonic acid (AA) after the consumption of n-6PUFA+LCn-3PUFA diet, while no significant change in LA and AA was observed after the SFA+LCn-3PUFA diet.

Lipoprotein profiles at baseline were not significantly different between groups (Tables 1 and 2). Both diets decreased cholesterol and triglyceride concentrations in VLDL particles (n-SFA+LCn-3PUFA diet,  $p < 0.001$ , n-6PUFA+LCn-3PUFA diet  $p = 0.002$  and  $p < 0.001$ , respectively). After the n-6PUFA+LCn-3PUFA diet, there was a significant decrease in cholesterol and triglyceride levels in intermediate density lipoprotein (IDL) particles ( $p = 0.001$  for both). After the SFA+LCn-3PUFA there was a significant increase in the concentration of LDL triglycerides ( $p = 0.002$ ). Additionally, subjects on the SFA+LCn-3PUFA diet presented significantly higher triglyceride levels in IDL and LDL particles after intervention than subjects on the n-6PUFA+LCn-3PUFA. There was also an increase in cholesterol levels in HDL particles after consumption of both diets, although this increase was significant only for subjects consuming the n-6PUFA-LCn-3PUFA diet ( $p = 0.012$ ) (Table 1).

**Table 1.** Plasma lipid concentrations of subjects at pre and post intervention, measured using nuclear magnetic resonance spectroscopy.

<i>mmol/l</i>		<i>Pre-intervention</i>	<i>Post-intervention</i>	$\Delta$ <i>Change</i>	<i>P-value</i> <sup>a</sup>
VLDL-C	SFA+LCn-3PUFA	0.12 (0.12)	0.02 (0.02)	- 0.05 (0.08) <sup>b</sup>	0.129
	n-6PUFA+LCn-3PUFA	0.14 (0.15)	0.02 (0.07)	- 0.11 (0.15) <sup>b</sup>	
IDL-C	SFA+LCn-3PUFA	0.09 (0.06)	0.09 (0.06)	- 0.01 (0.06)	0.076
	n-6PUFA+LCn-3PUFA	0.09 (0.07)	0.04 (0.07)	- 0.04 (0.08) <sup>b</sup>	
LDL-C	SFA+LCn-3PUFA	2.70 (0.51)	2.71 (0.59)	0.13 (0.57)	0.425
	n-6PUFA+LCn-3PUFA	2.50 (0.72)	2.43 (0.29)	0.01 (0.47)	
HDL-C	SFA+LCn-3PUFA	1.39 (0.40)	1.55 (0.23)	0.07 (0.32)	0.857
	n-6PUFA+LCn-3PUFA	1.24 (0.45)	1.27 (0.58)	0.08 (0.17) <sup>b</sup>	

Total C	SFA+LCn-3PUFA	4.23 (0.78)	4.57 (1.09)	0.13 (0.67)	0.355
	n-6PUFA+LCn-3PUFA	4.01 (0.93)	3.99 (0.57)	- 0.06 (0.49)	
VLDL-TG	SFA+LCn-3PUFA	0.44 (0.30)	0.29 (0.27)	- 0.17 (0.18) <sup>b</sup>	0.857
	n-6PUFA+LCn-3PUFA	0.46 (0.11)	0.29 (0.15)	- 0.20 (0.18) <sup>b</sup>	
IDL-TG	SFA+LCn-3PUFA	0.06 (0.02)	0.05 (0.02)	- 0.00 (0.02)	0.033
	n-6PUFA+LCn-3PUFA	0.06 (0.02)	0.06 (0.02)	- 0.02 (0.02) <sup>b</sup>	
LDL-TG	SFA+LCn-3PUFA	0.12 (0.15)	0.12 (0.09)	0.02 (0.02) <sup>b</sup>	0.042
	n-6PUFA+LCn-3PUFA	0.10 (0.06)	0.11 (0.03)	- 0.01 (0.04)	
HDL-TG	SFA+LCn-3PUFA	0.04 (0.08)	0.05 (0.05)	0.01 (0.03)	0.117
	n-6PUFA+LCn-3PUFA	0.06 (0.05)	0.05 (0.04)	- 0.01 (0.03)	
Total TG	SFA+LCn-3PUFA	0.70 (0.20)	0.54 (0.24)	- 0.16 (0.24) <sup>b</sup>	0.503
	n-6PUFA+LCn-3PUFA	0.67 (0.18)	0.49 (0.15)	- 0.19 (0.28) <sup>b</sup>	

Abbreviations: C, cholesterol; HDL, high-density lipoprotein; IDL, intermediate-density lipoprotein; LCn-3PUFA, long-chain omega-3 polyunsaturated fatty acids; LDL, low density lipoprotein; n-6PUFA, omega-6 polyunsaturated fatty acid; SFA, saturated fatty acid; TG, triglycerides; VLDL, very-low-density lipoprotein. <sup>a</sup>*P*-values for comparison of change values between diets. <sup>b</sup>Significant difference between pre and post intervention (*P*<0.05). Data presented as median (interquartile range) for the SFA+LCn-3PUFA diet (*n* = 14; 3 males and 11 females) and the n-6PUFA+LCn-3PUFA diet (*n* = 12; 3 males and 9 females). Bold values in the delta- change column indicate significant difference between pre and post intervention (*P*<0.05). Bold values in the *P*-value column indicate *P*<0.05.

Total, large, medium and small VLDL particles were decreased after the consumption of both diets (n-SFA+LCn-3PUFA diet, *p*<0.001, *p*=0.025, *p*<0.001 and *p*<0.001; n-6PUFA+LCn-3PUFA diet *p*<0.001, respectively). A decrease was also observed in very large HDL particles after both diets (n-SFA+LCn-3PUFA diet, *p*=0.01; n-6PUFA+LCn-3PUFA diet, *p*<0.001, respectively), with no change in total HDL particle concentration and a tendency for increase in medium-large HDL particles after the SFA+LCn-3PUFA (*p*=0.058) and the n-6PUFA+LCn-3PUFA (*p*=0.064) diet. After the SFA+LCn-3PUFA there was a significant increase in the concentration of medium-large LDL particles (*p*=0.011). However, change in medium-large LDL was not significantly different between the two diets. Increases in VLDL and LDL particle size were not

## Chapter 4

significantly different between both diets (Table 2). For all other parameters there was no significant difference between diets.

**Table 2.** Lipoprotein profiles (distribution in subclasses, concentration and size) of subjects at pre at pre and post intervention.

		Pre-intervention	Post-intervention	Δ Change	P-value <sup>a</sup>	P-value <sup>b</sup>
<b>Particle concentrations</b>						
VLDL-P (nmol/L)	SFA+LCn-3PUFA	23.93 (17.27)	13.85 (16.28)	<b>-10.85 (9.53)</b>	<b>&lt;0.001</b>	0,939
	n-6PUFA+LCn-3PUFA	26.03 (8.76)	13.63 (9.09)	<b>-13.34 (12.53)</b>	<b>&lt;0.001</b>	
Large VLDL-P (nmol/L)	SFA+LCn-3PUFA	0.73 (0.26)	0.55 (0.45)	<b>-0.20 (0.33)</b>	<b>0,025</b>	0,625
	n-6PUFA+LCn-3PUFA	0.77 (0.31)	0.57 (0.25)	<b>-0.21 (0.24)</b>	<b>&lt;0.001</b>	
Medium VLDL-P (nmol/L)	SFA+LCn-3PUFA	3.77 (2.36)	2.32 (1.90)	<b>-1.44 (1.74)</b>	<b>&lt;0.001</b>	0,979
	n-6PUFA+LCn-3PUFA	4.01 (1.19)	2.40 (1.09)	<b>-1.80 (1.58)</b>	<b>&lt;0.001</b>	
Small VLDL-P (nmol/L)	SFA+LCn-3PUFA	19.35 (14.74)	10.77 (14.01)	<b>-9.33 (7.91)</b>	<b>&lt;0.001</b>	0,898
	n-6PUFA+LCn-3PUFA	20.96 (7.46)	10.45 (6.67)	<b>-11.28 (10.65)</b>	<b>&lt;0.001</b>	
LDL-P (nmol/L)	SFA+LCn-3PUFA	725.9 (126.2)	739.0 (189.5)	39.6 (159.4)	0,173	0,292
	n-6PUFA+LCn-3PUFA	682.6 (210.3)	667.7 (79.5)	2.5 (146.5)	0,91	
Very large LDL-P (nmol/L)	SFA+LCn-3PUFA	107.9 (29.0)	108.7 (39.0)	7.1 (20.7)	0,119	0,341
	n-6PUFA+LCn-3PUFA	99.9 (27.2)	100.1 (15.6)	1.5 (14.1)	0,301	
Medium-large LDL-P (nmol/L)	SFA+LCn-3PUFA	243.4 (54.7)	249.2 (72.7)	<b>21.5 (47.6)</b>	<b>0,011</b>	0,173
	n-6PUFA+LCn-3PUFA	229.3 (66.9)	235.7 (42.6)	3.85 (32.9)	0,519	
Small LDL-P (nmol/L)	SFA+LCn-3PUFA	380.2 (88.8)	388.2 (100.5)	6.5 (88.0)	0,426	0,341
	n-6PUFA+LCn-3PUFA	353.0 (105.2)	328.8 (46.4)	-5.3 (90.2)	0,519	
HDL-P (μmol/L)	SFA+LCn-3PUFA	24.44 (6.79)	27.13 (3.99)	1.40 (4.35)	0,173	1,000
	n-6PUFA+LCn-3PUFA	23.10 (6.43)	23.32 (9.35)	0.60 (1.97)	0,077	
Very large HDL-P (μmol/L)	SFA+LCn-3PUFA	0.10 (0.07)	0.06 (0.06)	<b>-0.04 (0.05)</b>	<b>0,011</b>	0,738
	n-6PUFA+LCn-3PUFA	0.10 (0.05)	0.06 (0.05)	<b>-0.05 (0.05)</b>	<b>&lt;0.001</b>	
Medium-large HDL-P (μmol/L)	SFA+LCn-3PUFA	8.11 (1.36)	8.95 (1.41)	0.56 (1.63)	0,058	1,000
	n-6PUFA+LCn-3PUFA	7.03 (2.52)	7.54 (3.71)	0.65 (1.06)	0,064	
Small HDL-P (μmol/L)	SFA+LCn-3PUFA	16.53 (4.03)	18.00 (2.21)	0.95 (3.30)	0,217	0,817
	n-6PUFA+LCn-3PUFA	15.96 (4.26)	15.83 (6.21)	0.06 (1.26)	0,519	
<b>Lipoprotein particle size (nm)</b>						
VLDL-Z	SFA+LCn-3PUFA	42.17 (0.53)	42.48 (0.67)	<b>0.27 (0.45)</b>	<b>0,042</b>	0,662
	n-6PUFA+LCn-3PUFA	42.22 (0.62)	42.46 (0.80)	<b>0.37 (0.46)</b>	<b>0,007</b>	
LDL-Z	SFA+LCn-3PUFA	21.11 (0.10)	21.16 (0.15)	<b>0.04 (0.08)</b>	<b>0,030</b>	0,341
	n-6PUFA+LCn-3PUFA	21.11 (0.08)	21.16 (0.12)	<b>0.06 (0.10)</b>	<b>0,027</b>	
HDL-Z	SFA+LCn-3PUFA	8.23 (0.03)	8.24 (0.05)	0.00 (0.04)	0,670	0,662
	n-6PUFA+LCn-3PUFA	8.23 (0.01)	8.22 (0.04)	-0.01 (0.05)	0,970	

Abbreviations: HDL, high-density lipoprotein; IDL, intermediate-density lipoprotein; LCn-3PUFA, long-chain omega-3 polyunsaturated fatty acids; LDL, low

density lipoprotein; n-6PUFA, omega-6 polyunsaturated fatty acid; P, particle; SFA, saturated fatty acid; VLDL, very-low-density lipoprotein; Z, size (diameter in nm).<sup>a</sup>*P*-values for comparison for comparison between pre and post intervention. <sup>b</sup>*P*-values for comparison of change values between diets.

Data presented as median (interquartile range) for the SFA+LCn-3PUFA diet ( $n = 14$ ; 3 males and 11 females) and the n-6PUFA+LCn-3PUFA diet ( $n = 12$ ; 3 males and 9 females). Bold values in the delta-change and *P*-value (a) indicate significant difference for comparison between pre and post intervention ( $P < 0.05$ ). Bold value (b) column represent significant difference for comparison of values between diets.

#### 4.4.5 Discussion

The present intervention trial was designed to evaluate the effect of diets enriched with either SFA or n-6PUFA and supplemented with LCn-3PUFA, on lipoprotein profiles as a secondary outcome. Both diets produced similar changes in lipoprotein profiles, suggesting that neither SFA nor n-6PUFA modulate LCn-3PUFA induced changes in lipoprotein profiles. Additionally, both diets increased LDL particle size, profile that has been associated with a reduced risk for atherosclerosis in epidemiological studies.

Subjects consuming either of the diets presented comparable reductions in total, large, medium and small VLDL particle concentrations, as well as in VLDL triglycerides, consistent with the decrease in total triglycerides and VLDL particle concentration following LCn-3PUFA supplementation observed in other studies<sup>23,28,29</sup>. Decrease in plasma triglycerides and VLDL particles have been associated with a protective profile against atherosclerosis and CVD risk<sup>6,30</sup>. Supplementation with n-3PUFA has been shown to inhibit VLDL synthesis<sup>31</sup> and secretion by the liver<sup>32</sup>, improve VLDL clearance<sup>33</sup> and enhance VLDL conversion to LDL<sup>29</sup>. One of the mechanisms by which LCn-3PUFA may act is the stimulation of lipoprotein lipase expression;

## Chapter 4

resulting in triglyceride hydrolysis in chylomicrons and VLDL particles, forming lipoprotein remnants (small VLDL and IDL particles). Lipoprotein remnants have more affinity to the LDL receptor (LDL-r) <sup>28,34</sup>, and compete with LDL particles for clearance<sup>35,36</sup>. Additionally, both LCn-3PUFA and SFA decrease expression of hepatic LDL-r<sup>33,37</sup>, also explaining the increase in large LDL particle concentration after consumption of the SFA+LCn-3PUFA diet. N-6PUFA are also known to reduce circulating VLDL particle concentration, by increasing VLDL uptake and lipolysis<sup>38</sup>. The n-6PUFA lipolysis effect in VLDL may also explain the reduction in triglycerides in IDL particles that occurred after the consumption of the n-6PUFA+LCn-3PUFA diet, but not after the SFA+LCn-3PUFA diet. Despite the VLDL lowering ability of both n-6 and LCn-3PUFA, the n-6PUFA+LCn-3PUFA diet did not affect VLDL particle concentration and subclass distribution differently than the SFA+LCn-3PUFA diet, suggesting no increased benefit obtained in VLDL particle modulation by combining n-6 and LCn-3PUFA.

N-6PUFA have also been demonstrated to reduce plasma LDL particle concentration by increasing the fractional catabolism of apoB-100<sup>39</sup>, the main apolipoprotein in VLDL and LDL particles, and by increasing LDL-r transcription and synthesis<sup>35,40</sup>. However, no significant change was observed in LDL particle concentration or distribution after the consumption of the n-6PUFA+LCn-3PUFA diet in our study, suggesting that LCn-3PUFA may have neutralized the LDL lowering effect of n-6PUFA.

The size of VLDL particles increased in both groups, conflicting with findings from Mostad et al<sup>21</sup> and Maki et al<sup>41</sup>, who observed a

decrease in VLDL particle size in type 2 diabetes and hypercholesterolaemic patients, respectively, after supplementation with LCn-3PUFA compared to placebo (corn oil and soya oil, respectively). This may suggest that either both background dietary fats (n-6PUFA and SFA) suppress the ability of LCn-3PUFA to reduce VLDL size or LCn-3PUFA modulate VLDL size differently in healthy subjects.

After the consumption of both diets, there was an increase in LDL size and medium-large LDL particle concentration. Epidemiological studies suggest that serum LCn-3PUFA level is positively correlated with LDL particle size<sup>7,42</sup>. Furthermore, intervention trials suggested an increase in LDL particle size<sup>43</sup>, especially when DHA is supplemented in the diet<sup>13</sup>. The increase in medium-large LDL particle concentration is also consistent with previously published studies<sup>14,22</sup>.

No change in total HDL particle concentration was observed, despite a decrease in very large HDL particle concentration. Indeed, there was a trend for an increase in medium-large HDL particle concentration after both diets, which counter-balanced the decrease of very large HDL particles. This is consistent with previous epidemiological and interventional studies. In epidemiological studies a positive correlation between dietary LCn-3PUFA and serum large HDL particle concentration was observed<sup>7,44</sup>. In interventional trials, an increase in large HDL particle concentration was observed in the plasma of mildly and hypercholesterolaemic subjects during a DHA supplementation trial<sup>13,14</sup>; and no change in plasma small, medium or large HDL particles after supplementation with EPA<sup>17</sup>. The very large HDL particles (10.5-13.5nm) in the present intervention are just a small proportion of the



## Chapter 4

total HDL particles and even a small change in magnitude may result in a significant change. Nevertheless, medium-large HDL particles (8.5-10.5nm) represent mature HDL particles and therefore active in the reverse transport of cholesterol, conferring a profile protective against atherosclerosis risk.

The decrease in very large HDL particles after consumption of both diets is consistent with an increase in the activity of cholesteryl ester transfer protein (CETP) caused by LCn-3PUFA supplementation, especially DHA<sup>37</sup>. An increase in CETP activity consequently increases the exchange of cholesterol from HDL particles for triglycerides from VLDL particles, improving the reverse cholesterol transport and facilitating the conversion of VLDL to LDL. This mechanism may also be responsible for the concomitant decrease in VLDL particles and increase in LDL triglycerides. Triglyceride-rich HDL particles have their triglycerides hydrolysed by hepatic lipase, which may explain the shift in the subclass distribution of HDL particles<sup>45</sup>.

Comparison between the different studies performed on lipoprotein profiles is limited by the lack of standardization between the different analytical methods used for the determination of lipoprotein profiles<sup>46</sup>, although the gap between methods has been closing with recent studies<sup>47</sup>. Furthermore, the literature on the classification of lipoprotein subclasses according to their diameter and density is heterogeneous. The method used was limited by the fact that intermediate density particles were not measured separately<sup>25</sup>, but were combined with very large LDL particles. However, large and small LDL subclasses and VLDL particles seem to be of more importance to

atherosclerosis management<sup>1</sup>. Another limitation in the discussion about the effect of LCn-3PUFA on lipoprotein profiles is the difference in composition and dose of LCn-3PUFA used across different studies, as well as the lack of dietary information. Additionally, sample size and power were calculated for determining change in plasma triglycerides and not specifically for determining changes in lipoprotein profiles. Thus, the sample size may have been small to assess differences in lipoprotein profiles, as the changes are small in magnitude, especially for HDL profile. The results may also have been confounded by sex and age dependent effects, as a mixed population was assessed. Moreover, it is possible that a small increase in LCn-3PUFA in tissues may produce a desirable effect on lipoprotein profiles that is not improved with a further increase in LCn-3PUFA. In which case, the high LCn-3PUFA dose may have masked the effects of the background dietary fat consumed.

In conclusion, a background diet rich in saturated fatty acids versus n-6PUFA did not modulate the effect of LCn-3PUFA on lipoprotein profiles, despite the enhanced LCn-3PUFA incorporation into plasma and erythrocyte lipids with consumption of a diet rich in saturated fatty acids compared to n-6PUFA<sup>24</sup>. Further investigation of the interaction of LCn-3PUFA with saturated fats is warranted, in order to clarify the role of LCn-3PUFA status in modulating dietary SFA-induced changes in circulating lipoproteins. However, the changes to lipoprotein profiles observed suggest an improvement towards a less atherogenic profile after intervention with both diets, supporting the hypothesis that a diet rich in saturated fatty acids does not modulate cardiovascular risk factors differently than a diet rich in n-6PUFA when

## Chapter 4

an adequate amount of LCn-3PUFA is consumed. Furthermore, sex differences, as well as age, dose and intervention length, should be considered in future studies.

Supplementary Information accompanies this paper on European Journal of Clinical Nutrition website (<http://www.nature.com/ejcn>).

### 4.4.6 References

1. Carmena, R., Duriez, P. & Fruchart, J.-C. Atherogenic Lipoprotein Particles in Atherosclerosis. *Circulation* **109**, III-2-III-7 (2004).
2. Mackey RH, McTigue KM, Chang YF, Barinas-Mitchell E, Evans RW, Tinker LF, et al. Lipoprotein particles and size, total and high molecular weight adiponectin, and leptin in relation to incident coronary heart disease among severely obese postmenopausal women: The Women's Health Initiative Observational Study. *BBA Clin.* **3**, 243–250 (2015).
3. Akinkuolie, A. O., Paynter, N. P., Padmanabhan, L. & Mora, S. High-density lipoprotein particle subclass heterogeneity and incident coronary heart disease. *Circ. Cardiovasc. Qual. Outcomes* **7**, 55–63 (2014).
4. Mora, S. et al. Lipoprotein Particle Profiles by Nuclear Magnetic Resonance Compared With Standard Lipids and Apolipoproteins in Predicting Incident Cardiovascular Disease in Women. *Circulation* **119**, 931–939 (2009).
5. Mackey RH, Kuller LH, Sutton-Tyrrell K, Evans RW, Holubkov R, M. K. Lipoprotein subclasses and coronary artery calcium in postmenopausal women from the healthy women study. *Am. J. Cardiol.* **90**, 71–76 (2002).
6. Cromwell, W. C. et al. LDL particle number and risk of future cardiovascular disease in the Framingham Offspring Study—Implications for LDL management. *J. Clin. Lipidol.* **1**, 583–592 (2007).

7. Bogl, L. H. *et al.* Association between habitual dietary intake and lipoprotein subclass profile in healthy young adults. *Nutr. Metab. Cardiovasc. Dis.* **23**, 1071–8 (2013).
8. Ahmed, H. M., Blaha, M. J., Nasir, K., Rivera, J. J. & Blumenthal, R. S. Effects of Physical Activity on Cardiovascular Disease. *Am. J. Cardiol.* **109**, 288–295 (2012).
9. Rizos, E. C., Ntzani, E. E., Bika, E., Kostapanos, M. S. & Elisaf, M. S. Association between omega-3 fatty acid supplementation and risk of major cardiovascular disease events: a systematic review and meta-analysis. *JAMA* **308**, 1024–33 (2012).
10. Eslick, G. D., Howe, P. R. C., Smith, C., Priest, R. & Bensoussan, A. Benefits of fish oil supplementation in hyperlipidemia: a systematic review and meta-analysis. *Int. J. Cardiol.* **136**, 4–16 (2009).
11. Russo, G. L. Dietary n-6 and n-3 polyunsaturated fatty acids: From biochemistry to clinical implications in cardiovascular prevention. *Biochemical Pharmacology* **77**, 937–946 (2009).
12. Phang, M., Lincz, L. F. & Garg, M. L. Eicosapentaenoic and Docosahexaenoic Acid Supplementations Reduce Platelet Aggregation and Hemostatic Markers Differentially in Men and Women. *J. Nutr.* **143**, 457–463 (2013).
13. Mori, T. A. *et al.* Purified eicosapentaenoic and docosahexaenoic acids have differential effects on serum lipids and lipoproteins, LDL particle size, glucose, and insulin in mildly hyperlipidemic men. *Am. J. Clin. Nutr.* **71**, 1085–94 (2000).
14. Neff, L. M. *et al.* Algal docosahexaenoic acid affects plasma lipoprotein particle size distribution in overweight and obese adults. *J. Nutr.* **141**, 207–13 (2011).
15. Kelley, D. S., Siegel, D., Vemuri, M. & Mackey, B. E. Docosahexaenoic acid supplementation improves fasting and postprandial lipid profiles in hypertriglyceridemic men. *Am. J. Clin. Nutr.* **86**, 324–33 (2007).
16. Erkkilä, A. *et al.* Effect of fatty and lean fish intake on lipoprotein subclasses in subjects with coronary heart disease: A controlled trial. *J. Clin. Lipidol.* **8**, 126–133 (2014).

## Chapter 4

17. Bays, H. *et al.* Icosapent ethyl, a pure EPA omega-3 fatty acid: Effects on lipoprotein particle concentration and size in patients with very high triglyceride levels (the MARINE study). *J. Clin. Lipidol.* **6**, 565–572 (2012).
18. Mostad, I. L., Bjerve, K. S., Lydersen, S. & Grill, V. Effects of marine n-3 fatty acid supplementation on lipoprotein subclasses measured by nuclear magnetic resonance in subjects with type II diabetes. *Eur. J. Clin. Nutr.* **62**, 419–429 (2008).
19. Satoh, N. *et al.* Purified eicosapentaenoic acid reduces small dense LDL, remnant lipoprotein particles, and C-reactive protein in metabolic syndrome. *Diabetes Care* **30**, 144–6 (2007).
20. Shigemasa Tani, MD; Ken Nagao, MD; Michiaki Matsumoto, MD; Atsushi Hirayama, M. Highly Purified Eicosapentaenoic Acid May Increase Low-Density Lipoprotein Particle Size by Improving Triglyceride Metabolism in Patients With Hypertriglyceridemia. *Circ. J.* **77**, 2349–2357 (2013).
21. Mostad, I L; Bjerve, K S; Lydersen, S; Grill, V. Effects of marine n-3 fatty acid supplementation on lipoprotein subclasses measured by nuclear magnetic resonance in subjects with type II diabetes - ProQuest. *Eur. J. Clin. Nutr.* **62**, 419–29 (2007).
22. Oelrich, B., Dewell, A. & Gardner, C. D. Effect of fish oil supplementation on serum triglycerides, LDL cholesterol and LDL subfractions in hypertriglyceridemic adults. *Nutr. Metab. Cardiovasc. Dis.* **23**, 350–7 (2013).
23. Rivellese, A. A. *et al.* Effects of dietary saturated, monounsaturated and n-3 fatty acids on fasting lipoproteins, LDL size and post-prandial lipid metabolism in healthy subjects. *Atherosclerosis* **167**, 149–158 (2003).
24. Dias, C., Wood, L. & Garg, M. Effects of dietary saturated and n - 6 polyunsaturated fatty acids on the incorporation of long - chain n - 3 polyunsaturated fatty acids into blood lipids. *Eur. J. Clin. Nutr. Adv. online Publ.* **13**, (2016).

25. Mallol, R. *et al.* Liposcale: a novel advanced lipoprotein test based on 2D diffusion-ordered <sup>1</sup>H NMR spectroscopy. *J. Lipid Res.* **56**, 737–746 (2015).
26. Jeyarajah, E. J., Cromwell, W. C., Otvos, J. D. & al., *et.* Lipoprotein particle analysis by nuclear magnetic resonance spectroscopy. *Clin. Lab. Med.* **26**, 847–70 (2006).
27. Wood, L. G., Fitzgerald, D. A., Gibson, P. G., Cooper, D. M. & Garg, M. L. Increased plasma fatty acid concentrations after respiratory exacerbations are associated with elevated oxidative stress in cystic fibrosis patients. *Am. J. Clin. Nutr.* **75**, 668–75 (2002).
28. Mori, T. A. *et al.* Effects of varying dietary fat, fish, and fish oils on blood lipids in a randomized controlled trial in men at risk of heart disease. *Am. J. Clin. Nutr.* **59**, 1060–8 (1994).
29. Chan, D. C. *et al.* Randomized controlled trial of the effect of n–3 fatty acid supplementation on the metabolism of apolipoprotein B-100 and chylomicron remnants in men with visceral obesity. *Am. J. Clin. Nutr.* **77**, 300–307 (2003).
30. Nordestgaard, B. & Varbo, A. Triglycerides and cardiovascular disease. *Lancet* **384**, 626–635 (2014).
31. Schoonjans, K., Staels, B. & Auwerx, J. Role of the peroxisome proliferator-activated receptor (PPAR) in mediating the effects of fibrates and fatty acids on gene expression. *J. Lipid Res.* **37**, 907–25 (1996).
32. López-Soldado, I., Avella, M. & Botham, K. M. Suppression of VLDL secretion by cultured hepatocytes incubated with chylomicron remnants enriched in n–3 polyunsaturated fatty acids is regulated by hepatic nuclear factor-4 $\alpha$ . *Biochim. Biophys. Acta - Mol. Cell Biol. Lipids* **1791**, 1181–1189 (2009).
33. Fernandez, M. L. & West, K. L. Mechanisms by which dietary fatty acids modulate plasma lipids. *J. Nutr.* **135**, 2075–8 (2005).
34. Griffin, B. A. The effect of n–3 fatty acids on low density lipoprotein subfractions. *Lipids* **36**, S91–S97 (2001).

## Chapter 4

35. Jackson, K. G., Maitin, V., Leake, D. S., Yaqoob, P. & Williams, C. M. Saturated fat-induced changes in Sf 60-400 particle composition reduces uptake of LDL by HepG2 cells. *J. Lipid Res.* **47**, 393–403 (2006).
36. Olano-Martin E, Anil E, Caslake MJ, Packard CJ, Bedford D, Stewart G, et al. Contribution of apolipoprotein E genotype and docosahexaenoic acid to the LDL-cholesterol response to fish oil. *Atherosclerosis* **209**, 104–110 (2010).
37. Ishida T, Ohta M, Nakakuki M, Kami H, Uchiyama R, Kawano H, et al. Distinct regulation of plasma LDL cholesterol by eicosapentaenoic acid and docosahexaenoic acid in high fat diet-fed hamsters: Participation of cholesterol ester transfer protein and LDL receptor. *Prostaglandins, Leukot. Essent. Fat. Acids* **88**, 281–288 (2013).
38. van Schalkwijk, D. B. et al. Dietary Medium Chain Fatty Acid Supplementation Leads to Reduced VLDL Lipolysis and Uptake Rates in Comparison to Linoleic Acid Supplementation. *PLoS One* **9**, e100376 (2014).
39. Ooi, E., Watts, G., Ng, T. & Barrett, P. Effect of Dietary Fatty Acids on Human Lipoprotein Metabolism: A Comprehensive Update. *Nutrients* **7**, 4416–4425 (2015).
40. Mustad, V. A., Ellsworth, J. L., Cooper, A. D., Kris-Etherton, P. M. & Etherton, T. D. Dietary linoleic acid increases and palmitic acid decreases hepatic LDL receptor protein and mRNA abundance in young pigs. *J. Lipid Res.* **37**, 2310–23 (1996).
41. Maki, K. C. et al. Effects of Prescription Omega-3-Acid Ethyl Esters on Fasting Lipid Profile in Subjects With Primary Hypercholesterolemia. *J. Cardiovasc. Pharmacol.* **57**, 489–494 (2011).
42. Mäntyselkä, P. et al. Cross-sectional and longitudinal associations of circulating omega-3 and omega-6 fatty acids with lipoprotein particle concentrations and sizes: population-based cohort study with 6-year follow-up. *Lipids Health Dis.* **13**, 28 (2014).
43. Lee, M. W. et al. Beneficial Effects of Omega-3 Fatty Acids on Low Density Lipoprotein Particle Size in Patients with Type 2 Diabetes Already under Statin Therapy. *Diabetes Metab. J.* **37**, 207 (2013).

44. Annuzzi, G. *et al.* Lipoprotein subfractions and dietary intake of n-3 fatty acid: the Genetics of Coronary Artery Disease in Alaska Natives study. *Am. J. Clin. Nutr.* **95**, 1315–1322 (2012).
45. Kuang, Y.-L., Eric Paulson, K., Lichtenstein, A. H. & Lamon-Fava, S. Regulation of the expression of key genes involved in HDL metabolism by unsaturated fatty acids. *Br. J. Nutr.* **108**, 1351–1359 (2012).
46. Ensign, W. *et al.* Disparate LDL phenotypic classification among 4 different methods assessing LDL particle characteristics. *Clin. Chem.* **52**, 1722–7 (2006).
47. Sninsky, J. J., Rowland, C. M., Baca, A. M., Caulfield, M. P. & Superko, H. R. Classification of LDL phenotypes by 4 methods of determining lipoprotein particle size. *J. Investig. Med.* **61**, 942–9 (2013).



## **Chapter 5: Discussion and conclusions**



**Perspectives on NMR-based advanced lipoprotein tests (ALTs) into clinical practice**

The exhaustive characterization of the lipoprotein profile is anything but trivial. The main reason for this is that the chemical compositions, density and size of lipoproteins vary greatly, limiting the possibility of clearly establishing the relationships amongst these three fundamental properties. The wide variety of methodologies used, the non-uniform definitions or descriptions of lipoprotein subfractions and the heterogeneity limit the comparability among and within analytical techniques.

Due to its inherent quantitative nature and sensitivity to size and density, NMR spectroscopy has increasingly gained attention as a valuable method for lipoproteins measurement, attracting several research groups to test and apply the methodology. However, so far, the applications with coherent NMR and reference data (e.g. UC) have been limited to relatively small cohorts, and the lack of appropriate standards both for the UC measurements and the NMR measurements have made meta-studies extremely difficult if not impossible. Several commercial companies are now offering lipoprotein analysis through NMR spectroscopy, but there is still some controversy about the introduction of NMR-based ALTs into clinical practice, partly because current methods do not provide a direct measure of lipoprotein sizes.

Currently, most NMR-based molecular profiles base the results on empirical models developed by correlation between the crude NMR spectrum and laboratory biochemical measurements of lipid concentrations, which make the scientific and clinical community

somewhat distrustful, taking into account that the size of the particles is the most relevant parameter to estimate the particle number. In this context, the approximation proposed by the research group for the lipoprotein characterization, the Liposcale test, using two-dimensional NMR experiments, whose signal is modulated by the diffusion of the particles in the mixture (DOSY-NMR), allows the hydrodynamic characteristics of the molecules, such as the size, to be included in the obtained information.

On the other hand, for the introduction of the NMR-based tests for the lipoprotein characterization, it is not only necessary to create trust and understanding in relation to a particular technology, but also attention should be given to the standardization between the different NMR platforms and approaches.

Current efforts towards extreme standardization of NMR measurements of blood samples and similar efforts on standardization of the reference methods will become game changers that will revolutionize the field of lipoprotein profiling. In particular, the development of NMR-specific standard operation procedures will allow the comparison of different cohorts and will generate new knowledge on the lipoprotein particle distribution with the possibility of turning it into a biomarker of lifestyle, diseases and healthiness.

The long-term application of NMR-based lipoprotein analysis in medical research is obviously an encouraging example of the epidemiological and clinical prospects of NMR-based technologies.

In the present thesis, it has been demonstrated that  $^1\text{H}$ -NMR spectroscopy is a suitable technique for the characterization of

## Chapter 5

lipoprotein particles and related parameters, reflecting its function and the cardio-metabolic health. We have tested this hypothesis within different contexts and approximations, from the analysis of lipoprotein fractions previously isolated using ultracentrifugation to the analysis of serum/plasma samples without the need for separation protocols and with minimal sample manipulation by using 1 and 2-dimensional NMR approaches in pharmacological, nutritional and epidemiological studies.

In Chapter 2, we presented our patented methodology for the lipoprotein characterization based on the DOSY NMR experiments, the Liposcale test, as well as the industrial development carried out by the spin off company Biosfer Teslab.

The Liposcale test<sup>1</sup> was created in a pure research framework, and therefore, with some limitations to coexist in the market with other NMR based on technologies for lipoprotein characterization. Thus, an industrial development and regulatory requirements for clinical applications were needed to become competitive enough. In this regard, **Section 2.3.2** offers an overview of the industrial development and milestones achieved by the spin off company Biosfer Teslab in order to introduce the advance lipoprotein test Liposcale in the market for its distribution and commercialization from its constitution.

During the industrial development of the Liposcale test, with the objective to favor the introduction of the NMR based on tests for lipoprotein characterization into the clinical practice, the research group has been involved in multiple and diverse research studies in collaboration with different national and international entities in which

the Liposcale test has been applied to characterize the lipoprotein profile in different pathologies, interventions and population studies.

Importantly, the main difference between our 2D NMR approach and current 1D NMR methods is that the addition of a second dimension in the NMR spectrum by means of a diffusion experiment allows the separation of the lipoprotein subclasses according to their diffusion coefficient, and with the use of the Stokes-Einstein equation<sup>2</sup>, DOSY NMR yields an objective separation of lipoprotein subclasses based on their size and favors the uniqueness of mathematical solutions compared to 1D NMR, and therefore is a potentially useful alternative to other available approaches for measuring lipoprotein fraction particle sizes or discrete size distributions for an arbitrary number of NMR-derived lipoprotein subclasses due to its inherent robustness and minimal sample manipulation<sup>3</sup>, ready to be used in the clinical routine to determine whether there are progressive changes in lipoproteins and to identify certain subgroups of individuals with lipoprotein abnormalities contributing to the understanding of the physiopathology of lipid-mediated cardiometabolic disorders.

### **Lipoproteins, beyond the lipidic content**

NMR has successfully been applied to identify the presence of pro-atherogenic particles, particularly smaller and dense LDL particles, reflecting a higher risk for the development of atherosclerosis and therefore the possibility of developing cardiovascular disease<sup>1</sup>.

On the other hand, the HDL hypothesis considers that a low level of cholesterol carried by this fraction accelerates also the development

## Chapter 5

of atherosclerosis. However, the development of drugs that increase its concentration, although increasing the level of HDL cholesterol, has been unsuccessful due to the lack of efficacy or increasing cardiovascular risk<sup>4</sup>.

The NMR derived results, presented in Chapter 3 **Section 3.2**, introduce a radically new attempt to explain the above facts, considering that HDL undergo alterations in their size that determine its structure and composition.

Since the 1970s, it has been known that the cholesterol concentration of the HDL fraction of lipoproteins (HDL-C) is inversely related to cardiovascular risk<sup>4</sup>. The protective function of HDL is characterized by its anti-inflammatory and anti-oxidant properties and reverse cholesterol transport (CRT)<sup>5</sup>, that is, the uptake of cholesterol from peripheral tissue cells and its transport to the liver for its subsequent elimination. Clinical trials with treatments which tend to increase HDL cholesterol concentration have revealed that increasing cholesterol from pharmacological interventions does not necessarily translate into a benefit for the patient as it does naturally. The mechanisms affecting the functionality of the HDL particles are unknown. As a consequence, the validity of HDL-C as a marker of cardiovascular risk protection is questioned. There is currently no procedure to evaluate the functionality of HDL in clinical practice and therefore no HDL-associated biomarker, alternative to HDL cholesterol, has been found which can be used universally to estimate cardiovascular risk.

Currently the HDL functionality is evaluated from *in-vitro* experiments in which the cholesterol reverse transport efficiency of HDL particles is calculated from measurement of the incorporation of radioactive isotope-labeled cholesterol molecules<sup>5</sup> or fluorescent labels<sup>6</sup> from macrophages. However, these tests are slow, tedious and poorly reproducible. Therefore, they can only be carried out in the framework of research studies. In addition, they do not generate information about the structure and composition of HDL. Some studies of lipidomics and proteomics<sup>7,8</sup> have also been carried out, although the results have not been validated, and they not reveal structural information on HDL particles. Other studies indicate that the distribution of HDL's in their various subfractions, as well as the quantification of the number of particles of each subfraction, may be more informative parameters in relation to the cardiovascular protection function<sup>9</sup>. However, there is no consensus on which parameters are optimal and there is no clear correlation between these and their functionality / efficacy<sup>10</sup>. Direct measurement of the number of HDL (HDL-P) particles in serum / plasma can only be done by nuclear magnetic resonance (NMR)<sup>11</sup>.

The group of Samia Mora and colleagues published a relevant study comparing the number of HDL particles measured by NMR and those obtained with the HDL-C / ApoA-1<sup>12</sup> ratio and demonstrated a clear discrepancy between them in the Women's health study, the same study cohort that has been presented in Chapter 4 in the present thesis. In this study, they estimated the particle number considering the classic model of Shen<sup>13</sup>, valid for all fractions of lipoproteins and considered to be spherical. Its radius was calculated from lipid and protein volume



## Chapter 5

distribution criteria, taking into account that the surface layer measures 2 nm and that proteins (basically ApoA-I, ApoA-II) together with free cholesterol and phospholipids are on the surface and the esterified cholesterol and the triglycerides in the nucleus.

The reason for the discrepancy is based on the fact that the NMR technique measures smaller sizes than those calculated using the Shen model. This discrepancy has not been solved by the scientific community before the results presented in this thesis, in which we performed a preliminary experiment with a small number of control samples and patients with type 2 diabetic patients (DM2), reproducing the methodology of the mentioned article, although measuring the size of isolated HDL by means of ultracentrifugation by NMR with a method developed by the group<sup>14</sup>, seeing that our results<sup>15</sup> exhibited qualitatively similar discrepancy to that reported in the previously mentioned article.

Our hypothesis considers that the size of the HDL measured experimentally is correct and questions the validity of the classic model of HDL, proposed by Shen in 1977<sup>13</sup> and universally accepted by the scientific community without providing significant modifications to the original proposal. Our model update implies that the lipid distribution in HDL is not that predicted by the theory, in the sense that some of the hydrophobic lipids (triglycerides and esters of Cholesterol) that theoretically occupy the interior of the HDL particles must necessarily, by restriction of space, emerge towards the surface of the particles, and possibly modify its functionality.

The existence of surface hydrophobic lipids would change the hydrophobicity of HDL, modify the conformation of the proteins found on the surface (basically Apo A-1 and Apo A-2) and therefore affect its functionality.

The results presented in this thesis open the door to the development of new procedures to directly identify and distinguish lipoprotein abnormalities in this specific fraction, in which the ratio surface/volume is crucial due to the particular small size. The novelty of the proposal resides in the application, for the first time, of the most modern biophysical techniques to the study of lipoproteins combining atomic force microscopy (AFM), microscopy equipment and classic fluorimetric scattering to analyze the polarity of the surface of the HDL particles as well as their viscoelastic properties from the electromechanical interactions of the microscope sensor complemented by the visualization of lipoproteins with NMR, a technique capable to provide the hydrodynamic size information of the particles.

### **Lipoprotein profile characterization as an evaluation tool for nutritional habits and nutritional interventions**

Finally, in Chapter 4, we have applied two different approaches for the lipoprotein characterization, the Liposcale test<sup>1</sup> and the Lipoprofile test developed by Otvos et al.<sup>11</sup>, demonstrating the utility of the lipoprotein NMR characterization for the assessment of the nutritional habits and evaluation of nutritional interventions affecting the lipoprotein profile opening the fundamental application of NMR

## Chapter 5

spectroscopy to the study of the non-pharmacologically modulation of the lipoprotein profile.

In the first study presented in **Section 4.2**, with a large cohort of 26,034 female healthcare professionals, we found that higher intake of fish and n-3 were significantly associated with lower triglycerides and larger VLDL particles. On the other hand, there was a positive association between the intake of fish and n-3 fatty acids and the LDL size, consistent with increased levels of large LDL particles. Total n-3, DHA and ALA intake were associated with larger HDL size and elevated levels of large HDL particles, factors that may be associated with lower CVD risk.

Importantly, we report for the first time that higher habitual fish consumption and higher levels of dietary derived n-3 fatty acid intake were both found to be associated with much larger magnitudes of association with lipoproteins fractions than the corresponding magnitudes of associations observed with traditional lipids. This finding suggests that dietary derived n-3 fatty acids influence CVD risk through lipid and lipoprotein metabolism perhaps more than previously appreciated, given that lipoprotein particles, particularly LDL and HDL particles concentration or number, have both been shown to perform better than their respective major lipid components for assessing CVD risk<sup>16–18</sup>.

In the same direction, the two intervention trials presented in **Section 4.3**<sup>19</sup> and **Section 4.4**<sup>20</sup>, designed to evaluate the effect of diets enriched with either SFA or n-6PUFA, and supplemented with LCn-3PUFA, produced similar changes in lipoprotein profiles. Both diets

increased the LDL particle size, a parameter that has been associated with a reduced risk for atherosclerosis in epidemiological studies. In addition, they produced a reduction in total, large, medium and small VLDL particle concentrations, as well as in VLDL triglycerides, consistent with the decrease in total triglycerides and VLDL particle concentration, in agreement with the previous association study.

Altogether, the results presented in this thesis demonstrate that the use of NMR is ideal for the routine characterization of lipoproteins in the research, the clinical and the epidemiological frameworks, due to the simplicity of the preparation of the sample, the reliability and the robustness of the  $^1\text{H}$ -NMR spectroscopy and the possibility of automatization; and could be the basis for a revolution in clinical lipid analysis, which would provide invaluable help in the evaluation of the lipid-mediated cardiovascular risk as well as the development and evaluation of new drugs and diet intervention to combat dyslipidemia and metabolic disorders.

### References

1. Mallol, R. *et al.* Liposcale: a novel advanced lipoprotein test based on 2D diffusion-ordered  $^1\text{H}$  NMR spectroscopy. *J. Lipid Res.* **56**, 737–746 (2015).
2. Liu, M., Tang, H., Nicholson, J. K. & Lindon, J. C. Use of  $^1\text{H}$  NMR-determined diffusion coefficients to characterize lipoprotein fractions in human blood plasma. *Magn. Reson. Chem.* **40**, S83–S88 (2002).
3. Mallol, R. *et al.* Particle size measurement of lipoprotein fractions using diffusion-ordered NMR spectroscopy. *Anal. Bioanal. Chem.* **402**, 2407–2415 (2012).

## Chapter 5

4. Kingwell, B. A., Chapman, M. J., Kontush, A. & Miller, N. E. HDL-targeted therapies: progress, failures and future. *Nat. Rev. Drug Discov.* **13**, 445–64 (2014).
5. Rohatgi, A. *et al.* HDL Cholesterol Efflux Capacity and Incident Cardiovascular Events. *N. Engl. J. Med.* **371**, 2383–2393 (2014).
6. Sankaranarayanan, S. *et al.* A sensitive assay for ABCA1-mediated cholesterol efflux using BODIPY-cholesterol. *J. Lipid Res.* (2011). doi:10.1194/jlr.D018051
7. Inazu, A. *et al.* Increased high-density lipoprotein levels caused by a common cholesteryl-ester transfer protein gene mutation. *N. Engl. J. Med.* (1990). doi:10.1056/NEJM199011013231803
8. Ishigami, M. *et al.* Large and cholesteryl ester-rich high-density lipoproteins in cholesteryl ester transfer protein (CETP) deficiency can not protect macrophages from cholesterol accumulation induced by acetylated low-density lipoproteins. *J. Biochem.* (1994).
9. Mora, S., Glynn, R. J. & Ridker, P. M. High-Density Lipoprotein Cholesterol, Size, Particle Number, and Residual Vascular Risk After Potent Statin Therapy. *Circulation* **128**, 1189–1197 (2013).
10. Robinson, J. G. What is the role of advanced lipoprotein analysis in practice? *J. Am. Coll. Cardiol.* (2012). doi:10.1016/j.jacc.2012.04.067
11. Jeyarajah, E. J., Cromwell, W. C., Otvos, J. D. & al., *et.* Lipoprotein particle analysis by nuclear magnetic resonance spectroscopy. *Clin. Lab. Med.* **26**, 847–70 (2006).
12. Mazer, N. A., Giulianini, F., Paynter, N. P., Jordan, P. & Mora, S. A comparison of the theoretical relationship between HDL size and the ratio of HDL cholesterol to apolipoprotein A-I with experimental results from the Women’s Health Study. *Clin. Chem.* **59**, 949–58 (2013).
13. Shen, B., Scanu, A. & Kezdy, F. Structure of human serum lipoproteins inferred from compositional analysis. *Proc. Natl. Acad. Sci. USA* **74**, 837–841 (1977).
14. Mallol, R. *et al.* Particle size measurement of lipoprotein fractions using diffusion-ordered NMR spectroscopy. *Anal Bioanal Chem.* **402**, 2407–2415 (2012).

15. Amigó, N. *et al.* Lipoprotein hydrophobic core lipids are partially extruded to surface in smaller HDL: "Herniated" HDL, a common feature in diabetes. *Sci. Rep.* **6**, 19249 (2016).
16. Stalenhoef, A. F. H. *et al.* The effect of concentrated n-3 fatty acids versus gemfibrozil on plasma lipoproteins, low density lipoprotein heterogeneity and oxidizability in patients with hypertriglyceridemia. *Atherosclerosis* **153**, 129–138 (2000).
17. Kris-Etherton, P. M. Fish Consumption, Fish Oil, Omega-3 Fatty Acids, and Cardiovascular Disease. *Circulation* **106**, 2747–2757 (2002).
18. Rivellese, A. A. *et al.* Effects of dietary saturated, monounsaturated and n-3 fatty acids on fasting lipoproteins, LDL size and post-prandial lipid metabolism in healthy subjects. *Atherosclerosis* **167**, 149–58 (2003).
19. Dias, C. B. *et al.* Improvement of the omega 3 index of healthy subjects does not alter the effects of dietary saturated fats or n-6PUFA on LDL profiles. *Metabolism*. **68**, (2016).
20. Dias, C. B., Amigo, N., Wood, L. G., Correig, X. & Garg, M. L. Effect of diets rich in either saturated fat or n-6 polyunsaturated fatty acids and supplemented with long-chain n-3 polyunsaturated fatty acids on plasma lipoprotein profiles. *Eur. J. Clin. Nutr.* (2017). doi:10.1038/ejcn.2017.56